Aromatic Hydrocarbons from Pure Fatty Acids and Renewable Triglyceride Feedstocks via Hydrothermal Zeolite Catalysis

by

Na Mo

A dissertation submitted in partial fulfillment
of the requirements for the degree of
Doctor of Philosophy
(Chemical Engineering)
in The University of Michigan
2016

Doctoral Committee:

Emeritus Professor Phillip E. Savage, Chair
Professor H. Scott Fogler
Shawn Hunter, Dow Chemical Co.
Professor Adam Matzger
Professor Johannes W. Schwank

"To Learn"

To my parents and my dear husband, Alexander Crowell

ACKNOWLEDGEMENTS

Thanks to all the people who made this dissertation possible. I would especially like to thank my thesis advisor, Professor Phillip Savage. He has been as great an advisor as any graduate student could dream of. He helped me to recognize my specific research interest in renewable chemical production at the very beginning and encouraged me to pursue it, even though it probably would have been an easier choice to pursue fuel over chemicals at that time. He is always there whenever I need him, I can just walk into his office when I want to have a discussion, and if I send him an email for a question the reply is always back very fast. He gives me enough freedom but always has key suggestions to keep me moving forward. I want to thank him not only for his great academic mentoring, but also for the friendship we have built during the past five years.

I would also like to thank all my committee members, including Professor H. Scott Fogler, Professor Johannes Schwank, Professor Adam Matzger, and Dr.Shawn Hunter. Every single discussion we have ever had was extremely helpful for the development of this work. This dissertation would not have been possible without their input.

I am very grateful to the group members I have. Peter Valdez, Jacob Dickinson, Chad Huelsman, Shujauddin Changi, Robert Levine, and Allison Frank, they all helped me with training to use different lab equipment and conduct general group business. In particular, I appreciate the great help in the lab and the unique humor of Thomas Yeh. I would also like to thank Jennifer Jocz, Le Yang, Yang Guo, and Zheng Li for their recommendations at certain points. I thank David Hielata for his help on

FAME analysis and other assistance over the past two years. I especially thank Julia Faeth, not only for her expertise but also for her friendship and encouragement.

I am lucky to have had the opportunity to mentor three undergraduate students, Ryan Hockstad, Wincent Tandar, and Jarrett Pennebacker. I thank them for their commitment and contribution to this work, and also for their help shaping me to be a better mentor. I thank Martin Goldbach, Chang Yup Seo, and Dr.Xiaoyin Chen for sharing their expertise on catalysis.

I thank Professor Timothy Scott for mentoring me as a student instructor for the course Thermodynamics. The experience was rewarding and memorable. I thank professor Ronald Larson and Dr. Susan Montgomery for their recommendations and encouragement.

I would like to thank all of my undergraduate professors at Michigan Technological University. They helped to cultivate my passion for chemical engineering and research. In particular, Professor Sarah Green, Professor Julia King, Professor Faith Morrison, Professor Tomas Co, Professor David Shonnard, and Professor Micheal Mullins.

I acknowledge the NSF Grant for financial support of this work.

I am grateful to my in-laws, especially my mother-in-law, Regina Crowell, who has been a constant source of love and support, and helped me achieve success in life. I am eternally obligated to my parents whose love and sacrifice made me what I am today.

Last, I thank my dear husband and best friend, Alexander Crowell, who has been by my side on each step through this long journey, and has given me endless support through thick and thin, and unconditional love at my strongest and weakest.

TABLE OF CONTENTS

LIST OF FIGURES

Figure

LIST OF TABLES

Table

LIST OF APPENDICES

Appendix

ABSTRACT

Aromatic Hydrocarbons from Pure Fatty Acids and Renewable Triglyceride Feedstocks via Hydrothermal Zeolite Catalysis

by

Na Mo

Chair: Professor Phillip E. Savage

Triglycerides and fatty acids are attractive renewable feedstocks, because they are the major components of many types of biomass. There are several proposed chemical processes that generate aqueous streams rich in fatty acids.[1–4] Thus, fatty acids in aqueous streams represent a renewable feedstock available for the production of chemicals. Zeolite catalysis is applied because these catalysts promote aromatization reaction, and aromatics are the targeted chemical products. The objective of this research is to use hydrothermal catalytic cracking with zeolite to generate key industrial chemicals, such as toluene and xylenes, from fatty acids.

I investigated the reactions of saturated (palmitic and stearic acids) and unsaturated fatty acids (oleic and linoleic acids) in water near the critical point at 400 ℃, at 12.5, 20, and 24 MPa, and over zeolites Y, beta, and ZSM-5. Zeolite ZSM-5 was found to be the most promising catalyst to produce aromatics from fatty acids in water among different types of zeolite that we have tested. The major liquid products were aromatics (e.g., xylenes, toluene), and alkanes (e.g., 2-methyl-pentane, heptane). Reaction condition of 400℃, 20 MPa, and 180 minutes gave the highest total product

yield. Additional hydrogen and water density have effect on product distribution. The lowest silica/alumina ratio (23) we have tested generated the most aromatics. The catalyst can be regenerated and reused. ZSM-5 with a silica/alumina ratio of 23 gave a total product yield of 76 ± 3 wt% at its third use, after undergoing regeneration twice previously. Finally, this methodology has been applied to fatty acid-rich lipids extracted directly from biomass, including algal oil, coconut oil, peanut oil, and lard, to assess the technical feasibility of the approach with a real plant-derived feedstock. Peanut oil (53 ± 15 wt%) and lard (48 ± 4 wt%) showed comparable total major aromatic yields to pure fatty acids (42 ± 4 wt%).

This research confirms the technical feasibility of producing appreciable yields of aromatic products from fatty acids in water over consecutive uses. Examining the influence of different process variables has revealed methods to tune the product distribution in order to favor desired products. Taken together, this work lays the foundation for an aromatics production process using renewable feedstocks.

CHAPTER I

Introduction

1.1 Background and Motivation

There has been a long interest in the production of chemicals from renewable feedstock in order to make the current chemical industry more environmentally friendly. Renewable chemicals are becoming increasingly essential due to large worldwide demand with fast developing countries, the growth of global population, and environmental concerns such as greenhouse gas release and the global warming phenomenon, which are associated with the conventional process of producing bulk chemicals from petroleum in the current chemical industry. For all of these reasons, interest in conversion of biomass to chemicals has increased sharply. The number of journal articles on this topic doubled from 2008 to 2010.[5] Chemical manufacturers are also interested in producing bulk and specialty chemicals from renewable feedstock because of the increasing global demand for certain chemicals and the potential sustainability advantage offered by renewables. In the U.S, the net import of benzene/toluene/xylene (BTX) has increased by 300 million liters from 2003 to 2013[6], indicating that demand is exceeding supply domestically.

This topic draws more attention especially with the recent shale gas revolution, which has the potential to affect not only the natural gas market, but also the entire energy mix of the world.[7] The US chemical and oil industry is very sensitive to

feedstock prices, and therefore has created a significant intentional shift from heavy feedstock to light feedstock with the shale gas discoveries in the US. The aromatics production routes are connected to naphtha from petroleum and its conversion by either steam cracking or by catalytic reforming. Therefore, this shift in cracker feedstock can have significant negative impact on the heavier refinery co-products such as aromatics. Some estimates suggest that aromatic cracker output is already down by 20% in the US. At the same time, the demand for aromatics is expected to rise by 5-10% annually.[8] The shale gas revolution might enable the large-scale implementation and production of the first wave of bio-based bulk chemicals. All of these factors point to the need to discover new methods to produce chemicals, especially aromatics, from renewable resources.

1.2 Relevance to Sustainability

Sustainability is generally measured by the Triple Bottom Line (TBL), which includes the traditional measure of economic profits as well as environmental and social dimensions. [9] Chemical production from renewable feedstocks can potentially be a more sustainable process than the traditional chemical production from fossil fuel by influencing some of these TBL dimensions.

According to Petrou and Pappis's survey[10], the most common positive impact of using renewable feedstocks is the reduction in the emission of greenhouse gases, particularity CO_2. This is because organisms (which the biomass comes from), during their lives absorb CO_2 equal to the amount emitted when biomass is burned. However, this is ignoring the GHG emission from the use of fossil transportation fuels in the complicated logistics needed for biomass collection. Another positive impact of using renewable feedstocks is the decrease in SO_2 emissions, which is due to the low content of biomass in sulfur. Among the negative impacts, the most serious problem arising from renewable feedstock-based chemical or fuel production is the increase in food

market prices.

Both benefits and risks exist with the process of chemical production from renewable feedstocks, and both sides should be considered in measuring the sustainability performance. Life Cycle Analysis (LCA) is a good approach for evaluating these pros and cons individually across the TBL dimensions and for different types of feedstocks. There are many factors that must be taken into consideration for each dimension. Cost factors for economic analysis include cost of feedstock, power and water supply, labor, taxes, and distribution, etc. Some indicators for the environmental dimension include greenhouse effect, ozone layer depletion, acidification, europhication, and energy. The results should be comprehensive and should come with trade-offs. For example, in a recent study, Singh and Olsen[11] suggested algal biofuels to be environmentally better than fossil fuels but economically it is not yet attractive based on LCA.

1.3 Properties of Water near the Critical Point

Interest in obviating a biomass drying step and the resulting energy savings has led many researchers to study and develop hydrothermal processes for conversion of biomass. A life-cycle assessment of algae biofuel production from Chlorella Vulgaris indicated that drying and extraction in the biofuel production process accounted for up to 90% of the total process energy.[12] Since there is a lot of water present in biomass, it is important to understand the role of water in the chemical process of biomass.

Water is widely considered a safe and inexpensive reaction medium. Water near its critical point (374 ℃, 22.1 MPa) is particularly an attractive reaction medium; compared to organic solvents in chemical processes, it offers potential environmental and economic advantages. The density and dielectric constant of the water medium play a major role in solubilizing organic compounds in subcritical and supercritical

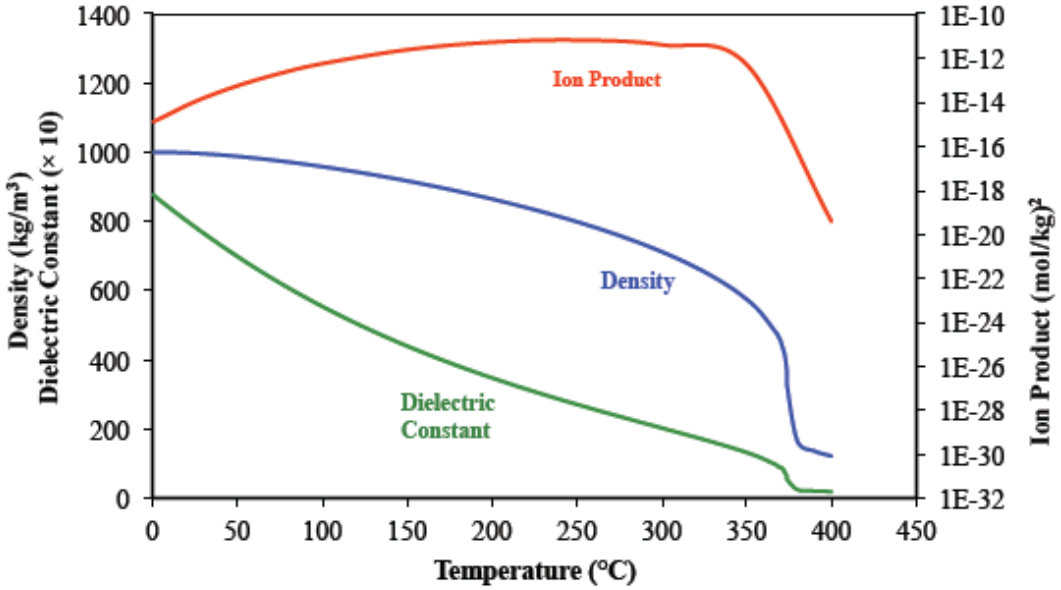

Figure 1.1: Effect of temperature on physical properties of water at a pressure of 25 MPa
[13]

water. As shown in Figure 1.1, the density, dielectric constant, and ion product of water decrease considerably near the critical point compared to room-temperature liquid water. The decrease of dielectric constant indicates that both the persistence and the number of hydrogen bonds decrease; therefore, enhancing the solubility of chemical compounds in the water. Water acts more like a polar organic solvent near the critical temperature of water, which would improve its solubility to polar chemicals, such as aromatics.

Conducting chemical reactions in subcritical or supercritical conditions affords some additional advantages. First, reducing the system temperature of post reaction would easily lead to the separation of organic and aqueous phases, so that product separation is convenient when using water as an alternative to organic solvents.[14] Second, it provides an opportunity to manipulate the reaction environment (solvent properties) by manipulating pressure.[15] Third, some reactions that follow conven-

tional acid- or base-catalyzed mechanisms at room temperature have been proposed to be catalyzed by water molecules in subcritical or supercritical reaction conditions, which suggests that the subcritical or supercritical condition may promote acid- or base- catalyzed reactions.

Since water is already present in harvested biomass, and considering the advantages of using water near the critical point as a solvent as we have discussed above, it is believed that this water could serve as a promising solvent alternative for our proposed methodology for producing industrial bulk chemicals from renewable feedstock.

1.4 Selection of Reactants and Targeted Products

Fatty acids are attractive renewable feedstocks for producing hydrocarbon chemicals, because they can be major components of both terrestrial and aquatic biomass (e.g., jatropha, palm, microalgae). Lipids in both terrestrial and aquatic biomass contain free fatty acids and acylglycerides, which include triglycerides, diglycerides, and monoglycerides (with triglycerides as the majority). Acylglycerides, however, can be easily broken down to fatty acids via thermal reaction or hydrolysis.

There are several proposed chemical processes that generate aqueous streams rich in fatty acids. For example, Immer et al.[16] and Wang et al.[17] describe a fuel production process that includes hydrolysis of triglycerides and thereby produces fatty acids in water at elevated temperatures. Kusdiana and Saka [2] have proposed making biodiesel from vegetable oils by first hydrolyzing triglycerides to produce fatty acids in water. Hydrothermal liquefaction of lipid-rich algal biomass is another process that generates aqueous streams rich in fatty acids.[1] These accumulated examples show that fatty acids can be readily produced in aqueous streams. Hence, fatty acids are chosen as our starting reactant for developing the method of producing high-value chemicals.

Palmitic acid is one of the most common fatty acids that can be found in plants and animals. For example, palmitic acid makes up to 20 wt% of the total fatty acids produced from liquefaction of microalgae. [1] Palmitic acid is a saturated fatty acid with 16 carbon atoms (C16:0). We use it as a model saturated fatty acid in this study. Some unsaturated fatty acids such as oleic acid and linoleic acid were also investigated. If valuable chemical products, such as aromatics, can be generated from the fatty acid in a water environment, then there is reason to be optimistic that they can be generated from wet biomass feedstock. Therefore, real triglyceride feedstocks are also introduced after the methodology is tested and determined to be technically feasible. The real triglyceride feedstocks include algal oil, coconut oil, peanut oil, and lard. They are chosen mainly due to their popularity and high content of fatty acids. The findings are presented in Chapter 7.

Our targeted products are high-value industrial bulk chemicals, mainly aromatics in this case. This is not only because of the high selling price of aromatics compared to gasoline, but also their increasing demand worldwide, as well as potential reduction of their supply due to the recent shale gas discovery as discussed earlier.

Some representative aromatic compounds include benzene, toluene, different isomers of xylene: o-xylene (1,2-dimethyl-benzene), m-xylene (1,3-dimethyl-benzene), p-xylene (1,4-dimethyl-benzene), and ethylbenzene. Those aromatic hydrocarbons are chemicals produced in very large volumes worldwide; for example, the global market is about 30 Mt/year for benzene, 14.5 Mt/year for toluene, 24 Mt/year for mixed xylenes, and 17 Mt/year for p-xylene, according to the International Energy Agency's analysis in 2012. [18] In traditional gasoline production, a considerable amount of aromatics are often generated by the catalytic reforming of naphtha in a petroleum refinery.[19]

Chemicals such as benzene, toluene, and xylene are considered valuable as chemical building blocks and are thus removed to some extent in the traditional gasoline

production process. Aromatic hydrocarbons have various uses in the chemical industry. Many are used as starting materials for a wide range of consumer products. For example, p-xylene is a precursor of terephthalic acid, which is a monomer used to make polyethylene terephthalate, a plastic widely used in the production of fibers and beverage bottles.

1.5 Proposed Methodology and Catalyst Application

Since the reactants and the targeted products are clear, the proposed approach would be hydrothermal cracking and aromatization reactions. Cracking is necessary to break down the long carbon chain in fatty acids. Aromatization is needed to form aromatic rings from the hydrocarbon molecules that are produced from cracking. It is a hydrothermal process because subcritical or supercritical water is chosen to be the reaction medium for many reasons, for example, to avoid drying and the use of organic solvent.

Zeolite catalysts are hydrated aluminosilicate minerals made from interlinked tetrahedra of alumina and silica. They are widely used in both petroleum and bio-oil refining. [20–22] They are active for catalytic cracking and aromatization.[23] Zeolite catalyst was selected for this work because prior research,[24–26] though not done in an aqueous phase, indicates that zeolite (HZSM-5) can convert fatty acids to paraffins, olefins, and aromatic compounds that fall within the gasoline and kerosene boiling point fractions. Additionally, zeolite (HZSM-5) has been shown to be useful in other biomass processing contexts.[20, 27–29] Detailed discussion of these prior works is in Chapter 2, the literature review section.

A traditional zeolite cracking process in petroleum refining normally occurs at a very high temperature (around 700 ℃). In the presence of steam, framework aluminum atoms can be removed from the zeolite lattice. [30–32] A severe hydrothermal reaction condition may reduce the catalyst stability. Therefore, a temperature near

the critical point of water (400 ℃) was chosen for this catalytic hydrothermal reaction to study.

To summarize, palmitic acid (PA), which is one of the most common fatty acids in nature, serves as a key reactant. We identify and quantify all of the major reaction products (in Chapter 4, Products and Kinetics), and we elucidate the effects of reaction time, temperature, hydrogen pressure, water density, and degree of saturation of the reactant, on the yield of each (in Chapter 5, Effect of Reaction Process). We also examine catalyst regeneration and catalyst characterization (in Chapter 6, Catalyst Composition, Regeneration, and Characterization). Finally, we applied this method to renewable triglyceride feedstocks and report the results in Chapter 7. Chapter 8 concludes with the significant findings of this study and suggests some future directions.

CHAPTER II

Literature Review

The previous chapter summarized the reasoning behind the selection of feedstock, catalyst, targeted products, and the proposed method. This chapter features a comprehensive literature review of relevant work. The first section presents an overview of hydrothermal processing of biomass and particularly of fatty acids, which includes some literature highlights at the time this work was first undertaken. The second section provides a understanding of application of zeolite catalyst with its reaction activity and hydrothermal stability. The third section focuses on possible reaction pathways and potential products for our proposed process based on literature surveys. Lastly, this chapter concludes with gaps in prior literature, which motivated our research.

2.1 Hydrothermal Processing

Researchers have a long history of studying biomass conversion, and this approach includes many different technological pathways, such as pyrolysis, fermentation of sugars, gasification, and aqueous phase reforming. Most recently, more attention has been attracted to hydrothermal processing of biomass, mainly because it can apply to biomass with high water content. Hydrothermal processing of plant oils has been studied for decades. It is believed that lipids in biomass are a good source for bio-fuel.

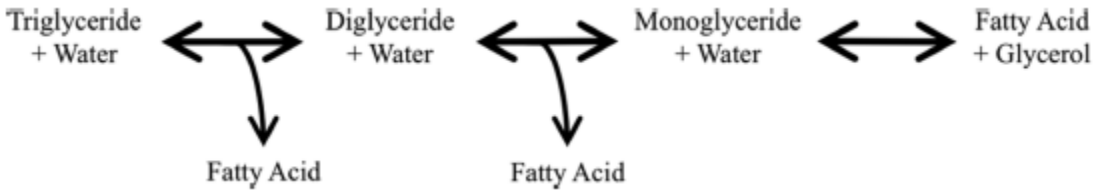

Figure 2.1: Reaction network for acylglyceride hydrolysis in hydrothermal condition [33]

As mentioned briefly in the introduction section (Chapter1), lipids contain acylglycerides and free fatty acids. Acylglycerides include triglycerides (TG), diglycerides (DG), and monoglycerides (MG), where triglyverides are the majority in terrestrial plant. Fatty acids can be obtained from them by either thermal reaction or hydrolysis. Figure 2.1 shows the reaction network for acylglyceride hydrolysis in hydrothermal condition to produce fatty acids.

2.1.1 Hydrothermal Processing of Triglyceride Feedstocks

Holliday et al.[3] studied soybean, linseed, and coconut oils in subcritical water (water density of 0.7 g/mL and temperatures at 260-280℃). The oils were successfully and reproducibly hydrolyzed to free fatty acids with conversion of greater than 97% after 15-20 minutes. Higher temperature reactions were also performed, where soybean oil was subjected to subcritical temperature at 300 ℃ for 11 and 25 minutes and 320 ℃ for 13 minutes. The reported results indicated severe decomposition, pyrolysis, or polymerization of the fatty acids, but there was no further information to confirm any of these reactions.

Alenezi et al. [4] studied sunflower oil with subcritical water in a tubular reactor over a range of temperature from 270 to 350 ℃ for 30 minutes, at 20 MPa. The sunflower oil consisted of about 77 wt% triglycerides, 20 wt% diglycerides, 2.5 wt% monoglycrides, and only 0.3-0.5 wt% free fatty acids. In all the experiments the water to oil feed ratio is kept at 50/50 (volume/volume). At 350 ℃ and 20 MPa, the yield

of fatty acids was 76 wt% at only 5 minutes of reaction time. This yield increased to 93 wt% at reaction time of 15 minutes. It is believed that the reaction is autocatlyzed by the acidity of fatty acids.

This work does not just test the feasibility of fatty acids production from sunflower oil in subcritical water, but also investigated the reaction kinetics. The oil hydrolysis reaction is a first-order reversible reaction. As shown in Figure 2.1, in the first step, TG is hydrolyzed to DG, in the second step, DG is hydrolyzed to MG, and in the third step, MG is hydrolyzed to glyceride. Fatty acid is generated with each step. The authors have implemented a kinetics model for the reversible oil hydrolysis reaction that gives good fitting with experimental data and has a maximum variance of less than 5.4 %.

Kusdiana and Saka [2] took a further step after hydrolysis of vegetable oil. The study proposed a two-step catalyst-free method for biodiesel fuel production, which includes step 1, hydrolysis of triglycerides of rapeseed oil in subcritical water to obtain fatty acids, and step 2, methyl esterification of the hydrolyzed products with supercritical methanol to achieve fatty acid methyl esters. We are more interested in the first step where the process provided fatty acids in a water stream. This first step was carried out at various temperatures ranging from 255 to 350 ℃, and a pressure ranging from 5 to 20 MPa. A flow reactor was used and the results were recorded from reaction time 0 to 30 minutes. The hydrolysis reaction is a reversible reaction, so it would be completed only if a large excess of water is used or if one of the products is removed from the reaction mixture. Therefore, the work extended the experiments to study the effect of the amount of water in the system. Consequently, the various volumetric ratios of water to rapeseed oil did affect the yield of fatty acids. A higher water to rapeseed oil ratio gave a higher fatty acids yield.

These studies mentioned above[2–4] confirmed that vegetable oils can be a good source for fatty acids, and provided a good range of reaction temperatures and pres-

sures for hydrolysis of vegetable oils to produce fatty acids.

Besides vegetable oils, aquatic biomass has been a primary target for hydrothermal processing as well. The work published by Brown et al.[1] in 2010 was a highlight in this field, which was cited for 296 times up to date. The study is on hydrothermal liquefaction and gasification of Nannochloropsis sp, which is a type of microalgae. Microalgae offer several advantages relative to terrestrial lignocellulosic biomass. Microalgae have a higher photosynthetic efficiency, and large lipid content, which means, they can be rich in oil (triglycerides). They grow rapidly and can be cultivated in marginal and non-arable land, and grow in contaminated water environments. Furthermore, unlike the land plants, such as soy or sunflower, microalgae have no competition with food supply. Hydrothermal treatment of microalgae at low temperatures (around 200 ℃) to make carbonized solids is referred to as carbonization (HTC). Hydrothermal treatment of microalgae at intermediate temperatures (around 300 ℃) to make crude bio-oil, is referred to as liquefaction (HTL). Hydrothermal treatment of microalgae at high/supercritical temperatures (about 400 ℃) to make fuel gas, is referred to as gasification.[33]

The conventional approach for biofuel production from microalgae involves extraction of triglycerides from the algae and then transesterification into biodiesel fuel, while Brown et al[1] used a one-step method for making biocrude from microalgae. The work was performed under temperatures from 200 to 500 ℃, to cover both liquefaction and gasification of Nannochloropsis sp. microalgae. A moderate temperature of 350 ℃ with a batch holding time of 60 minutes led to the highest bio-oil yield of 43 wt%. Major products include fatty acids, alkanes, alkenes, and N-containing compounds. The products include five free fatty acids, myristic, palmitoleic, palmitic, oleic, and stearic acids. They likely arise from hydrolysis of triaclyglcerol present in the Nannochloropsis sp., which has about 28 wt% lipids. The most abundant gas product is always carbon dioxide. The paper was the first to report in detail yields

and molecular compositions of both the oil and gas products from a systematic study of hydrothermal treatment over a broad temperature range (from subcritical to supercritical water state). This work lays a great foundation, but more work is needed to improve the bio-oil quality, for example to increase the carbon recovery and to remove the nitrogen in the bio-oil. However, the significance of this work to the thesis is that this hydrothermal liquefaction method of microalgae can serve as one path to provide a good renewable feedstock of fatty acids in a stream that also contains primarily water.

Another hydrothermal study of microalgae was explored by Lu et al. [34]. They used hydrothermal carbonization (HTC) of wet microalgae to facilitate extraction of algal lipids (fatty acids). Approximately 3 g of the homogenized 15 wt% microalgae slurry was loaded into each batch reactor. The carbonization temperatures were examined between 180 to 220 ℃, and reaction times from 15 minutes to 30 minutes. The retained fatty acids were extracted using ethanol, which was claimed to be a renewable and less toxic non-petroleum-derived solvent. An overall recovery of fatty acids from microalgae of 74 wt% was achieved by the combination of hydrothermal carbonization and ethanol extraction. The highest total fatty acids recovery occurs at 180 ℃ at 30 minutes, 200 ℃ at 30 minutes, and 220 ℃ at 15 minutes. This study provides good treatment conditions of a potential feedstock, microalgae, to produce fatty acids.

Lu et al. [34] proposed a possible process of using HTC to obtain nutraceuticals and biofuels from microalgae based on the results from their work. The process starts with dewatering the harvested algae to a slurry that is then treated by hydrothermal carbonization to produce hydrochar and an aqueous stream containing nutrients. Using catalytic hydrothermal gasification on this latter stream can produce fuel gases to supply heat and power in the bio-refinery. The nutrients and water can be potentially be recycled back to the cultivation of microalgae. The hydrochar is extracted with

ethanol to recover the lipids, which then could be fractionated to nutraceuticals and bio-oil.

All the studies discussed above are catalyst free hydrothermal processing of biomass. There are also many work that focus on catalytic hydrothermal processing of biomass. For example, Satyarthi et al. [35] conducted experiments on hydrolysis of vegetable oils (i.e. coconut oil, plmolein oil, used soybean oil, castor oil, jatropha oil, karnja oil, palm oil, rubber seed oil) and chicken fat to fatty acids over solid acid catalysts. The hydrolysis of triglycerides is a three-step, consecutive and reversible reaction, which is shown in Figure 2.1. The third step of the reaction which is the conversion of MG into fatty acids, is relatively more endothermic than the first two steps. Similar thermodynamics is expected for the vegetable oil and fats, where the activation energy was reported to be in the range of 45 to 75 kJ/mol. The catalysts applied in this work include acidic, macroporous polymeric resin (Amberlst 70), zeolite (SAPO-11, HY and H-beta), supported oxide (Manganese oxide/alumina), sulfated zironia, Fe-Zn double metal cyanide (DMC), and basic ZnO. The catalysts (except for HY and SAPO-11) increased the TG conversion significantly. Complete conversion of vegetable oil triglcerides to fatty acids with selectivity greater than 73% was obtained at about 190 ℃.

Catalysis has also been used in hydrothermal liquefaction of microalgae. Duan and Savage [20] tested six different heterogenous catalysts (shown in Table 2.1) on bio-oil that was obtained from HTL of Nannochloroposis sp. microalgae. The catalytic reactions were carried out under inert (helium) and high-pressure reducing (hydrogen) conditions. The elemental compositions and heating values of the crude oil (about 38 MJ/kg) were largely insensitive to the catalyst used. The crude bio-oil yield ranged from a low of 35 % (from uncatalyzed liquefaction without hydrogen) to a high of 57 % (from Pd/C catalyzed liquefaction without hydrogen). The authors reported that the crude bio-oil yields exceed the crude lipid content (28 wt%) of the feedstock

Table 2.1: Catalyst types and compositions

catalyst	composition (from supplier)
Pd/C	Pd (5 wt %)
Pt/C	Pt (5 wt %)
Ru/C	Ru (5 wt %)
$Ni/SiO_2{-}Al_2O_3$	Ni (65 wt %)
$CoMo/\gamma\text{-}Al_2O_3$	CoO (4.4 wt %), Mo_2O_3 (11.9 wt %), sulfided
zeolite	SiO_2 and Al_2O_3, in various proportions plus metal oxides

[20]

because not only the triglycerides but also other cellular components such as protein, fiber, and carbohydrate, must be converted into crude bio-oil via catalyzed HTL.

Steam reforming reaction (2.1) and water-gas shift reaction (2.2) were believed involved in the gas production pathways. Since so much more of the carbon dioxide than hydrogen was formed from the reaction, the pathways for carbon dioxide and hydrogen formation must be separate. This was also supported by the disparity in their activation energies for the formation from microalgae (38 kJ/mol vs 99 kJ/mol).

$$C_xH_yO_z + (2x - z)H_2O \rightarrow xCO_2 + (y/2 + 2x - z)H_2 \tag{2.1}$$

$$CO + H_2O \rightarrow CO_2 + H_2 \tag{2.2}$$

This was the first application of common hydrocarbon processing catalyst to microalgae liquefaction in water. Because Pd/C catalyst is active for the conversion of triglycerides to fatty acids and also for the conversion of fatty acid into alkanes, the idea that catalytic hydrothermal liquefaction (with Pd/C) may be a way to produce a crude hydrocarbon bio-oil directly from wet microalgae in a single processing step is very similar to our objective, except that our target products are aromatic hydrocarbons. After reporting the success of hydrothermal liquefaction of microalgae with heterogeneous catalysts, Duan and Savage further determined the influence of high pressure hydrogen as a reaction variable on the upgrading of a crude algal bio-oil in

supercritical water. [36]

2.1.2 Hydrothermal Processing of Fatty Acids

After the overview of the prior relevant studies on hydrothermal processing of triglyceride feedstocks, we now discuss literature on hydrothermal processing of fatty acids in particular.

Fujii et al. [37] studied the decomposition kinetics of fatty acids in subcritical water under temperature-programmed heating conditions. The fatty acids they chose were caprylic acid (C8:0), capric acid (C10:0), and lauric acid (C12:0), which were studied as the corresponding fatty acids of monocaprylin, monocaprin, and monolaurin. The decomposition of fatty acids obeys first-order kinetics. The activation energy and frequency factors were smaller when the carbon number of the acyl chain of the fatty acids were longer.

Watanabe et al. [38] treated stearic acid (C17:0) using a batch reactor with supercritical water at 400 ℃ and a water density of 0.17 g/mL for 30 minutes. In the absence of catalyst, stearic acid was stable (2% conversion), and the main products were CO_2 and C16 alkene. An addition of alkali hydroxide (NaOH and KOH) in the supercritical water reaction enhanced the decarboxylation of stearic acid. Metal oxides also enhanced the decarboxylation of stearic acid with CO_2 and C16 alkene as the main products. Without supercritical water, the formation of CO and many carbonyl compounds were found, which suggested that stearic acid mainly underwent decarbonylation instead of decarboxylation. Monomolecular decarboxylation of stearic acid proceeded by added KOH to promote the dissociation of RCOOH into RCOO- and H+.

Catalytic deoxygenation of fatty acids can proceed via two pathways: decarboxylation wich yields CO_2 and n-alkane with one less carbon atom than the fatty acid reactant (2.3), and decarbonylation which yields CO, water and the corresponding

alkene (2.4).

$$R - CH_2 - CH_2 - COOH \rightarrow R - CH_2 - CH_3 + CO_2 \tag{2.3}$$

$$R - CH_2 - CH_2 - COOH \rightarrow R - CH_2 = CH_2 + CO + H_2O \tag{2.4}$$

Fu et al. [39] texted several different metal salts, bases, and high-surface-area supported metal catalysts for activity toward deoxygenation of palmitic acid in a hydrothermal reaction medium. Two heterogeneous catalysts, 5% platinum on activated carbon (Pt/C) and 5% palladium on activated carbon (Pd/C), proved to be very effective for hydrothermal deoxygenation of palmitic acid. They have examined the effect of the catalyst loading, reactant loading, batch holding time, and reaction temperature on the Pt/C-catalyzed deoxygenation rate.

Fu et al.[40] have also reported on hydrothermal decarboxylation and hydrogenation of different types of fatty acids over Pt/C. The conversion of saturated (stearic, palmitic, and lauric acid) and unsaturated (oleic and linoleic) fatty acids to alkanes happened over 5% Pt/C in high temperature water. The reactions were conducted in batch reactors under 330 ℃ for 30 to 150 minutes. No added hydrogen is required for these reactions. The saturated fatty acids gave the corresponding decarboxylation products (n-alkanes) with greater than 90% selectivity, and the formation rates were independent of the fatty acid carbon chain length. The unsaturated fatty acids showed low selectivities to the decarboxylation products. The main pathways were to form corresponding saturated fatty acids via hydrogenation, which then underwent decarboxylation to produce alkanes. Fu further studied the hydrothermal decarboxylation of fatty acids with activated carbons instead of Pt/C. [41] They successfully converted palmitic and oleic acids to fuel range hydrocarbons using two activated carbons in near- and supercritical water with no hydrogen added.

These previous studies on fatty acids not only provide insights of possible kinetics of fatty acids in high temperature water, but also showed that addition of hydrogen, carbon number, and the degree of saturation of fatty acids are some key topics when studying fatty acids.

2.2 Application of Zeolite

Zeolite is a well-known heterogeneous catalyst used in the petroleum industry and in the catalyzed pyrolysis process of biomass. Zeolites are attractive catalysts because they have well-defined pore structure, high activity per acid site, and can be produced at a reasonable price.[18] Zeolites are crystalline, hydrated aluminosilicates, and the conventional chemical formula for zeolites is shown below. Figure 2.4 shows one unit structure of the zeolite HZSM-5.

$$M_{x/n}[(AlO_2)_x(SiO_2)_y].wH_2O \tag{2.5}$$

Where M is the positive counter ion of valence +n that balances the charge due to the $x(AlO_2{}^-)$ groups. For example, M is hydrogen in Figure 2.2. The ratio y/x represents the Si/Al ratio, which can be rearranged as SiO_2/Al_2O_3. It is an important characteristic of zeolites that we will discuss further in Chapter 6.

Catalysts play a significant role in producing aromatics from biomass. The catalytic processing of pyrolysis oil has a yield of aromatic hydrocarbons that is as much as three times higher than that produced without catalyst.[43] In the fast pyrolysis process of lignocellulose biomass conversion, the zeolite catalyst converts products into light olefins and aromatic hydrocarbons. Among the various kinds of zeolite catalysts, HZSM-5 (ZSM-5 ion exchange sites are occupied by hydrogen ions) is favored in conversions of biomass into hydrocarbons, based on its conversion rate. Lestari et al. [23] reviewed a conversion of palm oil using three types of zeolites, zeolite HZSM-

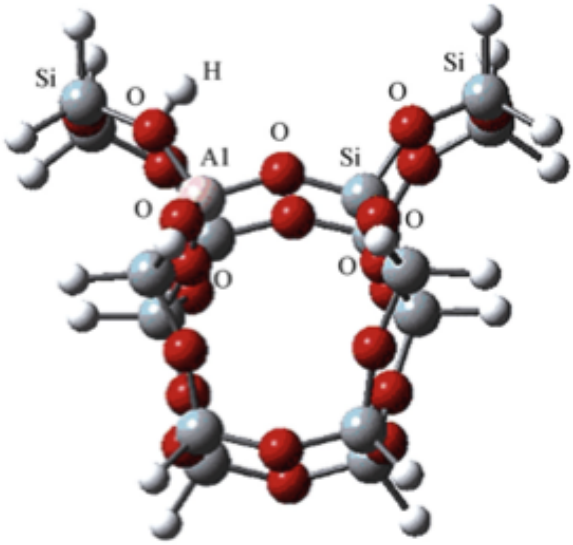

Figure 2.2: Structure illustration of a unit of zeolite HZSM-5 [42]

5, beta, and Y. HZSM-5 was reported as the most active catalyst, giving the highest conversion of 99%.

In 2013, Wang and Brown[44] presented a new study on catalytic pyrolysis of microalgae for production of aromatics and ammonia. They also studied a traditional lignocellulose biomass, red oak, for comparison with microalgae. They used Chlorella vulgaris algae, which were prepared by centrifugation, dewatering, and then freeze-drying. They chose zeolite catalyst ZSM-5 (silica/alumina ratio of 23) for the study. A micro-furnace pyrolyzer, with a quartz pyrolysis tube was used. The reaction temperature ranged from 40 to 800 ℃. Their results demonstrated that catalytic pyrolysis of microalgae produces better aromatic yields and better aromatic distributions than catalytic pyrolysis of red oak. At 700 ℃, with HZSM-5 to biomass ratio of 20, the product composition and yields are shown in Table 2.2.

Table 2.2 shows that benzene, toluene, and xylene (BTX) were their most abundant products. Napthalene and alkylnaphthalenes were the second major group of produced hydrocarbons. They have also reported the effect of catalyst loading and reaction temperature on product yields. Aromatic hydrocarbon production was favored

Table 2.2: Products from catalytic pyrolysis of Chlorella vulgaris algae

Compounds	Formula	Carbon yield/%	Aromatic selectivity[a]/%
Benzene	C_6H_6	4.24	18.5
Toluene	C_7H_8	6.72	29.3
Xylene	C_8H_{10}	6.03	26.3
Propyl-benzene	C_9H_{12}	0.02	0.1
1-Ethyl-2-methyl-benzene	C_9H_{12}	0.4	1.7
Trimethyl-benzene	C_9H_{12}	0.59	2.6
4-Ethyl-1,2-dimethyl-benzene	$C_{10}H_{14}$	0.05	0.2
Indane	C_9H_{10}	0.24	1.0
1-Propynyl-benzene	C_9H_8	0.35	1.5
1,Methyl-indan	$C_{10}H_{12}$	0.23	1.0
Methyl-1*H*-indene	$C_{10}H_{10}$	0.25	1.1
Naphthalene	$C_{10}H_8$	1.38	6.0
2-Methyl-naphthalene	$C_{11}H_{10}$	1.62	7.1
Ethyl-naphthalene	$C_{12}H_{12}$	0.07	0.3
Dimethyl-naphthalene	$C_{12}H_{12}$	0.54	2.4
Fluorene	$C_{13}H_{10}$	0.02	0.1
Anthracene	$C_{14}H_{10}$	0.09	0.4
2-Methylanthracene	$C_{15}H_{12}$	0.07	0.3
Total aromatics		22.95	100.0
Carbon monoxide	CO	13.90	—
Carbon dioxide	CO_2	28.34	—
Residue (coke/char)	—	33.10	—
Total carbon balance	—	98.29	—

[44]

Figure 2.3: A schematic diagram showing the diffusion limitations of xylene isomers inside zeolite pores
[45]

under reaction conditions of high catalyst to biomass ratio and high temperature. High catalyst loading is required to ensure that pyrolyzed vapor enters the pores of the zeolite catalyst instead of adsorbing on the external surface, where thermal decomposition produces coke and small oxygenates. In summary, this work shows a promising upgrading method of converting microalgae into fuels and chemicals using zeolite HZSM-5, however, it is limited to dried algae.

Chapter 1 discussed the advantages of having aromatics, such as xylenes, as targeted products. Cheng et al. [45] developed a catalytic fast pyrolysis method using ZSM-5 catalyst with reduced pore openings to produce p-xylene. They suggested that one possible option to improve the yield of p-xylene is to design a zeolite catalyst that allows only p-xylene but not m-xylene or o-xylene to diffuse out of the pores, shown in scheme(Figure2.3). In the study, furan and 2-methylfuran were converted by ZSM-5 and Ga/ZSM-5 in a continuous flow reactor. The modification of zeolite surface increased p-xylene selectivity from 32% to 96%.

These studies discussed above show that HZSM-5 is a potentially effective catalyst for biomass pyrolysis to produce aromatics. The next section then examines the application of zeolite in a hydrothermal system.

Duan and Savage [20] produced crude bio-oil from microalgae (Nannochloropsis sp.) via hydrothermal liquefaction with heterogeneous catalysts, include Pd/C, Pt/C,

Ru/C, $Ni/SiO_2 - Al_2O_3, C_oM_o/r - Al_2O_3$, and zeolite. The reactions were under inert (helium) and high pressure reducing (hydrogen) conditions at 350 ℃ in liquid water. Zeolite was tested because aluminosilicates in zeolite can facilitate cracking reactions that convert the heavier components of the biocrude into smaller fuel-range molecules. However, they found that the crude bio-oils produced from liquefaction with Pd/C, Pt/C, Ru/C, and C_oM_o/Al_2O_3 flowed easily and were much less viscous than the biocrude from the reactions with zeolite. They did not discuss the long-term hydrothermal stability of zeolite.

Rather than a catalyst screening study, a work that is more focused on HZSM-5 was performed by Li and Savage[28]. Crude bio-oil produced from hydrothermal liquefaction of Nannochloropsis sp. algae reacted over HZSM-5 at 400 to 500 ℃, with a reaction time of 30 to 240 minutes. This treatment greatly reduced the hetroatom (N,O,and S) content in the oil. In the work, they determined the influence of reaction temperature, reaction time, and catalyst loading on the yield and composition of treated bio-oil together with gaseous products. The gas yields were very sensitive to the reaction temperature, as higher temperatures generated more gas products. The gas products were primary light alkanes. At 500 ℃, the process produced a bio-oil that contains almost exclusively aromatic hydrocarbons, which indicated that HZSM-5 catalytic processing can be used to covert algae biocrude to a mixture that contains many industrial chemicals. They proposed that zeolite HZSM-5 maybe more economical than the supported Pt and Pd catalyst used in previous work, and can be an effective catalyst for treating algal biocrude. However, they did not further study the reuse of the catalyst to understand the activity or stability of zeolite under hydrothermal condition.

Dealumination and hydrolysis of the siloxane bonds (Si-O-Si) are possible causes of the degradation of zeolite in hot liquid water. However, little is known about the stability of zeolite in aqueous media at high temperatures. To the best of our

knowledge, Revenelle[46] was the only one who investigated in stability of zeolites in hot liquid water above 100 ℃.

Ravenelle[46] treated zeolite Y and ZSM-5 with varying Si/Al ratios in liquid water at 150 and 200 ℃ under autogenic pressure to assess their hydrothermal stability. The changes in the structure were characterized by X-ray diffraction, scanning electron microsopy, argon physisorption, MAS NMR spectrosopy, temperature-programmed desorption of ammonia, and pyridine adsorption followed by IR spectroscopy. The mechanisms of structural changes induced by water may go through two variants of hydrolysis, with one at the Si-O-Si sites and the other at Si-O-Al sites. The Si-O-Si hydrolysis is proton catalyzed, and the Si-O-Al hydrolysis is commonly refereed to as dealumination. In general, high-silica zeolites are strongly affected by basic solutions, while high-alumina zeolites transform more readily in acidic media.

They concluded that zeolite Y with a Si/Al ratio of 14 or higher is transformed into an amorphous material; the rate of this degradation increases with increasing Si/Al ratio. ZSM-5, in contrast, is not modified under the same conditions. The properties (e.g. crystallinity, acidity, micropore volume) of the ZSM-5 samples were found identical before and after treatment at 150 or 200 ℃ for 360 minutes, and this was also independent of the Si/Al ratio of the zeolite (Si/Al of 15, 25, 40). Therefore, ZSM-5 was illustrated to be a potentially effective zeolite in hot water environments.

2.3 Gaps in Prior Literature

After the literature review on hydrothermal processing of fatty acids, and application of zeolite in hydrothermal condition, we searched for studies that applied zeolite to fatty acids in water with a focus on producing aromatics. To the best of my knowledge, there is no prior work on this specific topic. The studies that are most close to our proposed hydrothermal catalytic reaction of fatty acids with zeolite to produce aromatics are Benson's[24] and Bielansky's[25] work, but neither study used

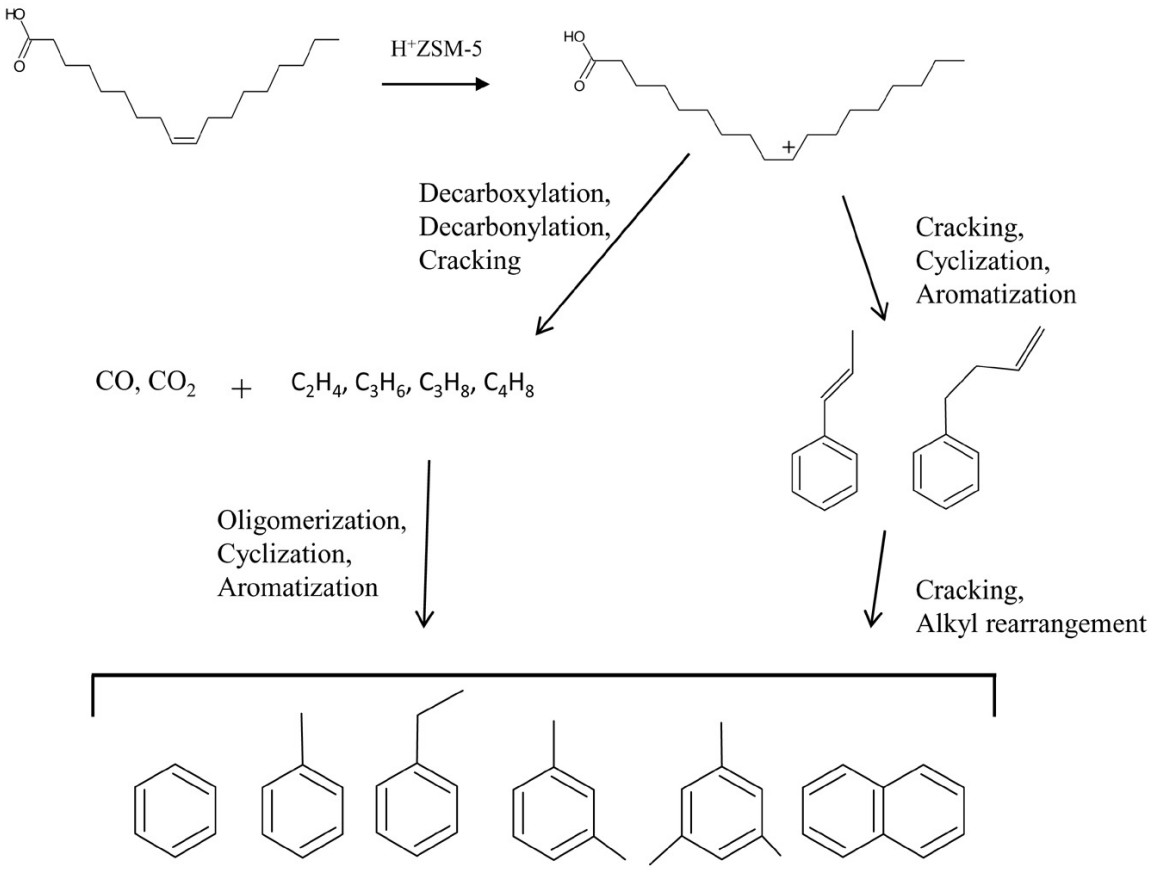

Figure 2.4: Proposed cracking chemistry for the transformation of oleic acid to green gasoline

[24]

hydrothermal conditions.

Oleic acid was used by Benson et al. [24] as a representative fatty acid. It was reacted at 400 ℃ with HZSM-5 catalyst, which has an elemental SiO_2/Al_2O_3 ratio of 23. Quatra C, a creative reaction/analysis device that combines catalyst bed and GC, was used for quick, online analysis of reaction products. The reaction produced a wide range of products, including paraffins, olefins, and aromatic compounds. In the proposed reaction pathway, aromatic compounds are believed to be the final products of cracking oleic acid (as shown in Figure 2.4), which also gives us some perspectives on the potential products and reaction pathway by cracking other kind of fatty acid.

Bielansky et al.[25] investigated palmitic acid as a model of fatty acid. The experiment was performed in the range of 485 to 550 ℃ in a fully continuous small-scale fluid catalytic (FCC) pilot plant with HZSM-5 applied. They reported that palmitic acid yielded the most gas from cracking at 550 ℃ with 44 wt%, and that product aromaticity clearly increased with temperature. The research demonstrated the ability of HZSM-5 at cracking gas phase palmitic acid, in turn generating aromatic hydrocarbons, in the temperature range of 485 to 550 ℃.

A gap has been observed after a review of the literature. According to the literature review on hydrothermal processing on biomass, there are many existing technologies that can produce fatty acids in water. However, most of the previous related analysis is either hydrothermal liquefaction of biomass to produce bio-oil, or catalytic conversion of fatty acids without water present. The only study on fatty acids to specific chemicals in water condition is by Fu et al.[40], which is still focused on catalytic hydrothermal deoxygenation to yield the corresponding alkane as potential diesel fuel.

We are unable to find any prior work on catalytic cracking of fatty acids to chemicals with zeolite in a hydrothermal environment. At the same time, the literature review suggested that the key ideas of this proposed process are promising, and if it succeeded, it would be an alternate environmental process for chemical production. Therefore, we are motivated to conduct the experiments to fill in the gap between literature and our objective.

CHAPTER III

Experimental Methods

3.1 Materials

This section starts with providing information on all the reactants, which include pure fatty acids for the initial study, and also the biomass feedstock reactants for the subsequent study. It is followed by information on the catalyst applied in the catalytic hydrothermal process, as well as preparation and regeneration of catalyst before usage in reactions.

3.1.1 Fatty acids and Biomass Feedstocks

Palmitic acid (PA, C16:0), stearic acid (SA, C18:0), oleic acid(OA, C18:1), and linoleic acid (LA, C18:2) were acquired from ACROS Organics in high purity (98%). Palmitic acid and stearic acid were white powders at room temperature. Oleic acid and linoleic acid were obtained and maintained in liquid form.

Nannochloropsis algae samples were supplied by Valicor Renewables. The algae slurry contains 21 wt% solid and 78 wt% water. Coconut oil (cold pressed), peanut oil, and lard were purchased from a retail grocery store.

3.1.2 Preparation and Regeneration of Catalyst

The zeolites ZSM-5 (with silica/alumina = 23, 30, 50, and 80), beta (silica/alumina = 38, 300), and Y (silica/alumina = 60) were obtained from Zeolyst International as white powders. All of the ZSM-5 materials and the zeolite beta with silica/alumina of 38 came in ammonium nominal cation form. The other materials were obtained in hydrogen form. We converted all of the catalysts that were in ammonium form to the hydrogen form by a calcination process. For example, we calcined the fresh zeolite ZSM-5 in air at 550 ℃ for 240 minutes to convert it to the hydrogen form HZSM-5, which increases the acidity of the zeolite and thus facilitates the cracking reactions.[47]

Many times, we regenerate and reuse catalysts from the reaction. We regenerated catalysts that had been used in an experiment by first drying them in an oven at 70 ℃ overnight. Next, controlled combustion (heating at 2 ℃/min up to 550 ℃) was carried out in air to burn off any coke. The 550 ℃ temperature was then maintained for 240 min to calcine the catalyst, after which the material naturally cooled to room temperature.[43, 48]

3.2 Reaction Experiments

This section explains the detail of all the reaction experimental procedures involved in this work. First, we introduce the experimental procedures to make crude algal oil via hydrothermal carbonization with ethanol extraction. Second, we explain the proposed hydrothermal catalytic reaction method that is applied on both pure fatty acids and real feedstock.

3.2.1 Algal Oil Production Method

The method we used to make crude algal oil from algae slurry was hydrothermal carbonization, also commonly known as HTC. We loaded 14 g of algae slurry and 6 g DI water into a 30 mL stainless steel Swagelok batch reactor. We then placed the reactor in a preheated sandbath at 180℃ for 30 minutes. This condition was chosen to achieve a high conversion of algae to fatty acid-containing solids. [34] When the reaction was complete, we quenched the reactor in cold water, cooling it down to room temperature. Next, we shook the reactor before opening it, rinsed the products inside the reactor with DI water, and transferred everything into two centrifuge tubes. These centrifuge tubes were then placed on a vortex mixter for 3 minutes at 2500 rpm, and finally centrifuged for 5 minutes at 4000 rpm. After the centrifuge, we removed the upper water phase and saved the bottom solid phase, hydrochar, which was then dried in an oven overnight at 70℃.

The next day, the char was ground and transferred into a flat bottom round bottle containing 30 mL of anhydrous ethanol and a magnetic stir bar. We then capped the bottle and placed it on a preheated stirring plate at 60℃, 220 rpm for 90 minutes. The contents of the bottle were transferred to a centrifuge tube and centrifuged at 4000 rpm for 5 minutes. Afterwards, the upper phase (oil with ethanol) was transferred to a round rotavapor bottle, and the bottom solid phase (hydrochar) to a flat bottom round bottle. Again, 30 mL of anhydrous ethanol and a magnetic stir bar was added. The bottle was capped and placed a preheated stirring plate at 60℃, 220 rpm for another 90 minutes. Once more, we transferred everything to a centrifuge tube for centrifugation at 4000 rpm for 5 minutes. And again, the upper phase from the centrifugation was added to the previous round rotavapor bottle (oil with ethanol inside). This bottle was set up in a rotavapor for 63 rpm, 200 bar, for 30 minutes. The final product is the crude algal oil we used for catalytic hydrothermal reaction with zeolite.

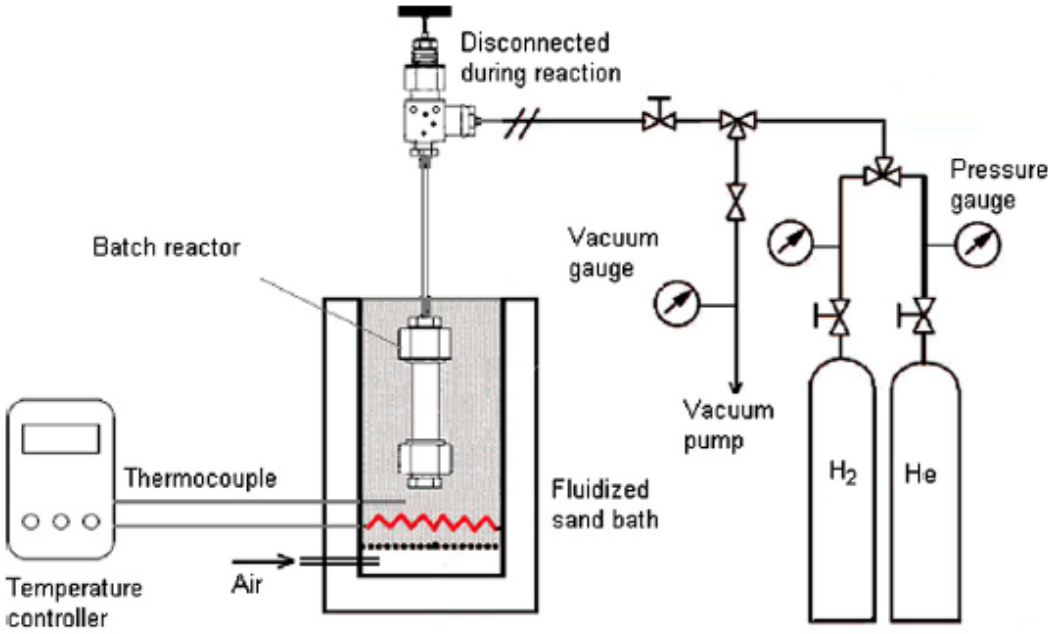

Figure 3.1: Schematic of apparatus and mini-batch stainless steel reactor for crude bio-oil upgrading
[36]

3.2.2 Hydrothermal Catalytic Reaction Method

Reactions were conducted in 4 mL 316-stainless steel Swagelok batch reactors with high-pressure valves that were connected by a length of 1/8 in. o.d. stainless steel tubing. Figure 3.1 shows the schematic of the reactor (not drawn to scale). Before their use in experiments, the reactors were loaded with water and seasoned at 400 ℃ for 240 minutes to remove any residual organic material from the reactors and to expose the fresh metal walls to high temperature water. After this conditioning process, potential catalytic reactor wall effects are likely reduced. Moreover, any small catalytic effect of the reactor walls should be the same in all runs and therefore not obscure the differences caused by added catalyst. [36]

In a typical reaction, a total of 150 mg of reactant (fatty acids, algal oil, coconut oil, peanut oil, and lard), 150 mg of precalcined catalyst zeolite (HZSM-5, beta, and HY) and the desired amount of water were loaded into each reactor. A different

amount of water loaded into a fixed volume reactor at a fixed temperature resulted in a different water density at the reaction condition, as well as a different reaction pressure.

For example, loading 0.6 mL of water leads to a water density of 0.15 g/mL and a pressure of 240 bar at 400 ℃. Loading 0.4 mL of water leads to a water density of 0.1 g/mL and a pressure of 200 bar at 400 ℃. The former condition exceeds the critical temperature and pressure of water, and the latter condition was in subcritical water state. Control reactions without water were also performed in some cases. Helium was added to each reactor at a pressure of 4 bar and was used as an internal standard for gas products analysis. In some cases, hydrogen was also added to the reactor. The sealed reactors were then attached to a wrist-action shaker and placed into an isothermal fluidized sand bath. The wrist-action shaker was used during the whole time of the reactions to improve the external mass transfer. The sand bath had been preheated to the desired reaction temperature, and reactions remained in the sandbath for the desired reaction time (from 20 minutes to 180 minutes). Upon removal from the sandbath, the reactors were submerged in a water bath at ambient temperature to quench the reaction.

3.3 Analysis of Algal Oil and Other Biomass Feedstocks

The fatty acid consituents of the different feedstocks were catalytically transesterified to fatty acid methyl esters (FAMEs) for quantitative analysis. About 50 mg sample was weighed into glass tubes and reacted with 2 mL of freshly prepared methanol (99%) containing 5% acetyl chloride as the acid catalyst. The reaction took place at 100 ℃ for 90 minutes with vigorous stirring. 1 mL of water was added into the glass tube after the reaction, and the FAMES were then extracted by 3 mL of n-heptane, which contains 250 mg/L tricosanoic methyl ester as an internal standard. The glass tubes were vortexed for 2 minutes, followed by centrifugation at 2000 rcf for

10 minutes. The upper phase from centrifugation was analyzed by an Agilent Model 7890A gas chromatograph with a flame ionization detector. FAMEs were identified by comparing with the C14-C24 standard FAME mix.

Calibration curves were created for quantification of FAMEs. The percentage of individual fatty acid methyl esters and their corresponding fatty acids were reported. The total fatty acids percentage in the oil or fat was also calculated and reported. We conducted replicates of runs, so standard deviation was used for the uncertainty of the data.

3.4 Sample Recovery and Analytically Procedure

This section provides information about procedures employed for getting maximum recovery of the material from the reactors and post-recovery analysis using different analytical techniques such as, gas chromatography with a mass spectrometric, thermal conductivity, or a flame ionization detector (GC-MS, GC-TCD, GC-FID).

3.4.1 Gas-phase Products Analysis

The gas products were collected and analyzed with a gas chromatograph (GC) with a thermal conductivity detector (GC/TCD) and argon as the carrier gas. A Carboxen column separated the light gases such as He, H2, CO, and C1 and C2 hydrocarbons, and a Porapak column separated the heavier gases including C3 to C5 hydrocarbons. Calibration curves were established by analyzing gas standards of known composition.

The temperature profile for the Carboxen column started at 35 ℃, increased to 225 ℃ at a rate of 20 ℃/min, and the oven then maintained 225 ℃ for 15 min, with a constant flow of argon at 15 mL/min. The temperature profile for the Porapak column started at 40 ℃ and increased to 225 ℃ at a rate of 10 ℃/min, with a constant flow of argon of 44 mL/min.

3.4.2 Liquid-phase Products Analysis

Upon completing the gas analysis, acetone was added to the reactor to recover the liquid- and solid-phase material from the reactor. The reactors were rinsed with repeated acetone washes until the total volume collected was 20 mL. The samples were transferred into a conical tube and then centrifuged at 4000 rpm for 10 minutes to facilitate recovery of the acetone-insoluble material (e.g., spent catalyst, coke). Liquid products referred to all the acetone-soluble products that were collected from the reactor after the reaction. The centrifugation separated the liquid and solid material from the reaction.

The liquid-phase products were identified and quantified using Agilent 6890 GCs with a mass spectrometric (GC/MS) and a flame ionization (GC/FID) detector. Helium served as the carrier gas. We used a nonpolar HP-5 (5% phenyl-methylpolysiloxane) capillary column. The quantification of acetic acid (one of the identified products) and palmitic acid was performed with an Agilent 7890 GC/FID with a high polarity DBFFAP column. Calibration curves of all the major identified liquid-phase products were made by analyzing various standards containing reaction products in known concentrations.

We injected 1 μL of the acetone-soluble sample into an inlet with a 50:1 split ratio. The oven temperatures were programmed to rise from 50 ℃ to 200 ℃ at a rate of 4 ℃/min and then rise further to 300 ℃ at a temperature ramp of 10 ℃/min.

Many experiments were replicated, and we report standard deviations as the experimental uncertainties in these cases. The reactions produced many products in yields too low to quantify reliably on an individual basis. Because the FID is a carbon counter, however, and because the products are primarily hydrocarbons, we used the total peak area of all of the products appearing in the GC/FID chromatogram to estimate the total mass of liquid-phase products as shown below (3.1). Molar yield and mass yield were both used in this work depending on the focus of the discussion.

Molar yields of reaction products were calculated as the number of moles of product formed divided by the number of moles of reactant loaded into the reactor. The mass yields were calculated as the mass of the individual or total product formed divided by the total mass of reactant loaded into the reactor. All cases, the conversion was calculated using the converted reactant mass divided by the total reactant mass loaded into the reactor.

$$\text{Total liquid product mass} = \frac{(\text{Total mass of quantified liquid products}) \times (\text{Sum of all GC/FID product peak areas})}{\text{Sum of all quantified liquid product peak areas}} \tag{3.1}$$

3.4.3 Solid-phase Material Analysis

The solid material (acetone-insoluble material from the centrifugation), was spent catalyst and coke generated from the hydrothermal reaction. The color of the solid material was observed and compared to the color of the fresh catalyst. The solid material was dried at 70 ℃ in an oven over night, and it was then oxidized in a tube furnace to remove the coke (carbon) to regenerate the catalyst. The procedures were given in section 3.1.2. We weighed the solid material before and after the regeneration process to calculate the weight difference, which was taken to be the mass of the coke generated from the reaction.

Spent catalyst was characterized by X-Ray Diffraction (XRD), Brunauer-Emmett-Teller (BET), and Barrett-Joyner-Halenda (BJH) surface analysis, and Scanning Electron Microscopy (SEM). The XRD experiments were carried out with Rigaku Rotating Anode X-Ray Diffractometer. The instrument is ageneral powder diffractometer with Pole figure attachment and scintillation counter detector. Nitrogen physisorption was carried out at liquid nitrogen temperature on a Micromeritics ASAP 2020 instrument for the characterization of BET specific surface area and pore volume. the

degassing pretreatment of the sample was 24 hours. Before the sample is analyzed, it was outgassed at 350 ℃ at about 3 mm Hg. Nitrogen physisorption was carried out at 77 K to obtain the isotherm. The relative pressures (P/P_0) were smaller than 0.30. SEM experiments were carried out using Philips XL30 FEG SEM, the accelerating voltage was 10 kV. The probe current or SPOT size was 6 A (amps), which is the total amount of current to be irradiated on the specimen. The control is done by varying the excitation of the SEM's condenser lens.

CHAPTER IV

Reaction Products and Kinetics

This chapter first presents results from control experiments that were performed to validate the experimental methods and determine the extent of chemical transformation from thermal energy alone. We next report the identities of the products (both gas and liquid-phase products) generated from the catalytic hydrothermal reactions of pure fatty acid, followed by showing the individual yields of the major liquid products, and the total yield of gas and liquid products combined. This chapter concludes with discussion of reaction kinetics.

4.1 Control Experiments

We completed two types of control experiments. The first involved loading PA, water, and HZSM-5 into reactors but not heating them. These experiments showed no detectable products, and an average PA recovery of 97 $\pm$ 4%. We expect SA, OA, and LA to give similar results as the amount of acetone (solvent) needed to dissolve the 150 mg of SA, OA, and LA loaded into the reactors is about two orders of magnitude lower than the 20 mL used experimentally. These calculations are based on the reported solubilities of SA, OA, and LA in acetone. [49, 50]

The second type of control experiments involved loading fatty acids and water into reactors (no HZSM-5) and placing them in the sandbath for 180 minutes at 400

℃. The average PA recovery was 66 ± 5%. The conversion was 34 ± 5%. The total liquid product yield was 12 ± 5 wt %. The most abundant products were xylenes, toluene, 2-methylpentane, and 2-methylhexane. The total gas product yield was 4 wt %, and the mass balance was 82%. The missing mass was presumably in the form of acetone-insolubles that were not quantified. Overall, the results indicated that no detectable amounts of products were generated without the elevated temperature, and that thermal cracking of PA could be responsible for no more than 12 wt % liquid product yield at 400 ℃ and 180 minutes, the most severe conditions examined in this investigation.

Besides palmitic acid (PA, C16:0), control runs were also performed with stearic acid (SA, C18:0), oleic acid(OA, C18:1), and linoleic acid (LA, C18:2). Gas yields were less than 4 wt%. The total yield of liquid products(acetone solubles) from SA, OA, and LA were 7 ± 2 wt%, 19 ± 12 wt%, and 41 ± 5 wt% respectively. Xylenes, toluene, and 2-methyl-pentane were the major products. The conversions were 54 ± 8%, 22 ± 11%, and 80 ± 18%, respectively.

These results above showed that non-zeolitic cracking could be responsible for up to only 12 wt% liquid product yield from the saturated fatty acids (PA and SA) at 400 ℃, 24 MPa, and 180 minutes. However, non-zeolitic cracking could be responsible for about 19 wt% and 41 wt% liquid products for the two unsaturated fatty acids (OA and LA). The higher conversion and product yields from the unsaturated fatty acids are reasonable since the presence of unsaturation would be expected to increase the thermal reactivity in general. It was also observed by Shin et al.[51], that unsaturated fatty acids have lower thermal stability in water near critical point.

4.2 Reaction Products

Figure 4.1 shows a representative total ion chromatogram for the reaction products appearing from HZSM-5-catalyzed palmitic acid cracking in supercritical wa-

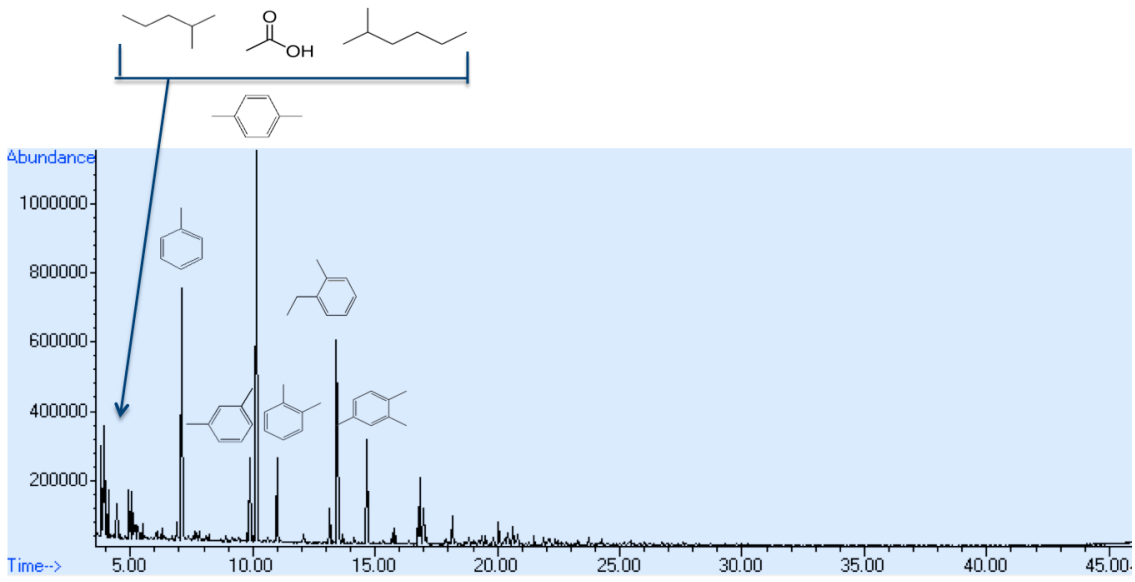

Figure 4.1: Identification of major liquid products, reaction condition: PA with HZSM-5 (PA/cat.=1), at 400 ℃, 24 MPa, 180 minutes.

ter. The major products were the aromatic compounds toluene, 1,4-dimethylbenzene (p-xylene), 1-ethyl-2-methyl-benzene, and 1,2,4-trimethylbenzene. The other xylene isomers and propylbenzene were also present. Toluene, p-xylene, 1-ethyl-2-methyl-benzene, and 1,2,4-trimethylbenzene were major products from cracking oleic acid at 400 ℃ with HZSM-5, but without water.[24] Thus, it appears that the presence of water in the present hydrothermal conversion experiments did not affect the types of major products generated from cracking fatty acids.

Some of the aromatic hydrocarbons in the product mixture are chemicals produced in very large volumes worldwide, often by the catalytic reforming of naphtha in a petroleum refinery. They have various uses in the chemical industry. For example, p-xylene is a precursor of terephthalic acid, which is a monomer used to make polyethylene terephthalate, a plastic widely used in the production of fibers and beverage bottles.

In addition to the aromatic products, 2-methyl-pentane, butanal, acetic acid, 2-methyl-hexane, 2-pentanone, heptane, and 4-methyl-heptane are also reaction prod-

ucts. The alkanes can be used as a fuel, and heptane is a raw material for manufacture of paints and coatings. Acetic acid is a key reactant in producing vinyl acetate monomer.

The gaseous products from cracking PA at 400 ℃ with HZSM-5 were C1 to C5 alkanes, CO, CO_2, and H_2. This product slate is largely consistent with previous reports on fatty acid cracking with zeolites (though not in water).[24, 25] The hydrocarbon gases are useful as a fuel in a biorefinery, and they also have uses as chemical feedstocks. Methane is a feedstock for producing hydrogen via steam reforming. Ethane is used in producing hydrogen and ethylene. n- and i-Butane can be blended as components of gasoline to give it a more desirable vapor pressure.[52] It is clear that hydrothermal catalytic conversion of palmitic acid over HZSM-5 produces molecules that are useful as chemicals and as components in liquid transportation fuels.

4.3 Quantification of Reaction Products

For a reaction of 150 mg palmitic acid with 150 mg HZSM-5 with water at 400 ℃ for 180 minutes, the quantifiable liquid products were 2-methyl-pentane, butanal, 2-methyl-hexane, 2-pentanone, heptane, 4-methyl-heptane, toluene, p-xylene, m-xylene, o-xylene, propyl-benzene, 2-ethyl-toluene, 1,2,4-trimethyl-benzene, and acetic acid. There were many products in yields too low to quantify reliably on an individual basis, which were considered as minor liquid products and were not reported individually. Figure 4.2 is a pie chart that shows the distribution of quantified liquid products in weight percentage for this reaction.

Mixed xylenes (includes p, m, o- xylene) were the most abundant liquid product at 50 wt% of all the quantified liquid products, followed by toluene (19.4 wt%), acetic acid (6.2 wt%), 2-methyl-pentane (5.2 wt%), and some significant amount of other aromatics, such as propyl-benzene (3.9 wt%), 2-ethyl-toluene (4.2 wt%), and 1,2,4-

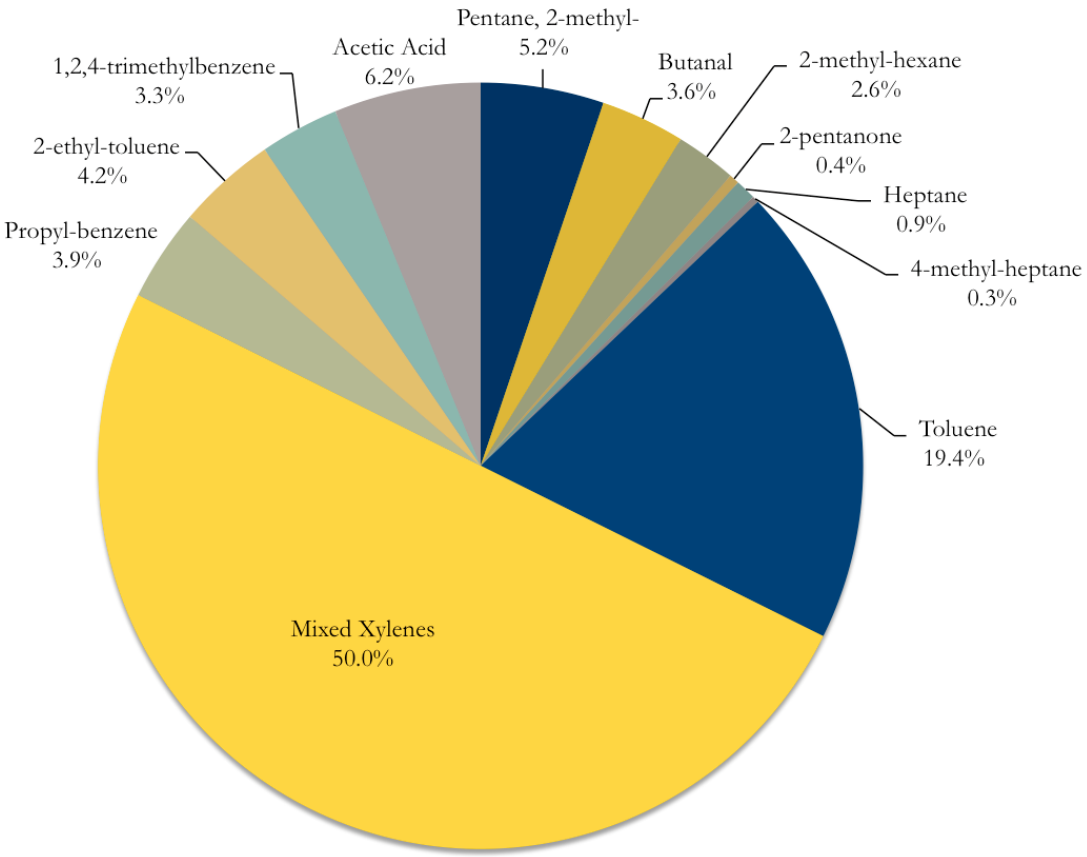

Figure 4.2: Distribution of quantified liquid products in wt%, reaction condition: PA with HZSM-5 (PA/cat.=1), at 400 ℃, 24 MPa, 180 minutes.

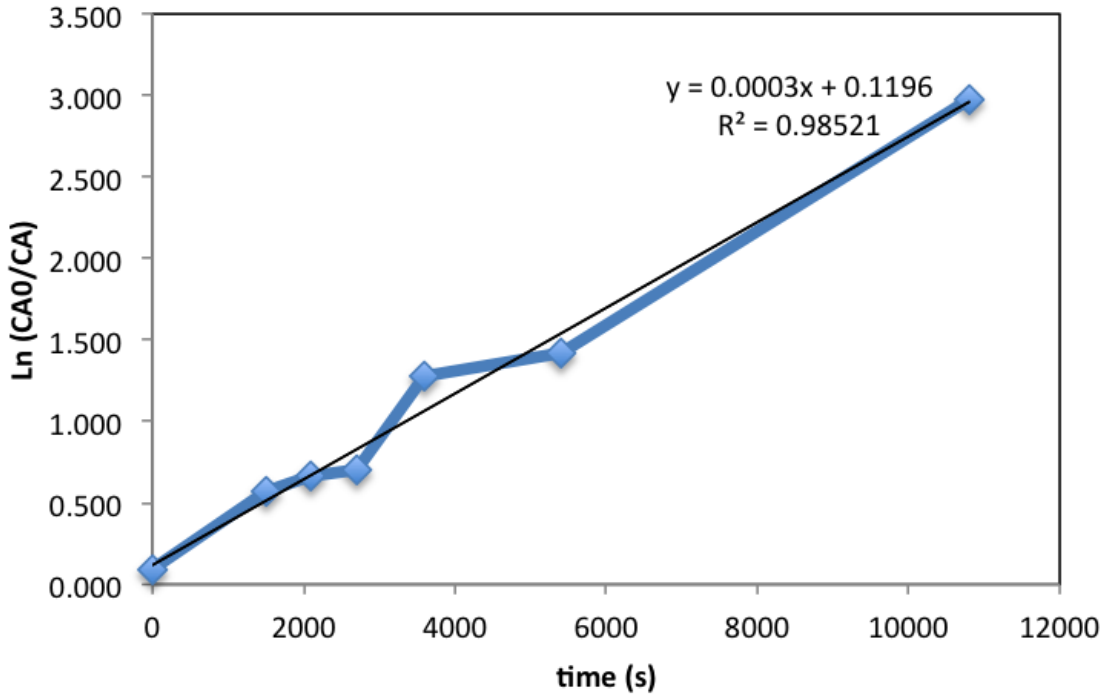

Figure 4.3: First order correlation, reaction condition: 150 mg of PA with 150 mg of HZSM-5 with water, at 400 ℃, 24 MPa

trimethyl-benzene (3.3 wt%).

4.4 Reaction Kinetics for Palmitic Acid

Figure 4.3 shows the natural log of the ratio of initial concentration of palmitic acid to the concentration of palmitic acid at different reaction time v.s. reaction time for experiments of 400 ℃. For a first-order reaction, the plot is linear.

The data at 400 ℃ are consistent with first-order kinetics, and the rate constant was $2.6 * 10^{-4} s^{-1} \pm 3.8 * 10^{-6} s^{-1}$. Using conversions measured at 180 minutes, we calculated that the rate constants at 200 and 300 ℃ are $2.6 * 10^{-5} s^{-1}$ and $6.9 * 10^{-5} s^{-1}$, respectively. The activation energy for PA disappearance was then determined to be 31 ± 1 kJ/mol. The Arrhenius pre-exponential factor was $5.6 * 10^{-2} \pm 2.2 * 10^{-3} s^{-1}$ or $1.5 * 10^{-3} \pm 5.9 * 10^{-5} L * gcat^{-1} s^{-1}$.

4.5 Possible Reaction Pathways Based on Product Analysis

Palmitic acid is a C16 fatty acid. It must undergo cracking to form fuel gases and short chain alkanes, such as 2-methyl-pentane, 2-methyl-hexane, heptane, and 4-methyl-heptane. Since not all of these products were formed in the thermal cracking of palmitic acid (control runs), we believe zeolite catalytic cracking of palmitic acid was the process that generated those products. Catalytic cracking is used to convert higher molecular weight hydrocarbons to lighter but more valuable products through contact with a powdered catalyst (traditionally zeolite) at high temperatures (510 to 550 ℃ for FCC (Fluid Catalytic Cracking) and 760 to 870 ℃ for SC (Steam Cracking)). Equations below show examples of catalytic cracking of ethane to ethene and hydrogen, and dodecane to hexane, ethene, and butene. We observed $C_2H_6, C_2H_4, and\ H_2$ generated from the reaction, so it is possible that eqn 4.1 occurred in the process, while some process similar to eqn 4.2 must have happened too, but we don't have enough evidence to confirm the exact reactions.

$$C_2H_6 \rightarrow C_2H_4 + H_2 \tag{4.1}$$

$$C_{12}H_{26} \rightarrow C_6H_{14} + C_2H_4 + C_4H_8 \tag{4.2}$$

Toluene, 1,2,3-trimethyl-benzene, and p,m,o-xylenes were all present in our liquid phase products, the transalkylation reaction, which is often performed over zeolite [53], should also took place under the reaction condition we tested. The illustration of this reaction is in Figure 4.4.

Decarboxylation and decarbonylation may also occurred under the reaction conditions based on the observation of carbon dioxide and carbon monoxide as products, especially with the most abundant gas product as carbon dioxide at all various reaction conditions. Palmitic acid must undergo a decarboxylation reaction which

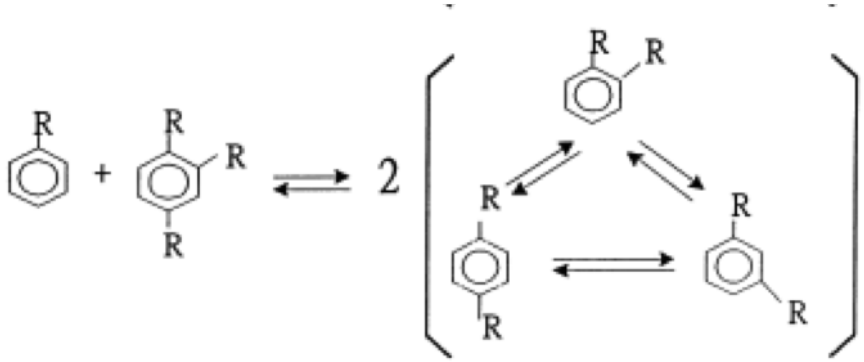

Figure 4.4: Transalkylation from toluene and 1,2,4-trimethyl-benzene to mixed xylenes

[54]

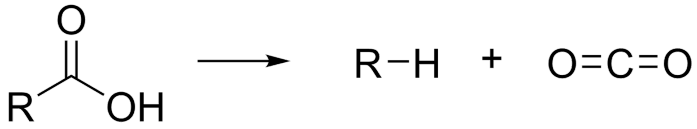

Figure 4.5: Decarboxylation reaction of a carboxylic acid

removed its carboxylic group and released carbon dioxide, as shown in Figure 4.5, with R as $C_{15}H_{31}-$ group.

$C_{15}H_{32}$ alkane, however, was not detected as a product in our reaction of palmitic acid at 400 ℃ and 180 minutes. It is very possible that $C_{15}H_{32}$ alkane underwent a catalytic cracking similar to the reaction in eqn 4.2.

CHAPTER V

Effect of Process Variables

This chapter first discusses the results from experiments with palmitic acid in water with zeolite HZSM-5 conducted at different reaction time and temperature. Some other process variables that were studied include water density and addition of hydrogen in the system. The effect of different types of catalyst, effect of reactant-to-catalyst loading, and effect of degree of saturation of fatty acids on the products were also elucidated in this chapter.

5.1 Effect of Time and Temperature

We conducted experiments at 400 ℃ and several different reaction times to explore the influence of this process variable on the product yields. We also did experiments for 180 minutes at 200, 300, and 400 ℃ to explore the effect of temperature on this hydrothermal catalytic conversion. Table 5.1 (Runs 1 - 6) lists the molar yields of the identified products from the reaction at 400 ℃ and at the different batch holding times explored. In Table 5.1, NA indicates "not applied", which means these were not measured. ND indicates "not detected", which means they were not able to be detected reliably by the equipment we used. There is uncertainty in time in the data because it takes some time (about one minute) for the batch reactor to heat up and cool down.

The most abundant products at short times were 2-methyl-pentane, butanal, 2-ethyltoluene, toluene, and mixed xylenes. The molar yields of 2-methyl-pentane and butanal reached maxima at 60 and 90 minutes, respectively, and then decreased. The change in yield of 2-ethyltoluene with time is less than the experimental uncertainty, so we consider this yield to be essentially time invariant. In contrast, the yields of toluene and xylenes, as shown in Figure 5.1, increased steadily with reaction time, and they are the major products from the reactions. Acetic acid is below detection limits through 45 minutes, but its molar yield increases to be greater than 10% at 180 minutes. The conversion of palmitic acid increased with reaction time and reached 95% at 180 minutes as shown in Figure 5.2 and meanwhile the total liquid product yield reached 59 wt% at 180 minutes.

Figure 5.1 and Figure 5.2 show a shared trend of a possible induction period at short reaction times. This kind of induction period was found by other researchers as well. For example, Riekett and Zhou noticed an induction period when cracking n-decane and n-hexane using zeolite HZSM-5. They suggested that the induction period can be suppressed by addition of olefin, and they confirmed this by adding propene, n-butene, and n-hexene to n-decane. One possible explanation for this observation is that olefin can serve as autocatalytic agent in this type of reaction. As indicated in Figure 5.2, we stopped the reaction at 180 minutes and did not carry out reactions at longer times, because the PA conversion was very close to 100% (i.e. 95%) at 180 minutes already.

The final row in Table 5.1 shows the overall mass balance for the two reaction times (60 and 180 minutes) at 400 ℃ where gas products were quantified. The mass balance is 81 ± 11% for the 180 min reaction and 78 ± 8% for the 60 minutes reaction. One possible contributor to the incomplete mass balance is the generation of coke during the reaction, which is common during hydrocarbon processing with zeolites.[55] Coke formation during these experiments seems likely given the color change observed for

Table 5.1: Molar yields of major products from palmitic acid cracking over HZSM-5 at different reaction times, temperature, and water density

Run Number	1	2	3	4	5	6	7	8	9	10	11
Reaction Temperature (°C)	400	400	400	400	400	400	400	400	400	300	200
Reaction Time (min)	25	35	45	60	90	180	180	180	180	180	180
Water loading (mL)	0.6	0.6	0.6	0.6	0.6	0.6	0.4	0.2	0	0.6	0.6
auto generated pressure (bar)	240	240	240	240	240	240	200	125	NA	86	15
Water density (g/mL)	0.15	0.15	0.15	0.15	0.15	0.15	0.1	0.05	0	NA	NA
Product yield (mol/mol PA)											
2-methyl-pentane	0.023 ± 0.016	0.040 ± 0.038	0.068 ± 0.027	0.078 ± 0.032	0.11 ± 0.02	0.062 ± 0.053	0.047 ± 0.008	0.028 ± 0.009	ND	ND	ND
Butanal	0.019 ± 0.006	0.029 ± 0.014	0.017 ± 0.006	0.056 ± 0.025	0.037 ± 0.003	0.051 ± 0.022	0.032 ± 0.004	0.015 ± 0.008	0.0045 ± 0.0063	0.0023	ND
2-methyl-hexane	0.0045 ± 0.0089	0.020 ± 0.014	0.016 ± 0.011	0.020 ± 0.002	0.042 ± 0.010	0.026 ± 0.008	0.025 ± 0.008	0.0030 ± 0.0059	ND	ND	ND
2-pentanone	0.0098 ± 0.0048	0.014 ± 0.005	0.014 ± 0.003	0.0096 ± 0.0074	0.020 ± 0.009	0.0052 ± 0.0021	0.012 ± 0.003	0.028 ± 0.007	0.092 ± 0.072	ND	ND
Heptane	0.0055 ± 0.0042	0.0089 ± 0.0050	0.011 ± 0.003	0.016 ± 0.017	0.015 ± 0.013	0.0089 ± 0.0023	0.012 ± 0.005	0.0049 ± 0.0057	ND	ND	ND
4-methyl-heptane	0.0012 ± 0.0024	0.0049 ± 0.0030	0.0063 ± 0.0012	0.0041 ± 0.0028	0.0048 ± 0.0002	0.0025 ± 0.0028	0.0036 ± 0.0033	ND	ND	ND	ND
Toluene	0.090 ± 0.023	0.093 ± 0.050	0.082 ± 0.031	0.11 ± 0.05	0.187 ± 0.003	0.22 ± 0.03	0.36 ± 0.03	0.47 ± 0.05	0.53 ± 0.06	ND	ND
Xylene	0.25 ± 0.07	0.29 ± 0.14	0.29 ± 0.12	0.28 ± 0.02	0.44 ± 0.04	0.49 ± 0.08	0.68 ± 0.09	0.71 ± 0.09	0.62 ± 0.08	0.03	0.069
Propyl-benzene	0.011 ± 0.007	0.010 ± 0.007	0.0068 ± 0.008	0.015 ± 0.013	0.0170 ± 0.0001	0.034 ± 0.030	0.10 ± 0.02	0.076 ± 0.021	0.029 ± 0.002	ND	ND
2-ethyl-toluene	0.024 ± 0.010	0.029 ± 0.014	0.030 ± 0.018	0.025 ± 0.009	0.028 ± 0.004	0.036 ± 0.012	0.024 ± 0.006	0.023 ± 0.004	0.011 ± 0.002	ND	ND
1,2,4-trimethylbenzene	0.011 ± 0.008	0.015 ± 0.009	0.015 ± 0.012	0.018 ± 0.004	0.0302 ± 0.0006	0.029 ± 0.008	0.045 ± 0.006	0.050 ± 0.008	0.050 ± 0.010	ND	ND
Acetic Acid	ND	ND	ND	0.015 ± 0.027	0.0016 ± 0.0002	0.11 ± 0.04	0.043 ± 0.034	0.023 ± 0.005	0.0028 ± 0.0001	0.00073	ND
H_2	NA	NA	NA	0.013 ± 0.016	NA	0.085 ± 0.023	0.073 ± 0.016	0.063 ± 0.013	0.16 ± 0.01	NA	NA
CO	NA	NA	NA	0.14 ± 0.04	NA	0.126 ± 0.005	0.14 ± 0.08	0.14 ± 0.02	0.182 ± 0.003	NA	NA
CH_4	NA	NA	NA	0.038 ± 0.025	NA	0.020 ± 0.010	0.027 ± 0.003	0.038 ± 0.031	0.37 ± 0.08	NA	NA
CO_2	NA	NA	NA	0.23 ± 0.09	NA	0.30 ± 0.07	0.47± 0.16	0.37 ± 0.04	0.210 ± 0.001	NA	NA
C_2H_4	NA	NA	NA	0.0032 ± 0.0046	NA	0.090 ± 0.015	0.042 ± 0.049	0.10 ± 0.08	0.45 ± 0.23	NA	NA
C_2H_6	NA	NA	NA	0.021 ± 0.015	NA	0.0155 ± 0.0006	0.025 ± 0.006	0.044 ± 0.027	0.39 ± 0.08	NA	NA
C_3H_8	NA	NA	NA	0.24 ± 0.15	NA	0.13 ± 0.03	0.21 ± 0.06	0.27 ± 0.22	0.80 ± 0.10	NA	NA
n-C_4H_{10}	NA	NA	NA	0.25 ± 0.16	NA	0.10 ± 0.04	0.13 ± 0.06	0.097 ± 0.039	0.068 ± 0.013	NA	NA
i-C_4H_{10}	NA	NA	NA	0.10 ± 0.04	NA	0.051 ± 0.025	0.068 ± 0.037	0.060 ± 0.039	0.062 ± 0.008	NA	NA
C_5H_{12}	NA	NA	NA	0.050 ± 0.044	NA	0.037 ± 0.020	0.034 ± 0.023	0.025 ± 0.015	ND	NA	NA
Total liquid products (mg/mg PA)	0.31 ± 0.13	0.41 ± 0.19	0.40 ± 0.15	0.39 ± 0.03	0.57 ± 0.06	0.59 ± 0.12	0.73 ± 0.09	0.71 ± 0.08	0.65 ± 0.04	0.038	0.049
Total gas products (mg/mg PA)	NA	NA	NA	0.11 ± 0.01	NA	0.16 ± 0.04	0.20 ± 0.02	0.22 ± 0.07	0.34 ± 0.03	NA	NA
Total yield (wt%)	NA	NA	NA	50 ± 5.5	NA	76 ± 13	92 ± 7.7	93 ± 6.5	99 ± 7.0	NA	NA
PA conversion (%)	43	49	50	72 ± 13	76	95 ± 4.0	97 ± 1.8	99 ± 0.21	99 ± 0.03	52	25
Mass Balance (wt%)	NA	NA	NA	78 ± 7.6	NA	81 ± 11	95 ± 9.5	94 ± 6.7	99 ± 7.0	NA	NA

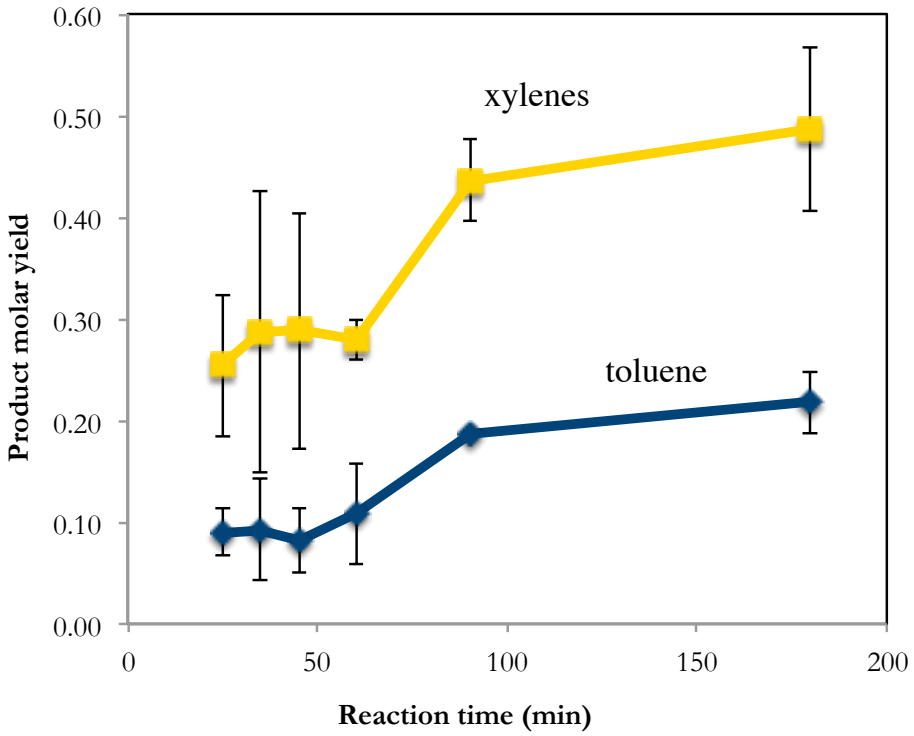

Figure 5.1: Temporal variation of toluene and xylenes molar yields, reaction condition: PA with HZSM-5 (PA/cat.=1), at 400 ℃, 24 MPa.

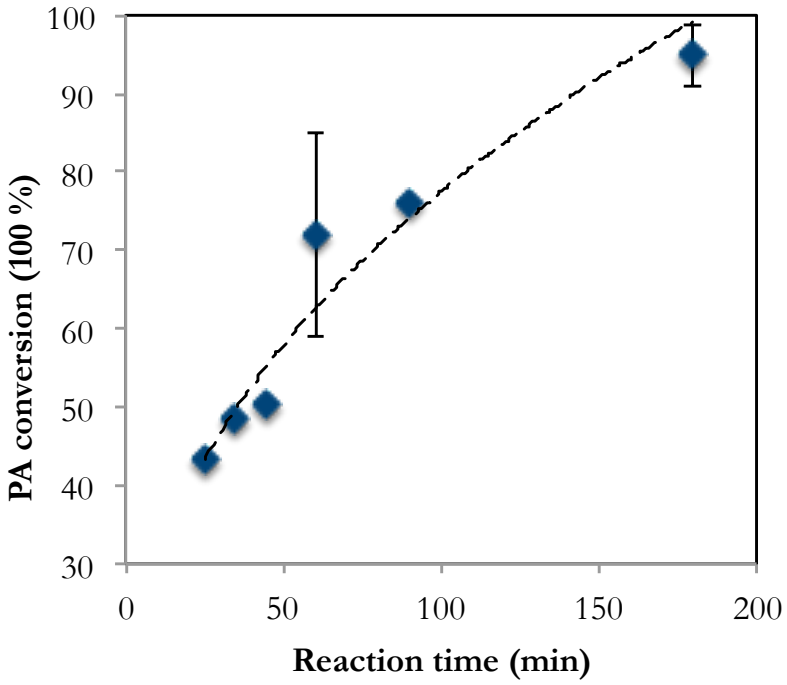

Figure 5.2: Temporal variation of PA conversion, reaction condition: PA with HZSM-5 (PA/cat.=1), at 400 ℃, 24 MPa.

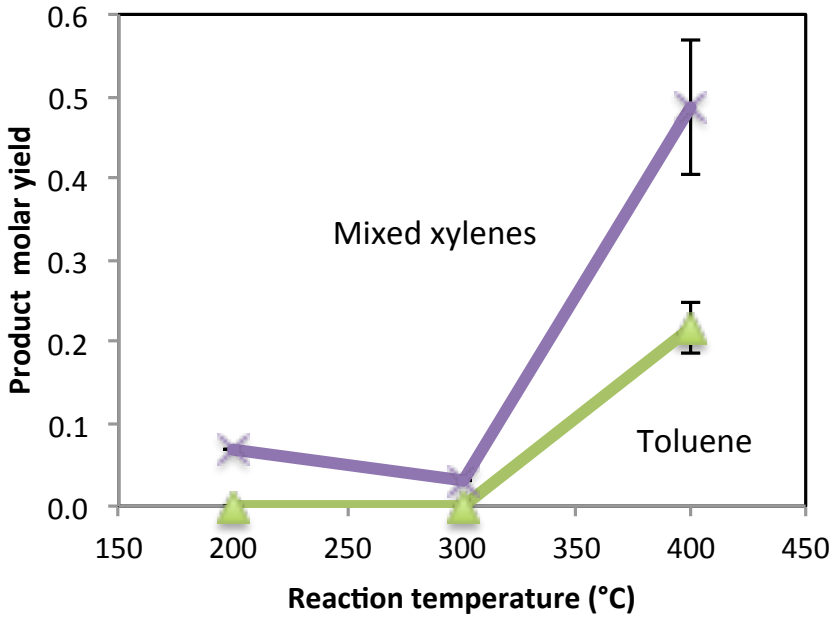

Figure 5.3: Temperature variation of toluene and xylenes molar yields, reaction condition: PA with HZSM-5 (PA/cat.=1), 180 minutes, with 0.6 mL water in 4 mL reactor.

the catalyst after each experiment. The catalyst recovered from the runs at short times, such as 25 and 35 minutes, retained its original white color. The catalysts recovered from runs at 45, 60, and 90 minutes were different shades of gray. The color turned into a darker gray for the 180 minutes reactions. It is likely that the amount of coke increased with increasing reaction time and that these higher coke contents corresponded to the increasingly dark color of the remaining solids.

Next, we fixed the batch holding time at 180 minutes, and changed the reaction temperature from 200 to 400 ℃. Reactions at 200 and 300 ℃ were in subcritical water state, while the reactions at 400 ℃ were in supercritical water state. Figure 5.3 shows the major liquid product yields (i.e. toluene and mixed xylenes) at different reaction temperatures. Runs 6, 10, and 11 in Table 5.1 show the detailed results of the effect of temperature on the product yields for a 180 minute batch holding time. With the same water loading of 0.6 mL in a 4 mL reactor, reaction conditions with 400 ℃ and

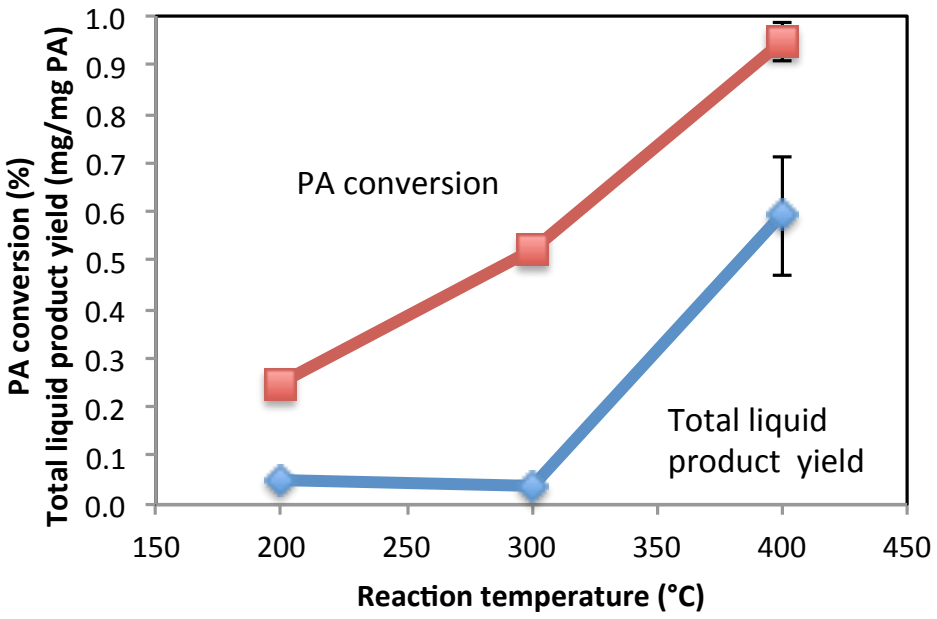

Figure 5.4: Temperature variation of PA conversion and total liquid product yield, reaction condition: PA with HZSM-5 (PA/cat.=1), 180 minutes, with 0.6 mL water in 4 mL reactor.

180 minutes gave the best results regarding with total liquid product yields and total product yield, which were 59 wt% and 76 wt%, respectively.

Figure 5.4 indicated that the PA conversion increased with increasing reaction temperature. The total liquid product yields were about the same at reaction temperature 200 and 300 ℃, while it significantly increased from 300 ℃ to 400 ℃. The PA conversion at 200 ℃ was only 25%, and mixed xylenes were the only products present in sufficiently high yield to quantify. At 300 ℃, the conversion was 52%, and some oxygenates appeared along with xylenes. At 400 ℃, the PA conversion was 97% and the complete product slate was illustrated in Figure 4.1 in Chapter 4. These results indicate that a reaction temperature around 400 ℃ is required to generate appreciable product yields from the hydrothermal catalytic cracking of palmitic acid over HZSM-5.

5.2 Effect of Water Density

The literature indicates that the water density can influence reaction rates and product selectivities for reactions at supercritical temperatures.[56, 57] Therefore, we desired to discover the effect of the water density on this reaction system.

A different amount of water loaded into the reactor at room temperature at a fixed reaction temperature, generated a different reaction pressure, and thus gave a different density of water during the reaction. Table 5.2 indicates the relationship between the amount of water loaded into the reactor with its reaction pressure, and the water density. The reaction condition with water density of 0.15 g/mL was in supercritical water region, and the reaction conditions with water density of 0.1 g/mL and 0.05 g/mL were in the subcritical pressure region.

Runs 6 to 8 in Table 5.1 show the product yields obtained from experiments at 400 ℃ and 180 minutes with water densities of 0.15, 0.10, and 0.05 g/mL. In the absence of water (run 9), aromatics dominate the product spectrum, with toluene

Table 5.2: Relationship between amount of water loaded into the reactor and water density

amount of water loaded into the reactor	temperature	auto generated pressure	water density
0.2 g	400 °C	125 bar	0.05 g/mL
0.4 g	400 °C	200 bar	0.1 g/mL
0.6 g	400 °C	240 bar	0.15 g/mL

and xylenes being the major products. Only one non-aromatic liquid-phase product, 2-pentanone, is present in a molar yield exceeding 1%. Hydrocarbons dominate the gaseous products, as the yield of each C1 to C3 hydrocarbon exceeds that of CO or CO_2. The palmitic acid conversion is essentially complete and about one-third of the initial mass appears as gaseous products, while the balance forms liquid-phase products.

Figure 5.5 shows the effect of water density on total liquid product yield, and the major product yields (i.e. mixed xylenes and toluene), where the red line separates the subcritical pressure region (to the left of the line) and the supercritical water region (to the right of the line). The total liquid product achieved a maximum yield at a water density of 0.1 g/mL.

The yields of the various products respond differently to the presence of water and to its density. The yield of acetic acid, for example, increases nearly 50-fold as the water density increased from zero to 0.15 g/mL. Other products showing consistently increasing yields (though less dramatic than acetic acid) with increasing water density include 2-methyl-pentane, butanal, 2-methyl hexane, 2-ethyl toluene, and pentane. In contrast to the behavior of the products just listed, the yields of other products either consistently decrease with increasing water density or exhibit a maximum yield at some intermediate density. Toluene, trimethyl-benzene, 2-pentanone, CO, methane, ethane, and propane are examples of the former, and heptane, 4-methyl-heptane, xylenes, and propyl benzene, butanes, and CO_2 are examples of the latter.

As shown in Table 5.1, methane, ethylene, ethane, and propane form in much

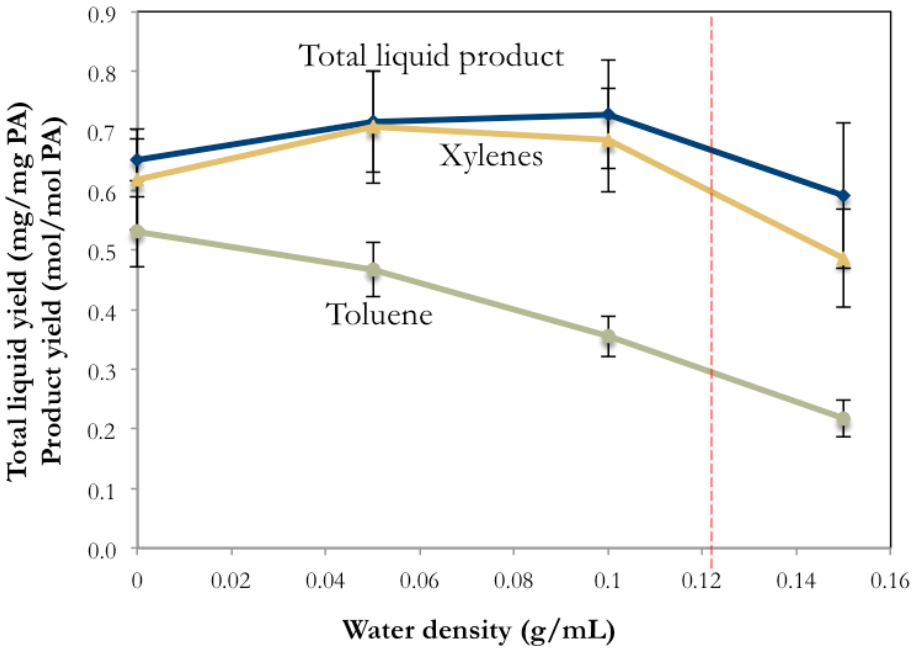

Figure 5.5: Effect of water density on total product yield and yields of xylenes and toluene, reaction condition: 150 mg PA with 150 mg HZSM-5, 400℃, 180 minutes (the red line separates the subcritical pressure region and the supercritical water region)

higher yields when there is no water in the reactor (run 9). In contrast, the yields of i- and n-butane and n-pentane are about the same (given the experimental uncertainties) with or without water. The presence of water reduces the yield of carbon monoxide and increases the yield of carbon dioxide. This outcome is consistent with the water gas shift reaction converting some of the CO produced into CO_2 demonstrated in eqn 5.1. The water gas shift reaction was believed involved in the gas production pathways in catalytic upgrading of microalgae in water by Duan and Savage.[36] HZSM-5 is not necessarily a good water gas shift catalyst, but this reaction can occur readily in supercritical water even in the absence of a catalyst.[58]

$$CO + H_2O \rightarrow CO_2 + H_2 \tag{5.1}$$

The reason(s) for these changes in product selectivity with changing water density is not clear at present, but it is clear that the water density can be used as a process

variable to direct the system to favor one product over another.

5.3 Effect of Hydrogen

Hydrogen is often used with zeolite Y or zeolite Beta (with or without metal) for hydrocracking reactions.[59] There is also precedent for using hydrogen to facilitate cracking reactions with HZSM-5.[60] More recently, high-pressure hydrogen was used with a zeolite catalyst for upgrading algal bio-oil, which contains a significant amount of fatty acids.[28, 36] Therefore, we deemed it relevant to determine the effect of added hydrogen on hydrothermal treatment of fatty acids with HZSM-5. We conducted experiments both with and without hydrogen but at otherwise identical reaction conditions. We added 4, 25, and 50 bar (at room temperature) of hydrogen pressure to the reactor, which results in mole ratios of hydrogen to palmitic acid of roughly 0.5:1, 3:1, and 6:1, respectively.

Table 5.3 shows all of the product yields, PA conversions, and mass balances, and Figure 5.6 displays selected results. The PA conversion, yields of the major products, and total yields of liquid and gas products were largely insensitive to the H_2 loading for H_2 pressures up to 25 bar. When the hydrogen loading increased from 25 to 50 bar, however, the total liquid product yield dropped from 73 to 50 wt %, while the total gas product yield climbed from 12 to 23 wt %. The yields of ethane, propane, butanes, and pentane more than doubled. On the other hand, the yields of toluene and xylenes decreased noticeably. The absence of ethylene at the highest H_2 pressure is consistent with it being more readily hydrogenated as more hydrogen is added to the system. Likewise, the reduced yields of aromatics are consistent with the additional hydrogen making the dehydrocyclization reactions more difficult. These results show that moderate hydrogen pressures do not adversely impact the total product yields but they do shift the product distribution to more gaseous products.

After the study of various levels of hydrogen pressure, we decided not to apply

Table 5.3: Effect of hydrogen on product molar yields, reaction condition: 150 mg PA with 150 mg HZSM-5, 0.15 g/mL water density, 400 ℃, 180 minutes

Product molar yield (mol/mol PA)	No hydrogen	4 bar hydrogen	25 bar hydrogen	50 bar hydrogen
2-methyl-pentane	0.062 ± 0.053	0.16 ± 0.02	0.16 ± 0.03	0.17 ± 0.02
Butanal	0.051 ± 0.022	0.051 ± 0.004	0.042 ± 0.006	0.039 ± 0.002
2-methyl-hexane	0.026 ± 0.008	0.045 ± 0.009	0.037 ± 0.011	0.039 ± 0.005
2-pentanone	0.0052 ± 0.0021	0.0119 ± 0.0008	0.0069 ± 0.0006	0.0063 ± 0.0003
Heptane	0.0089 ± 0.0023	0.03384 ± 0.00004	0.011 ± 0.001	0.01118 ± 0.00004
4-methyl-heptane	0.0025 ± 0.0028	0.0055 ± 0.0001	0.0055 ± 0.0006	0.0029 ± 0.0025
Toluene	0.22 ± 0.03	0.23 ± 0.02	0.22 ± 0.04	0.18 ± 0.03
Xylene	0.49 ± 0.08	0.47 ± 0.03	0.52 ± 0.07	0.34 ± 0.07
Propyl-benzene	0.034 ± 0.030	0.0191 ± 0.0004	0.019 ± 0.002	0.013 ± 0.002
2-ethyl-toluene	0.036 ± 0.012	0.046 ± 0.002	0.044 ± 0.004	0.027 ± 0.005
1,2,4-trimethylbenzene	0.029 ± 0.008	0.040 ± 0.001	0.034 ± 0.006	0.028 ± 0.002
Acetic Acid	0.11 ± 0.04	0.11 ± 0.01	0.14 ± 0.04	0.074 ± 0.004
CO	0.126 ± 0.005	NA	0.012 ± 0.016	0.087 ± 0.027
CH_4	0.020 ± 0.010	NA	0.060 ± 0.079	0.063 ± 0.021
CO_2	0.30 ± 0.07	NA	0.16 ± 0.09	0.100± 0.006
C_2H_4	0.090 ± 0.015	NA	0.0022 ± 0.0032	ND
C_2H_6	0.0155 ± 0.0006	NA	0.012 ± 0.005	0.041 ± 0.015
C_3H_8	0.13 ± 0.03	NA	0.17 ± 0.04	0.31 ± 0.03
n-C_4H_{10}	0.10 ± 0.04	NA	0.13 ± 0.02	0.33 ± 0.01
i-C_4H_{10}	0.051 ± 0.025	NA	0.059 ± 0.008	0.13 ± 0.01
C_5H_{12}	0.037 ± 0.020	NA	0.0398 ± 0.0001	0.11 ± 0.02
Total liquid products (mg/mg PA)	0.59 ± 0.12	0.68 ± 0.03	0.73 ± 0.08	0.50 ± 0.10
Total gas products (mg/mg PA)	0.16 ± 0.04	NA	0.12 ± 0.03	0.23 ± 0.01
Total yield (wt%)	76 ± 13	NA	85 ± 8	72 ± 9
PA conversion (%)	95 ± 4	98 ± 2	94 ± 3	95.5 ± 0.2
Mass Balance (wt%)	81 ± 11	NA	90 ± 6	77 ± 9

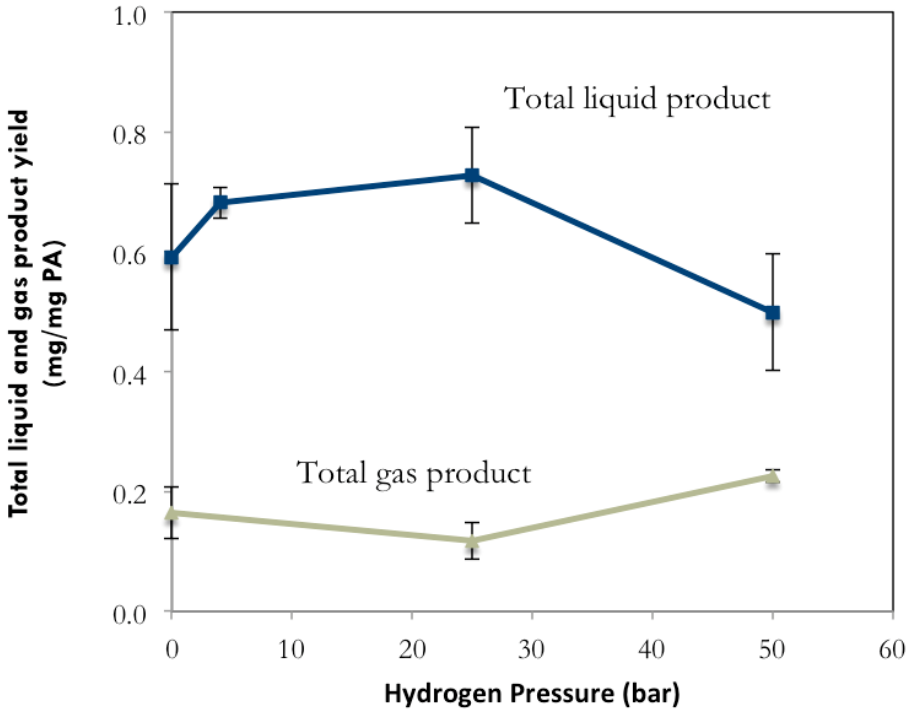

Figure 5.6: Effect of hydrogen pressure on total mass yields of liquid and gas products, reaction condition: 150 mg PA with 150 mg HZSM-5, 0.15 g/mL water density, 400℃, 180 minutes

Table 5.4: Typical properties of zeolite Y, beta, and ZSM-5

	Y	beta	HZSM-5
Pore size (Å)	12	5 ~ 7	5
Surface Area (m^2/g)	~ 700	600 ~ 700	400
Hydrothermal stability	less stable	less stable	more stable

hydrogen in our system. This is because first, by comparing reactions with no hydrogen and the reactions with additional hydrogen at 25 bar, which generated the highest total liquid product yield, the difference of the total liquid product yield was not large (only 0.1 mg/mg PA). Second, additional hydrogen increases the input of cost and energy, so it is beneficial only when it can create a significant increase of product value.

5.4 Effect of Different Catalysts

Zeolites ZSM-5, Beta, and Y are traditional cracking zeolites.[61] Therefore, we selected these three materials for the present study. The three types of zeolite are all composed of silica and alumina, but in different structures. ZSM-5 has a tube type micropore system with free diameters in the tubes of about 5 angstrom and a surface area of about 400 m^2/g. Zeolite beta has pore diameters of 5 - 7 angstrom and a surface area of 600 - 700 m^2/g. Zeolite Y has a three-dimensional pore network consisting of large spherical cavities with free diameters of about 12 angstrom and a surface area of about 700 m^2/g.[62] Thus, zeolites Y and beta generally have large pores and higher surface areas than zeolite ZSM-5. Those data are summarized in Table 5.4, and the structure of different types of zeolite are shown in Figure 5.7. Zeolites Y and beta, however, were less stable than zeolite ZSM-5 in hot liquid water at 150 and 200 ℃.[46] We desired to examine these different types of zeolites to determine their effectiveness for hydrothermal catalytic conversion of fatty acids to aromatics.

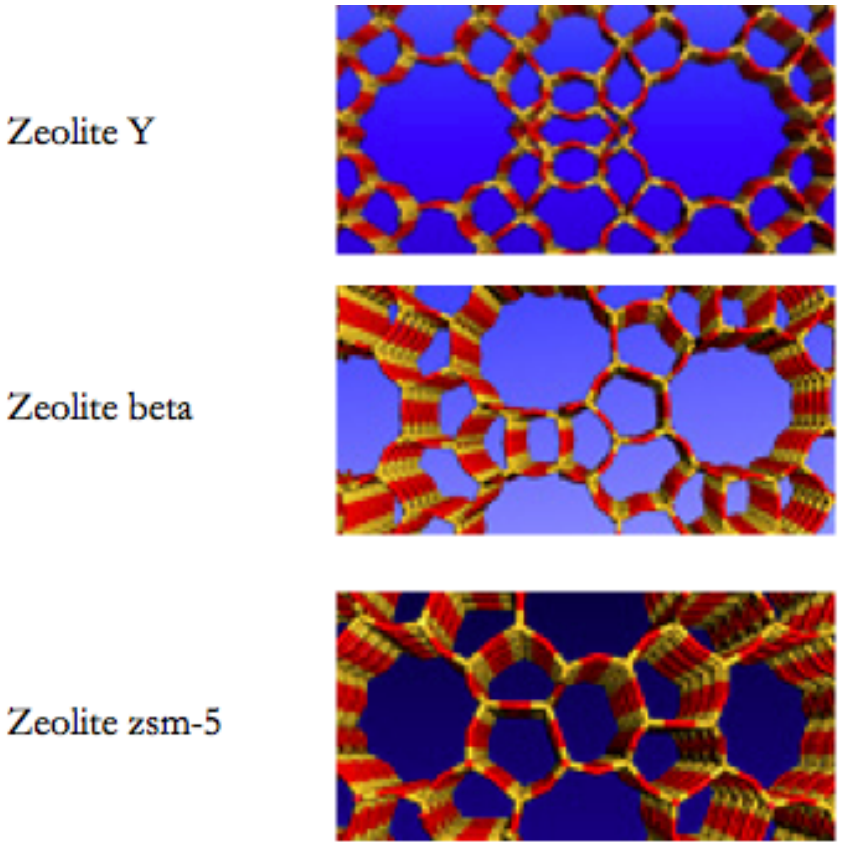

Figure 5.7: Structures of different zeolites (Y, beta, and zsm-5) [63]

Table 5.5: Molar yields of major products from palmitic acid over different zeolites (Y, beta, and zsm-5), reaction condition: 150 mg PA with 150 mg catalyst, water density of 0.15 g/mL, 400 ℃, 180 minutes.

Zeolite catalyst type	Y 60	beta 38	beta 300	HZSM-5 (30)
Product yield (mol/mol PA)				
Pentane, 2-methyl-	0.10 ± 0.02	0.13 ± 0.01	0.10 ± 0.005	0.062 ± 0.053
Butanal	0.0027 ± 0.0046	0.022 ± 0.006	0.0040 ± 0.0039	0.051 ± 0.021
2-methyl-hexane	0.0085 ± 0.0009	0.017 ± 0.007	0.011 ± 0.004	0.026 ± 0.008
2-pentanone	ND	0.0061 ± 0.0027	0.0056 ± 0.0053	0.0052 ± 0.0021
Heptane	0.0052 ± 0.0008	0.0028 ± 0.0020	0.0034 ± 0.0032	0.0089 ± 0.0023
4-methyl-heptane	ND	0.0017 ± 0.0020	0.0017 ± 0.0030	0.0025 ± 0.0028
Toluene	0.020 ± 0.007	0.040 ± 0.009	0.026 ± 0.027	0.22 ± 0.03
Xylene	0.039 ± 0.007	0.077 ± 0.018	0.046 ± 0.044	0.49 ± 0.08
Propyl-benzene	0.0041 ± 0.0035	0.0067 ± 0.0011	0.0024 ± 0.0042	0.034 ± 0.030
2-ethyl-toluene	0.0045 ± 0.0002	0.0047 ± 0.0020	0.0047 ± 0.0015	0.036 ± 0.012
1,2,4-trimethylbenzene	ND	0.0027 ± 0.0054	0.0088 ± 0.0090	0.029 ± 0.008
Acetic Acid	0.014 ± 0.012	0.013 ± 0.008	0.047 ± 0.028	0.11 ± 0.04
Total liquid products (mg/mg PA)	0.17 ± 0.01	0.14 ± 0.03	0.18 ± 0.06	0.59 ± 0.12
Total gas products (mg/mg PA)	0.075 ± 0.026	0.0065 ± 0.0024	0.024 ± 0.004	0.16 ± 0.04
Total yield (%)	24 ± 2	15 ± 3	21 ± 2	76 ± 13
PA conversion (%)	50 ± 2	29 ± 9	38 ± 1	95 ± 4
Mass Balance (%)	51 ± 1	66 ± 17	55 ± 4	81 ± 11

We performed reactions of palmitic acid with zeolites beta(silica/alumina = 38, 300), ZSM-5 (silica/alumina = 30), and Y (silica/alumina = 60) in supercritical water at 400 ℃, 240 bar, for 180 minutes. The mass balances in Table 5.5 being less than 100% can be attributed to the formation of products not detectable by our analytical methods. From Table 5.5, ZSM-5 gave the highest conversion of 95 ± 4%. The conversion with zeolite Y was about 50%, and zeolite beta gave the lowest PA conversion (30%). Zeolites beta and Y gave 2-methyl-pentane as the most abundant liquid product, while ZSM-5 gave toluene and xylenes as the major products. Some liquid products, such as 2-pentanone, 4-methyl-heptane, and 1,2,4-trimethylbenzene were not detected for reactions with zeolite Y. The molar yield of toluene was 22 ± 3% and that of xylenes was 49 ± 8% with ZSM-5. The highest yields of aromatics being obtained from ZSM-5 is consistent with previous work with these three materials in the gas phase cracking of n-octane at 500 ℃.[62]

We have also carried out experiments with an amorphous silica-alumina catalyst we synthesized in house. The generated amorphous silica-alumina catalyst has a

silica/alumina ratio of 35.6, which is very close to the silica/alumina ratio of 30 for the HZSM-5 used in reactions. For a 180 minutes reaction with amorphous silica-alumina, the major liquid products generated were the same as those from the HZSM-5 reactions, and the average conversion of palmitic acid was 88% with a standard deviation of 10%, was similar to that when HZSM-5 was used as the catalyst under the same circumstances. The procedure of making amorphous silica-alumina catalyst is in Appendix A.

The control experiment with palmitic acid with no catalyst, but at otherwise identical reaction conditions, produced 3.3% molar yield (1.2 wt%) of toluene, and 9.0% molar yield (3.7 wt%) of xylenes.The presence of zeolite ZSM-5 in the system significantly increased the yields of those major aromatic products. Among the zeolites ZSM-5, beta, Y, and amorphous silica-alumina, ZSM-5 shows the greatest potential for producing aromatic hydrocarbons from fatty acids in supercritical water under the conditions investigated here.

5.5 Effect of Catalyst Loading

Having shown that ZSM-5 is more effective than Y or beta for producing aromatics at the conditions of interest herein, we next examine the influence of the reactant-to-catalyst mass ratio for ZSM-5 with palmitic acid. Benson et al.[24] used oleic acid to ZSM-5 ratios of 0.2, 0.1, and 0.05 in their vapor-phase studies. Bielansky et al.[25] applied a REUSY catalyst partially coated with ZSM-5 to convert (not hydrothermally) palmitic acid into hydrocarbons in a continuous fluid catalytic cracking pilot plant. Converting their catalyst mass, flow rate, and residence time to batch reactor conditions leads to a reactant-to-catalyst ratio of unity for their study.[25] Of course, one prefers to operate with as high a reactant-to-catalyst ratio as possible that will provide the product yield and conversion required. Therefore, we assessed reactant-to-catalyst mass ratios of 1, 1.5, and 3.0 for the reaction of palmitic acid over ZSM-5.

Table 5.6: The effect of reactant-to-catalyst ratio on molar yields of major products, reaction condition: 150 mg of PA with different mass loading of HZSM-5, water density of 0.1 g/mL, 400 ℃, 180 minutes.

PA/catalyst mass ratio	3	1.5	1
Product yield (mol/mol PA)	50 mg cat.	100 mg cat.	150 mg cat.
Pentane, 2-methyl-	0.042 ± 0.025	0.020 ± 0.036	0.062 ± 0.053
Butanal	0.023 ± 0.007	0.018 ± 0.002	0.051 ± 0.021
2-methyl-hexane	0.0086 ± 0.0101	0.022 ± 0.004	0.026 ± 0.008
2-pentanone	0.0056 ± 0.0008	0.0079± 0.0024	0.0052 ± 0.0021
Heptane	0.0067 ± 0.0010	0.0066 ± 0.0004	0.0089 ± 0.0023
4-methyl-heptane	ND	0.0051 ± 0.0054	0.0025 ± 0.0028
Toluene	0.057 ± 0.026	0.13 ± 0.01	0.22 ± 0.03
Xylene	0.15 ± 0.08	0.34 ± 0.03	0.49 ± 0.08
Propyl-benzene	0.019 ± 0.007	0.012 ± 0.0008	0.034 ± 0.030
2-ethyl-toluene	0.0058 ± 0.0069	0.032 ± 0.002	0.036 ± 0.012
1,2,4-trimethylbenzene	0.0021 ± 0.0042	0.021 ± 0.001	0.029 ± 0.008
Acetic Acid	0.027 ± 0.021	0.037 ± 0.034	0.11 ± 0.04
Total liquid products (mg/mg PA)	0.17 ±0.07	0.35 ± 0.04	0.59 ± 0.12
Total gas products (mg/mg PA)	0.10 ± 0.02	0.17 ± 0.01	0.16 ± 0.04
Total yield (%)	27 ± 6	52 ± 3	76 ± 13
PA conversion (%)	40 ± 24	75 ± 25	95 ± 4
Mass Balance (%)	78 ±24	73 ± 22	81 ± 11

The palmitic acid loading remained at 150 mg in all of these experiments.

Table 5.6 shows the yields of the major liquid products and the palmitic acid conversions. The PA conversions and the total product yields both decrease as the reactant-to-catalyst ratio increases, as expected. Though one prefers a high reactant-to-catalyst ratio, the highest total product yield (76 wt%) and the highest PA conversion (95%) were achieved at the lowest reactant-to-catalyst ratio (1) examined. Figure 5.8 shows that the mass yield of total aromatics, and molar yields of toluene and xylenes decreased as the catalyst loading decreased.

Analysis of the data also reveals that the average rates of producing toluene with PA/catalyst ratios of 1, 1.5, and 3 were 8.5, 7.2, and 6.4 mmol/min/g catalyst, respectively, and the average rates of producing xylenes were 18,19, and 17 mmol/min/g catalyst, respectively. These rates were calculated as the product molar yield times the moles of PA loaded into the reactor, divided by the reaction time of 180 minutes and the catalyst loading in grams (0.15, 0.1, and 0.05 g). The production rates for each compound are almost the same at the various PA/catalyst ratios, which suggests

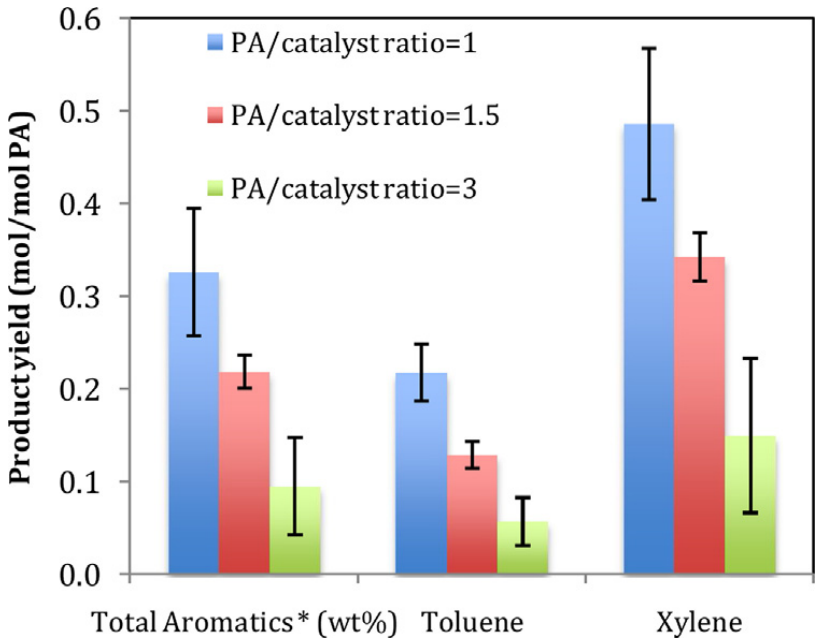

Figure 5.8: Effect of reactant-to-catalyst ratio on molar yields of toluene and xylene, and mass yield of total aromatics at water density of 0.1 g/mL, 400°C, 180 minutes (*denotes quantity given on a mass basis).

that the reaction that forms single-ring aromatics is first-order in catalyst. Thus, operating at even lower palmitic acid-to-ZSM-5 ratios should offer even higher yields of aromatics.

Figure 5.9 presents results for the gas yields. The yields of all gases shown increased first and then decreased as more catalyst was present in the reactors. This result is consistent with the additional catalyst promoting cracking reactions. As more catalyst is present with a fixed amount of palmitic acid, the additional cracking activity first produces more C3 - C5 gases as it reduces the sizes of the molecules that are present. As even more catalyst is added, and it effects an even greater amount of cracking, the molecules are sufficiently small that the C3 - C5 gases can no longer be formed as quickly as they are cracked to smaller products.

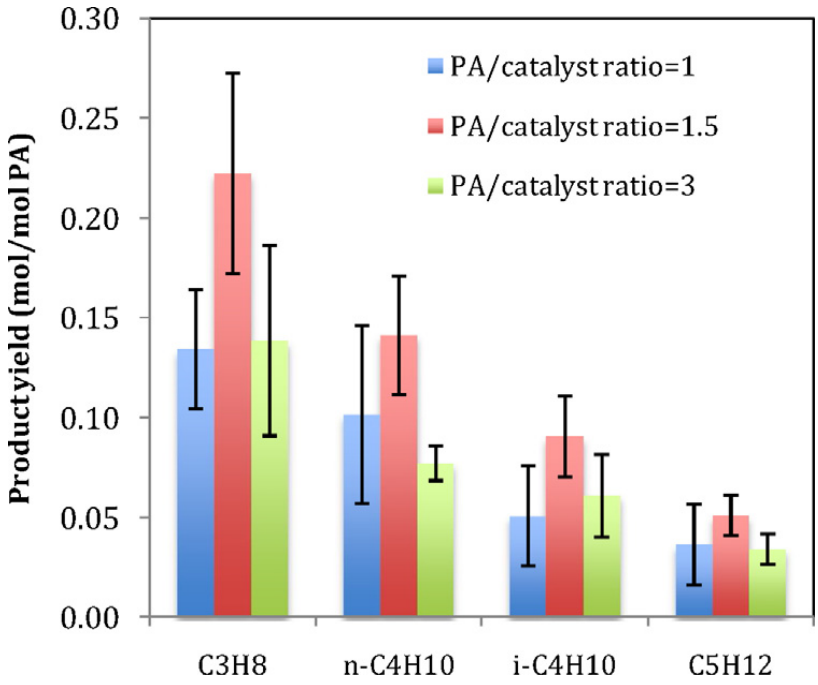

Figure 5.9: Effect of reactant-to-catalyst ratio on yields of major gas products at water density of 0.1 g/mL, 400℃, 180 minutes.

5.6 Effect of Degree of Saturation of Fatty acids

Most of the fatty acids in renewable plant oils contain one or more double bonds, which can influence the product distribution and pathways for acid-catalyzed hydrocarbon cracking.[64] The presence of unsaturation may play a role since protonation of a double bond is an easier route to the formation of a carbenium than is the direct formation of carbenium ions from saturated hydrocarbons. This section presents results for the hydrothermal zeolite-catalyzed cracking of unsaturated fatty acids.

To assess the influence of unsaturation on fatty acid cracking over zeolites, we conducted experiments with stearic acid (C18:0), oleic acid (C18:1), and linoleic acid (C18:2) with pre-calcined ZSM-5 (silica/alumina = 30) in supercritical water at 400℃, 240 bar, for 180 min. The results in Table 5.7 indicate that as the number of double bonds decreases, the total liquid product yield increases. Further, Figure 5.10 shows that the yields of the aromatic products decrease as the degree of unsaturation increases. These results suggest that hydrogenating unsaturated fatty acids before they

Table 5.7: Effect of number of double bonds on molar yields of products from C18 fatty acids over ZSM-5, reaction condition: 150 mg different types of FA, 150 mg HZSM-5, water density of 0.15 g/mL, 400 ℃, 180 minutes.

number of double bonds	2	1	0
Product yield (mol/mol FA)	linoelic acid	oleic acid	stearic acid
Pentane, 2-methyl-	0.015 ± 0.018	0.047 ± 0.035	0.12 ± 0.03
Butanal	0.0027 ± 0.0055	0.019 ± 0.012	0.027 ± 0.014
2-methyl-hexane	ND	0.021 ± 0.020	0.056 ± 0.008
2-pentanone	0.0012 ± 0.0025	0.0075 ± 0.0017	0.015 ± 0.003
Heptane	0.0024 ± 0.0048	ND	0.015 ± 0.007
4-methyl-heptane	0.0013 ± 0.0026	0.0029 ± 0.0051	0.0069 ± 0.0024
Toluene	0.060 ± 0.035	0.15 ± 0.02	0.22 ± 0.09
Xylene	0.23 ± 0.07	0.39 ± 0.01	0.50 ± 0.18
Propyl-benzene	0.0028 ± 0.0055	0.017 ± 0.004	0.030 ± 0.011
2-ethyl-toluene	0.028 ± 0.008	0.044 ± 0.006	0.028 ± 0.030
1,2,4-trimethylbenzene	0.027 ± 0.005	0.031 ± 0.007	0.021 ± 0.017
Acetic Acid	0.065 ± 0.050	0.052 ± 0.027	0.14 ± 0.02
Total liquid products (mg/mg FA)	0.18 ± 0.06	0.41 ± 0.12	0.56 ± 0.13
Total gas products (mg/mg FA)	0.25 ± 0.05	0.36 ± 0.12	0.15 ± 0.01
Total yield (wt%)	43 ± 0.6	77 ± 21	71 ± 12
FA conversion (%)	95 ± 3	85 ± 22	91 ± 1
Mass Balance (%)	45 ± 1	87 ± 12	78 ±8

react over the zeolite would increase the yields of aromatic liquid products. Previous work on fatty acid decarboxylation has also pointed to the potential advantage of hydrogenating unsaturated fatty acids prior to catalytic conversion.[16, 40]

The presence of catalyst increased the yield of liquid products for stearic and oleic acids, but not for linoleic acid. The total liquid product yield (18 ± 6 wt%) from hydrothermal catalytic cracking of linoleic acid is lower than the total liquid product yield (41 ± 5 wt%)from thermal cracking at otherwise identical conditions. The total product yields (gas plus liquid) were about 40 - 45 wt% in both cases, however.

The average mass balance for experiments with linoleic acid is much lower than those for oleic and stearic acids. One possible reason for the lower mass balance with LA is that the additional double bonds facilitate dimerization, oligomerization, and perhaps coke-forming reactions. None of these high-molecular weight products would be detected with the experimental methods we employed.

To determine how much coke is generated for reactions with the different fatty acids, we performed a controlled oxidation of the used catalyst and measured the

mass loss. The coke content on the catalysts accounted for 2.1, 0.4, and 0.3 wt% of the initial reactant mass for linoleic, oleic, and stearic acids, respectively. Therefore, coke formation was not a major contributor to the mass loss in the linoleic acid experiments, but linoleic acid generated more coke than did the more saturated fatty acids. We suspect that the missing material exists as high-molecular-weight compounds that were not amenable to GC analysis.

Figure 5.11 shows that the yields of major gaseous products increase first and then decrease as the degree of unsaturation increases. The total gas product yield was the highest at 36 ± 12 wt% for oleic acid, compared to 25 ± 4 wt% for linoleic acid, and 15 ± 1 wt% for stearic acid. This trend for the gases, along with that noted above for the liquid products, combine to show that the ratio of the total liquid product yield to the total gas product yield decreased with increasing unsaturation. This shift in the product distribution with the extent of unsaturation shows that changing the number of double bonds in the fatty acids can be a potential tool for controlling the product distribution.

5.7 Summary of the effect of reaction conditions

This chapter discussed how the reaction variables influence the product yield. The studied reaction variables include reaction time, temperature, water density, added hydrogen, different catalyst types, the reactant-to-catalyst loading, and the degree of saturation of fatty acids.

Reaction time and temperature are always important factors for a chemical reaction. Both the FA conversion and the production of the aromatics have an induction period at the short reaction times. Among tested reaction time and temperatures, the highest FA conversion (95%) was achieved at 400℃ and 180 minutes. With a fixed water density of 0.15 g/mL, the reaction condition of 400℃ and 180 minutes also generated the highest molar yields of toluene and xylenes, as well as the highest

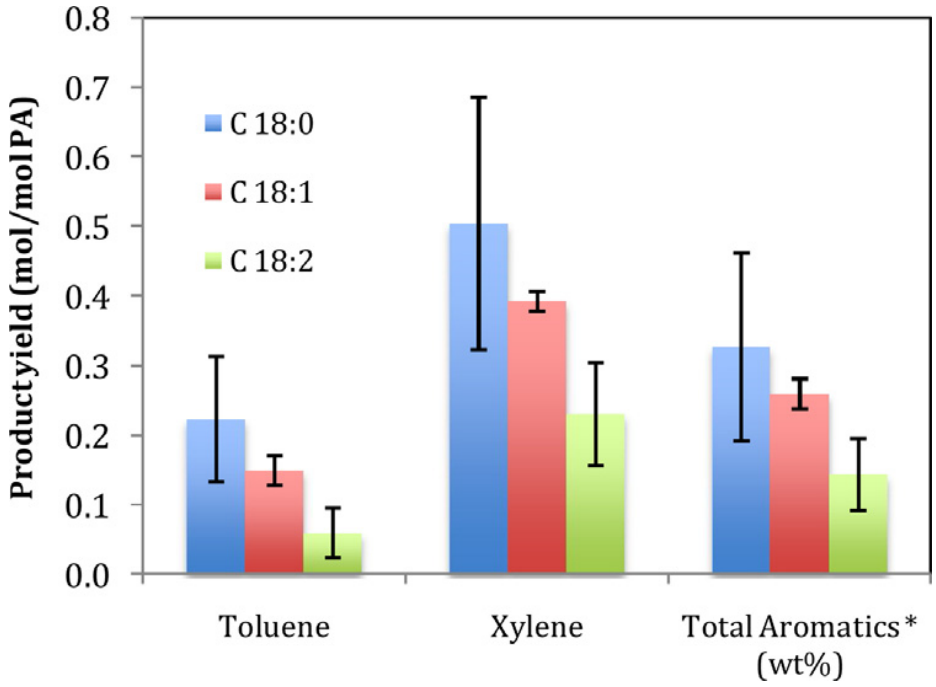

Figure 5.10: Effect of degree of unsaturation in C18 FA on molar yields of toluene and xylene, and mass yield of total aromatics at water density of 0.15 g/mL, 400℃, 180 minutes (*denotes quantity given on a mass basis).

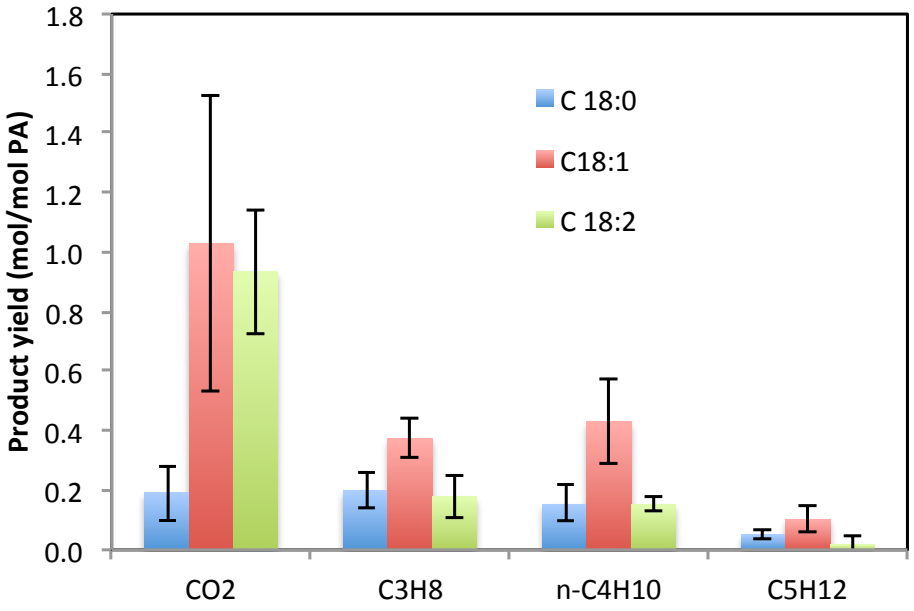

Figure 5.11: Effect of degree of unsaturation in C18 FA on yields of major gas products at water density of 0.15 g/mL, 400℃, 180 minutes.

total liquid product yield of 59 wt% (mainly aromatics), and the highest total product yield of 76 wt% (includes liquid and gas phase products).

The total liquid product achieved a maximum at a water density of 0.1 g/mL. The yields of the various products respond differently to the presence of water and to its density. Some of the products (2-methyl-pentane and 2-methyl-hexane) showed increased yields with increased water density, others (toluene and trimethyl-benzene) showed decreased yields with increased water density. In addition, the water gas shift reaction was believed involved in the gas production pathways of the reactions.

At mild hydrogen pressure (0 to 25 bar), there was no significant change of the product yields, however, the total liquid product yield dropped from 73 to 50 wt% while the gas product yield climbed from 12 to 23 wt% as hydrogen pressure increased from 25 to 50 bar. We decided not to add hydrogen in our subsequent reactions, due to the extra cost and small yield change cause by additional hydrogen.

Among zeolite ZSM-5, Beta, and Y, the highest molar yields of toluene (22%) and xylenes (49%) were obtained from reactions with ZSM-5. Zeolite ZSM-5 also gave the highest PA conversion of 95% compared to the other types of zeolite that we have examined.

The study of reactant-to-catalyst ratio showed the PA conversion, total liquid product yields, and the total product yields all decrease as the reactant-to-catalyst ratio increases. The product types, however, were the same at different reactant-to-catalyst ratios, except for 4-methyl-heptane not being detected for reactant-to-catalyst ratio of 3. The average rates of producing toluene and xylenes with reactant-to-catalyst ratios of 1, 1.5, and 3 were almost the same, which suggested that the reaction that forms single-ring aromatics is first-order in catalyst.

The number of double bonds in fatty acids was another variable. Among stearic acid (C18:0), oleic acid (C18:1), and linoleic acid (C18:2), stearic acid gave the highest total liquid product yields, while oleic acid gave the highest total gas product yield.

Overall, of the different zeolite catalysts examined to date, ZSM-5 was the most active for catalytic cracking of fatty acids in supercritical water to produce aromatic hydrocarbons. The reaction temperature, batch holding time, water density, and degree of saturation of the fatty acids all influence the product yields. On the other hand, added hydrogen has no significant effect on the product yields until the amount added is large enough (50 bar at room temperature) to inhibit the dehydrocyclization reactions that produce the aromatic products. Examination of the influence of different process variables reveals methods to tune the product distribution in order to favor desired products. For example, decreasing the reactant-to-catalyst ratio from 1.5 to 1 shifts the product distribution from fuel gases to aromatic products. The highest yield of liquid phase products (73 ± 9 wt %) occurred at 400 ℃, 180 minutes, with a water density of 0.1 g/mL, and in the absence of added hydrogen.

CHAPTER VI

Catalyst Composition, Regeneration, and Characterization

Chapter 5 discussed the reactions with different zeolite catalysts, including zeolite ZSM-5, Beta, and Y. The results showed that zeolite ZSM-5 was the most promising catalyst for hydrothermal reaction to produce aromatic hydrocarbon chemicals among the tested catalysts. This chapter provides further information about the zeolite catalyst used in the reactions. The study of catalyst includes investigation at the effect of silica-to-alumina ratio of zeolite ZSM-5, catalyst regeneration and reuse, catalyst characterization (surface area, bulk structure, pore size, etc.), and the calculation to determine if the reaction is diffusion limited.

6.1 Silica-to-alumina Ratio of Zeolite

Section 5.4 in Chapter 5 shows that ZSM-5 gave higher yields of aromatics than did zeolites beta or Y. Therefore, we used ZSM-5 for additional experiments that examined how the silica/alumina ratio affects the reaction outcome. This catalyst feature is important because the acidity of the zeolite increases as its silica/alumina ratio decreases. In acid-based zeolite catalysts, Bronsted acid site contains an H+ ion localized near a bridging Si-O-Al cluster, which is illustrated in Figure 6.1. The ratio

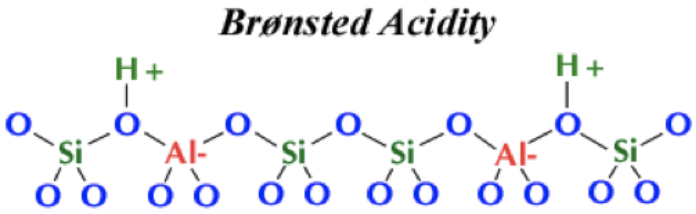

Figure 6.1: Demonstration of Bronsted acid sites, containing an H+ ion localized near a bridging Si-O-Al cluster
[68]

of Bronsted to Lewis acid sites also tends to increase with a decreasing silica/alumina ratio.[65] Bronsted acid sites are the ones typically implicated in cracking reactions. Although low silica/alumina ratio enhances acidity, increasing the silica/alumina ratio improves catalyst stability in hot liquid water and in steam, because it increases the hydrophobic character of the zeolite[66, 67]. To the best of our knowledge, no prior study has been done on the influence of the silica/alumina ratio on reactions in supercritical water.

We conducted experiments in supercritical water (400 ℃,240 bar) with palmitic acid and ZSM-5 with silica/alumina=23, 30, 50, and 80. Table 6.1 gives the product yields and conversions achieved with the different silica/alumina ratios. ZSM-5 with silica/alumina=23 gave the highest total product yield of 97 ± 2 wt% and the highest conversion of 98 ± 1%. As the silica/alumina ratio decreased the yields of the major products, toluene and xylenes, increased. The catalyst with silica/alumina=23 gave a 66% yield of xylenes, a 25% yield of toluene, and a 102% total molar yield of single-ring aromatics. Figure 6.2 gives a clear comparison of the xylene yield and toluene yield from reactions with different silica/alumina ratios. From the figure, we can tell that the silica/alumina ratio of 23 produces the most xylenes and toluene. These high yields demonstrate the efficacy of hydrothermal cracking for producing aromatics from fatty acids.

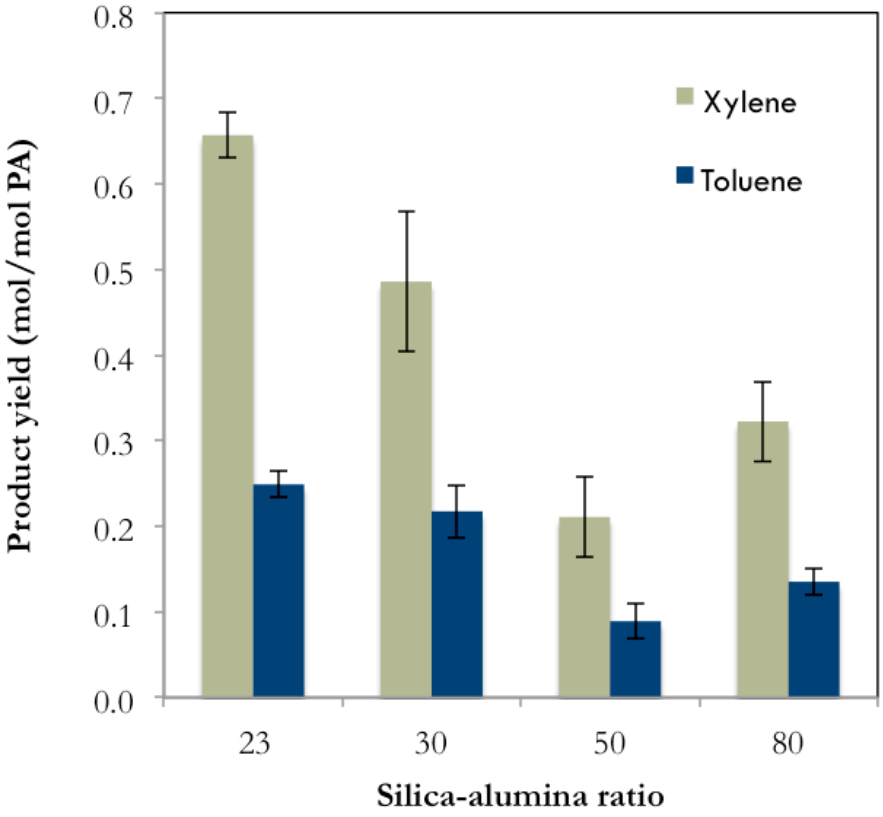

Figure 6.2: Effect of silica/alumina ratio of ZSM-5 on molar yields of xylenes and toluene, reaction condition: 150 mg PA with 150 mg HZSM-5, 0.15 g/mL water density. 400℃, 180 minutes.

Table 6.1: Effect of silica/alumina ratio of ZSM-5 on product yields, reaction condition: 150 mg PA with 150 mg HZSM-5, 0.15 g/mL water density. 400℃, 180 minutes.

silica-alumina ratio	23	30	50	80
Product yield (mol/mol PA)				
Pentane, 2-methyl-	0.10 ± 0.09	0.062 ± 0.053	0.026 ± 0.02	0.0089 ± 0.0077
Butanal	0.040 ± 0.034	0.051 ± 0.021	0.015 ± 0.014	0.013 ± 0.006
2-methyl-hexane	0.042 ± 0.005	0.026 ± 0.008	0.015 ± 0.004	0.014 ± 0.005
2-pentanone	0.017 ± 0.0006	0.0052 ± 0.0021	ND	0.007 ± 0.003
Heptane	0.012 ± 0.006	0.0089 ± 0.0023	0.00068 ± 0.0012	0.0040 ± 0.0050
4-methyl-heptane	0.0058 ± 0.0024	0.0025 ± 0.0028	0.0016 ± 0.0028	0.0034 ± 0.0033
Toluene	0.25 ± 0.02	0.22 ± 0.03	0.089 ± 0.021	0.14 ± 0.02
Xylene	0.66 ± 0.03	0.49 ± 0.08	0.21 ± 0.05	0.32 ± 0.05
Propyl-benzene	0.023 ± 0.002	0.034 ± 0.030	0.0080 ± 0.0012	0.012 ± 0.001
2-ethyl-toluene	0.064 ± 0.006	0.036 ± 0.012	0.021 ± 0.006	0.031 ± 0.003
1,2,4-trimethylbenzene	0.027 ± 0.016	0.029 ± 0.008	0.025 ± 0.004	0.032 ± 0.003
Acetic Acid	0.010 ± 0.058	0.11 ± 0.04	0.023 ± 0.03	0.088 ± 0.083
Total liquid products (mg/mg PA)	0.86 ± 0.01	0.59 ± 0.12	0.37 ± 0.09	0.54 ± 0.08
Total gas products (mg/mg PA)	0.11 ± 0.03	0.16 ± 0.04	0.23 ± 0.09	0.10 ± 0.03
Total yield (%)	97 ± 2	76 ± 13	60 ± 0.08	64 ± 5
PA conversion (%)	98 ± 1	95 ± 4	71 ± 0.6	80 ± 16
Mass Balance (%)	98 ± 2	81 ± 11	78 ± 4	86 ± 14

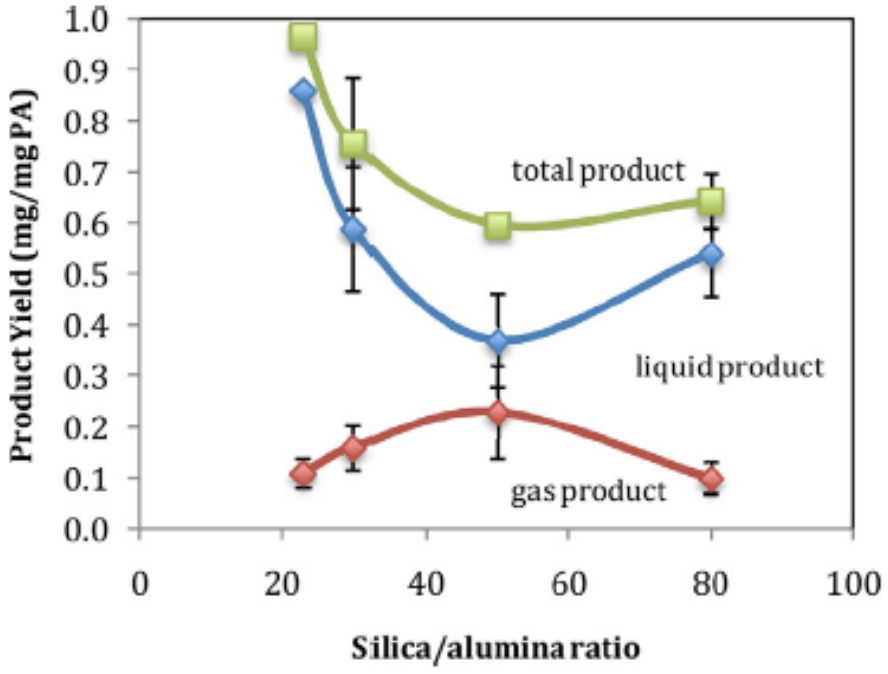

Figure 6.3: Effect of silica/alumina ratio of ZSM-5 on distribution of the total yields of all products, liquid, and gases, reaction condition: 150 mg PA with 150 mg HZSM-5, 0.15 g/mL water density. 400℃, 180 minutes.

Figure 6.3 illustrates the influence of the silica/alumina ratio on the distribution between liquid and gaseous products. ZSM-5 with a ratio of 23 gave the largest difference between the liquid and gas yields, with the liquid products dominating. Increasing the ratio to 50 led to this difference being nearly zero, but an additional increase to 80 again led to the mean liquid product yield being much higher than the mean gas yield. The uncertainties associated with the data obtained from the zeolite with a ratio of 50 are large enough that it is not clear whether that experiment represents a true extremum for the liquid and gas yields or whether the results from ratios of 30, 50, and 80 are all about the same. Regardless, the liquid yield is clearly highest for the material with a ratio of 23, which corresponds to the most acidic material.

6.2 Catalyst Regeneration and Reuse

Zeolites undergo coking reactions during hydrocarbon processing that can reduce the catalyst activity.[65] Additionally, some zeolites are unstable under certain hydrothermal conditions.[46] Given this background, we desired to determine whether HZSM-5 could be reused for fatty acid cracking in a hydrothermal environment. We first conducted an experiment wherein the catalyst zeolite HZSM-5 (silica/alumina ratio of 30) used in one reaction (400 ℃, 0.15 g/mL water density, 180 min) was collected, dried in an oven at 70 ℃ overnight, and then reused in a second run at the same conditions. The total product yield (liquid plus gas) was 76% with the fresh catalyst, but it dropped to only 2% with the once-used catalyst. It is clear that catalyst deactivation occurred either during the hydrothermal reaction or during the hydrothermal heating/cooling experienced by the catalyst. Regardless of where or how the deactivation occurs, the issue of practical significance becomes that of catalyst regeneration. We investigated catalyst regeneration by performing a controlled oxidation of the used catalyst to burn off any coke and then subjecting that material

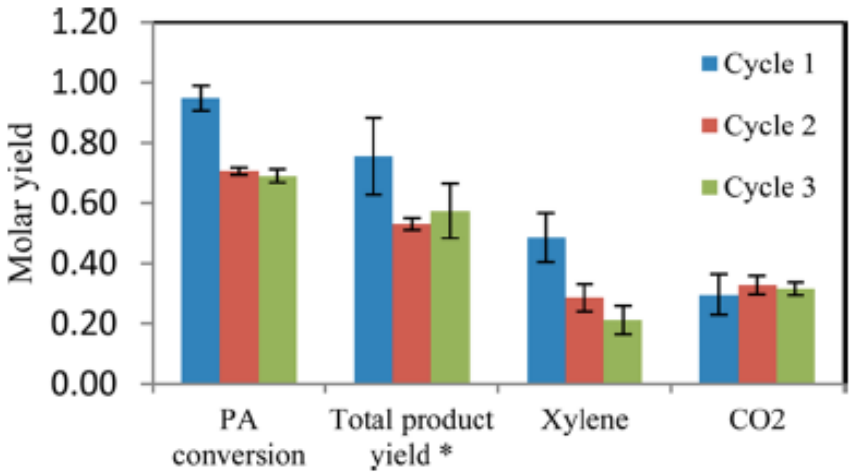

Figure 6.4: Effect of catalyst regeneration and reuse on palmitic acid conversion, molar yield of mixed xylenes and CO_2, and total *mass yield (not molar yield) of the liquid and gas products, reaction condition: 150 mg PA with 150 mg HZSM-5 (silica/alumina=30), 0.15 g/mL water density. 400℃, 180 minutes.

to a calcination step as described in the experimental section.

Figures 6.4 and 6.5 show the yields of selected products from experiments with fresh catalyst (cycle 1), with catalyst that had been used and regenerated once (cycle 2) and with catalyst that had been used twice and regenerated twice (cycle 3). Table 6.2 provides the details for all of the reaction products. As indicated in Figure 6.4, the total product yield decreased from 76 ± 13 wt% with the fresh catalyst to 53 ± 2 wt% upon its second use. This irreversible deactivation in the first reaction-regeneration cycle is typical of HZSM-5 zeolites, and one reason is the loss of a certain fraction of the Bronsted strong acid sites in hot compressed water, which are required for the cracking reactions.[65] Figure 6.4 also shows that the total product yields are about the same for the second and third uses of the catalyst, which suggests that this hydrothermal reaction-regeneration process might be effective for hydrothermal conversion of fatty acids to hydrocarbons with value as fuels or chemicals.

Figures 6.4 and 6.5 show that the molar yields of the major products (toluene and xylenes) decrease with each reuse and regeneration of the catalyst, but appreciable

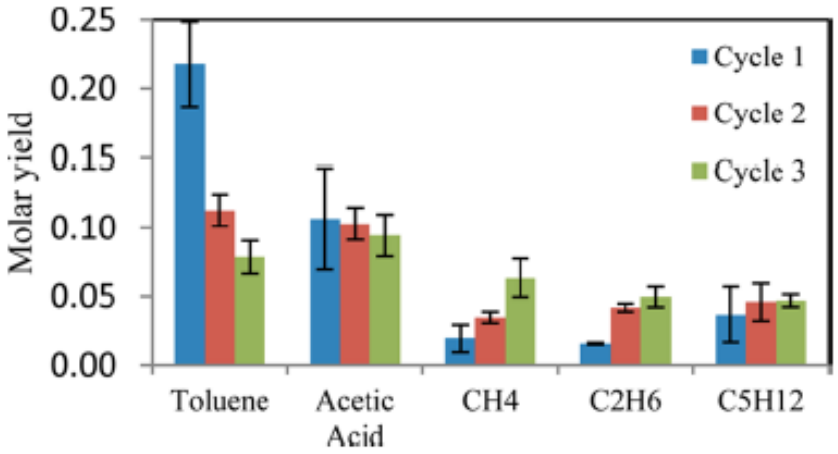

Figure 6.5: Effect of catalyst regeneration and reuse on molar yields of toluene, acetic acid, methane, ethane, and pentane, reaction condition: 150 mg PA with 150 mg HZSM-5 (silica/alumina=30), 0.15 g/mL water density. 400℃, 180 minutes.

yields of these desirable aromatic products are still obtained. Interestingly, the yield of acetic acid is unaffected by the reuse and regeneration of the catalyst (Figure 6.5). It seems that the aromatic compounds and acetic acid might be formed in two different paths, with one being insensitive to reuse of the catalyst. CO_2 and n-pentane also have similar yields with fresh and regenerated catalyst. The yields of methane and ethane slightly increased when using regenerated catalyst, as indicated in Figure 6.5.

Having determined in the present investigation that HZSM-5 with silica/alumina=23 is a better catalyst for making aromatics from fatty acids than HZSM-5 with silica/alumina=30, the material we used previously, we desired to discover whether this more acidic form of ZSM-5 could also be regenerated and reused for hydro-thermal cracking of palmitic acids. The reaction conditions were the same as for the reactions with HZSM-5 of silica/alumina ratio of 30.

Figure 6.6 shows the yields of selected products from these experiments. The conversion decreased from 98 $\pm$ 1% for the fresh catalyst to slightly lower values with the regenerated catalyst. Likewise,the yields of toluene and xylenes were lower with

Table 6.2: Effect of catalyst regeneration and reuse on product yields, reaction condition: 150 mg PA with 150 mg HZSM-5 (silica/alumina=30), 0.15 g/mL water density, 400℃, 180 minutes.

Product molar yield (mol/mol PA)	cycle 1	cycle 2	cycle 3
2-methyl-pentane	0.062 ± 0.053	0.0165 ± 0.0002	0.030 ± 0.017
Butanal	0.051 ± 0.021	0.043 ± 0.030	0.020 ± 0.002
2-methyl-hexane	0.026 ± 0.008	0.01759 ± 0.00003	0.018 ± 0.002
2-pentanone	0.0052 ± 0.0021	0.0061 ± 0.0038	0.0078 ± 0.0044
Heptane	0.0089 ± 0.0023	0.0049 ± 0.0070	0.0068 ± 0.0005
4-methyl-heptane	0.0025 ± 0.0028	0.014 ± 0.020	ND
Toluene	0.22 ± 0.03	0.11 ± 0.01	0.079 ± 0.012
Xylene	0.49 ± 0.08	0.29 ± 0.05	0.21 ± 0.05
Propyl-benzene	0.034 ± 0.030	0.039 ± 0.007	0.0081 ± 0.0015
2-ethyl-toluene	0.036 ± 0.012	0.019 ± 0.015	0.020 ± 0.005
1,2,4-trimethylbenzene	0.029 ± 0.008	0.024 ± 0.005	0.017 ± 0.004
Acetic Acid	0.11 ± 0.04	0.103 ± 0.012	0.095 ± 0.015
H_2	0.10 ± 0.03	0.14 ± 0.03	0.096 ± 0.057
CO	0.126 ± 0.005	0.111 ± 0.006	0.079 ± 0.023
CH_4	0.020 ± 0.010	0.035 ± 0.004	0.064 ± 0.014
CO_2	0.30 ± 0.07	0.33 ± 0.03	0.32 ± 0.21
C_2H_4	0.090 ± 0.015	0.047 ± 0.002	0.18 ± 0.03
C_2H_6	0.0155 ± 0.0006	0.042 ± 0.003	0.050 ± 0.008
C_3H_8	0.13 ± 0.03	0.20± 0.01	0.143 ± 0.003
n-C_4H_{10}	0.10 ± 0.04	0.15± 0.02	0.10 ± 0.02
i-C_4H_{10}	0.051 ± 0.025	0.071 ± 0.013	0.068 ± 0.007
C_5H_{12}	0.037 ± 0.020	0.046 ± 0.014	0.047 ± 0.005
Total liquid products (mg/mg PA)	0.59 ± 0.12	0.35 ± 0.01	0.40 ± 0.05
Total gas products (mg/mg PA)	0.16 ± 0.04	0.18 ± 0.01	0.17 ± 0.04
Total yield (wt%)	76 ± 13	53 ± 2	57 ± 9
PA conversion (%)	95 ± 4	71 ± 1	69 ± 2
Mass Balance (wt%)	81 ± 11	82.4 ± 0.7	88 ± 7

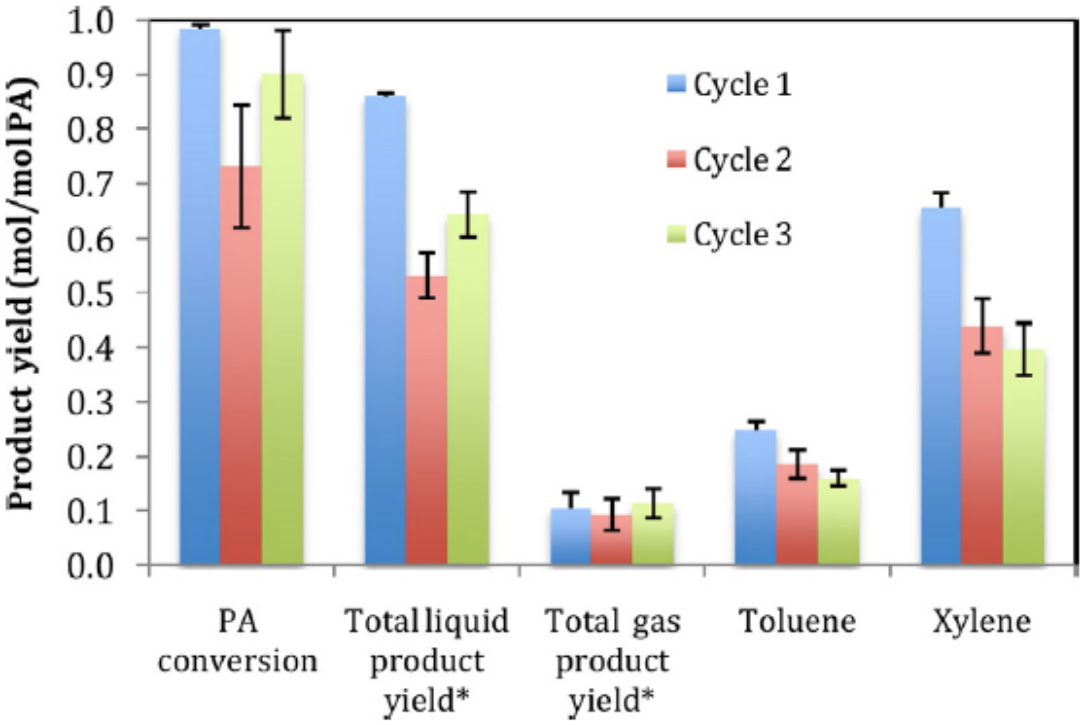

Figure 6.6: Effect of catalyst regeneration and reuse on palmitic acid conversion, molar yields of xylene and toluene, and total mass yield of liquid and gas products, * denotes quantity given on a mass basis, reaction condition: 150 mg PA with 150 mg HZSM-5 (silica/alumina=23), 0.15 g/mL water density. 400℃, 180 minutes.

the used and regenerated catalyst, but appreciable yields of the desirable aromatic products were still obtained. As was the case with the fresh catalyst, the regenerated materials with silica/alumina=23 gave higher product yields than did the regenerated zeolite with silica/alumina=30. Interestingly, the total yield of gas products was unaffected by the reuse and regeneration of the catalyst. Table 6.3 gives more details of the results.

These present results confirm the technical feasibility of producing appreciable yields of aromatic products from fatty acids in supercritical water in consecutive uses by applying regenerated catalyst.

Table 6.3: Effect of catalyst regeneration and reuse on product yields, reaction condition: 150 mg PA with 150 mg HZSM-5 (silica/alumina=23), 0.15 g/mL water density, 400℃, 180 minutes.

cycle number	1	2	3
Product yield (mol/mol PA)			
Pentane, 2-methyl-	0.10 ± 0.09	ND	0.24 ± 0.02
Butanal	0.040 ± 0.034	ND	0.064 ± 0.045
2-methyl-hexane	0.042 ± 0.005	0.026 ± 0.004	0.034 ± 0.004
2-pentanone	0.017 ± 0.0006	0.010 ± 0.002	0.018 ± 0.003
Heptane	0.012 ± 0.006	0.012 ± 0.002	0.013 ± 0.001
4-methyl-heptane	0.0058 ± 0.0024	0.0063 ± 0.0006	0.0069 ± 0.0002
Toluene	0.25 ± 0.02	0.19 ± 0.03	0.16 ± 0.01
Xylene	0.66 ± 0.03	0.44 ± 0.05	0.40 ± 0.05
Propyl-benzene	0.023 ± 0.002	0.042 ± 0.006	0.042 ± 0.004
2-ethyl-toluene	0.064 ± 0.006	0.016 ± 0.006	0.015 ± 0.0008
1,2,4-trimethylbenzene	0.027 ± 0.016	ND	0.015 ± 0.003
Acetic Acid	0.010 ± 0.058	0.061 ± 0.011	0.14 ± 0.001
Total liquid products (mg/mg PA)	0.86 ± 0.01	0.53 ± 0.04	0.64 ±0.04
Total gas products (mg/mg PA)	0.11 ± 0.03	0.094 ± 0.029	0.11 ± 0.03
Total yield (%)	97 ± 2	63 ± 4	76 ± 3
PA conversion (%)	98 ± 1	73 ± 11	90 ± 8
Mass Balance (%)	98 ± 2	86 ± 8	85 ± 8

6.3 Catalyst Characterization

Bronsted acidic zeolites are used widely in the petrochemical industry as catalysts for gas phase reactions of hydrocarbons at elevated temperatures (greater than 250 ℃), where issues of hydrothermal stability predominantly reflect steam-catalyzed cleavage of framework Al - O bonds that leads to dealumination.[69]

Ravenelle et al.[46] have reported that treatment in hot liquid water (150 and 200 ℃) transforms zeolite Y into an amorphous material. In contrast, HZSM-5 was not modified under the same conditions. In general, the main degradation mechanism is probably desilication and dealumination, as shown in Figure 6.7. Desilication is hydrolysis of the siloxane bonds (Si - O - Si), which dominates under neutral or basic liquid water conditions; while dealumination dominates under steaming, and acidic liquid water conditions. No work has been done on the stability of HZSM-5 in supercritical water at 400 ℃, to the best of our knowledge.

To better understand the hydrothermal stability of HZSM-5 under the present

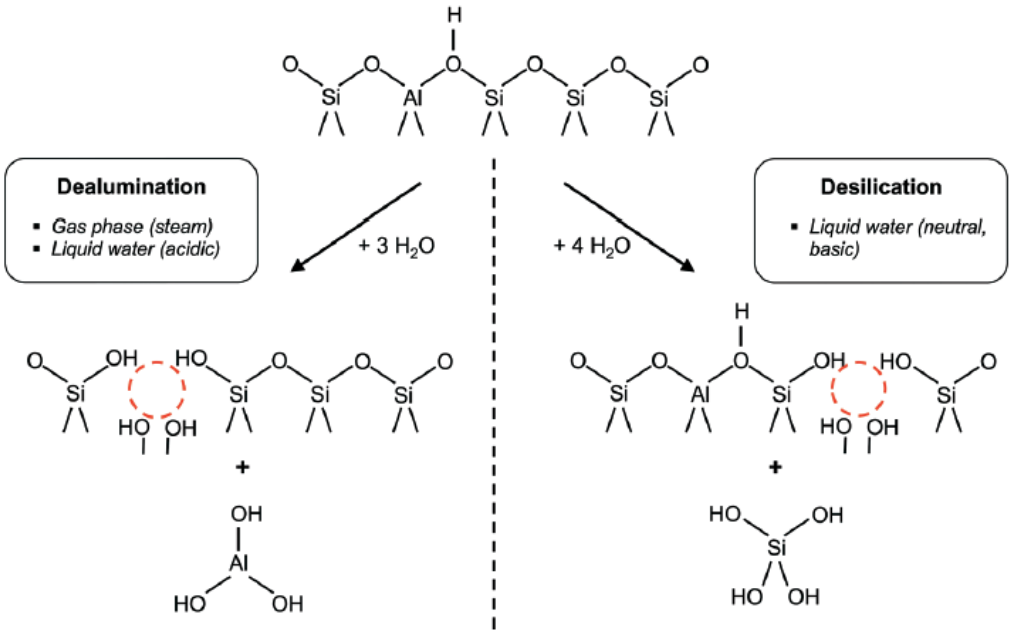

Figure 6.7: Hydrolysis reactions that lead to framework dealumination (left) prevail in the gas phase with steam and in liquid water under acidic conditions. Hydrolysis reactions that lead to framework desilication (right) prevail in liquid water under neutral and basic conditions.
[69]

reaction conditions, we used X-ray Powder Diffraction (XRD) to examine the fresh catalyst and samples of HZSM-5 recovered from reactors after use for 180 minutes. The XRD analysis gives information about the bulk structure of the material and the type of chemical bonds in the catalyst crystal. Figure 6.8 shows the XRD spectra. The fresh catalyst exhibits the XRD spectrum one expects for HZSM-5.[46] Two new peaks appear in the XRD spectrum of the HZSM-5 that was used for a 180 minute reaction, however. We were unable to identify the first new peak at 7.3°, but the second new peak at 21.48° corresponds to cristobalite high-SiO_2. Though the hydrothermal reaction conditions induced some changes in the HZSM-5, the persistence of the other characteristic peaks verifies that the HZSM-5 retained its major structural elements during the reaction.

Since the hydrothermal reaction changed a portion of the catalyst structure, we analyzed the regenerated catalyst to learn whether the regeneration process restores the catalyst to its original structure. Figure 6.8 shows that all of the characteristic peaks in the XRD spectrum for fresh HZSM-5 also appear for the once- and twice-regenerated material. This outcome indicates that the bulk structure of HZSM-5 after regeneration is the same as the bulk structure of the fresh HZSM-5 that has been calcined. Also, after the regeneration process, the two new peaks that appeared for the used catalyst vanish.

Figure 6.9 shows the pore size distributions for the fresh calcined catalyst and for materials that had been used once and regenerated and also used twice and re-generated. The majority of the pore volume for all of the materials resides in pores with diameters of 2 - 5 nm. This result for the fresh calcined ZSM-5 is consistent with the micropore sizes in fresh calcined ZSM-5 reported previously.[70] The curve for the catalyst regenerated once falls below that of the fresh catalyst. Likewise, the curve for the twice-regenerated material falls below that of the material regenerated just once. Thus, use and regeneration reduces the total pore volume in the material.

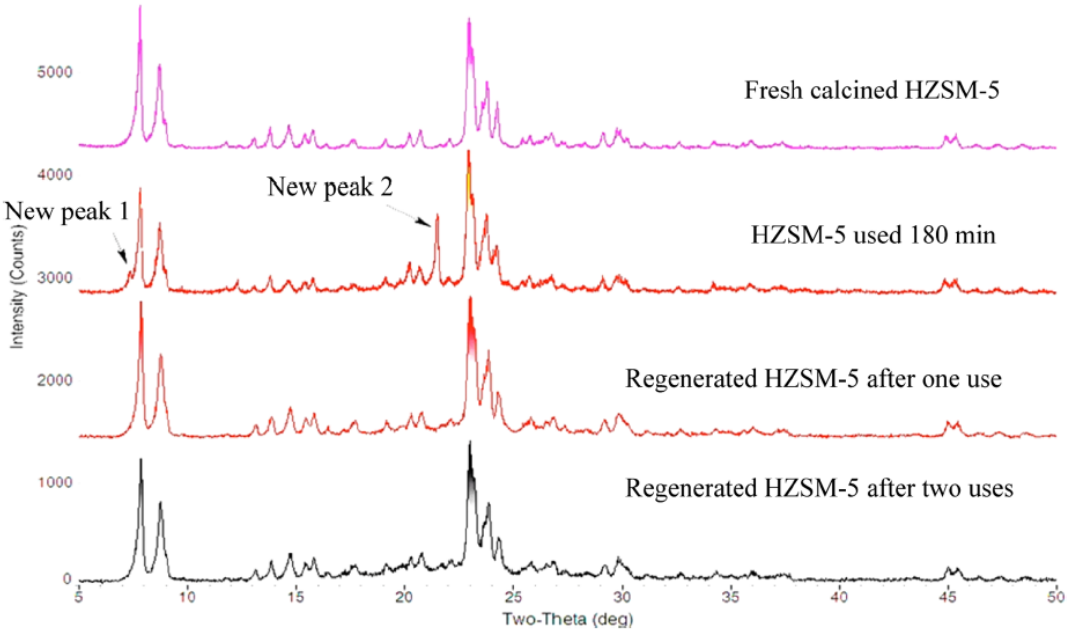

Figure 6.8: X-ray powder diffraction spectra for fresh calcined HZSM-5, HZSM-5 used after a 180 minutes reaction (reaction condition: at 400℃ with water density of 0.1 g/mL and PA-to-catalyst ratio of 1), and regenerated HZSM-5 after one and two uses. All the silica/alumina ratios are 23

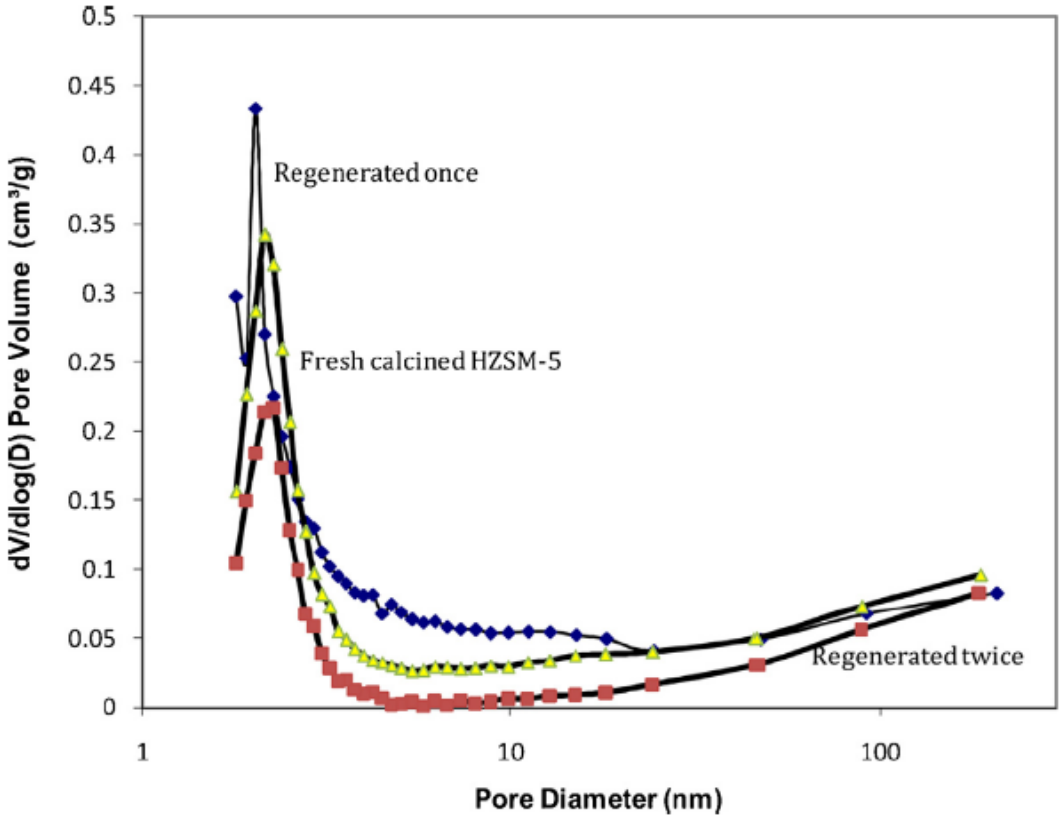

Figure 6.9: BJH pore size distribution for ZSM-5 fresh, used and regenerated once, and used and regenerated twice (silica/alumina =30), 400℃, 180 minutes.

A second effect of multiple uses and regeneration cycles evident in Figure 6.9 is the near elimination of pore volume in pores with diameters of 4 - 20 nm.

Table 6.4 shows the Brunauer-Emmett-Teller (BET) surface areas and the Barrett-Joyner-Halenda (BJH) adsorption pore volumes for the fresh ZSM-5 and for the catalysts that had been used and regenerated once and used and regenerated twice. The use and regeneration of the catalysts decreased both the surface area and the pore volume, but not the average pore diameter. These characterization results suggest that the modest reduction in activity with regeneration and reuse noted previously could be due to loss of surface area and pore volume.

Scanning Electron Microscope (SEM) analysis was carried out for three different types of catalyst(HZSM-5) samples, fresh calcined HZSM-5, HZSM-5 that has been

Table 6.4: Surface area, pore volume, and pore diameter for fresh calcined ZSM-5 and for ZSM-5 used and regenerated once and twice (silica/alumina=30, water density of 0.1 g/mL, PA-to-catalyst ratio of 1, 400℃, 180 minutes).

	Surface area (m^2/g)	Pore volume (cm^3/g)	Average pore diameter (nm)
Fresh calcined ZSM-5	370	0.19	5.2
Regenerated once	293	0.16	5.4
Regenerated twice	176	0.10	5.6

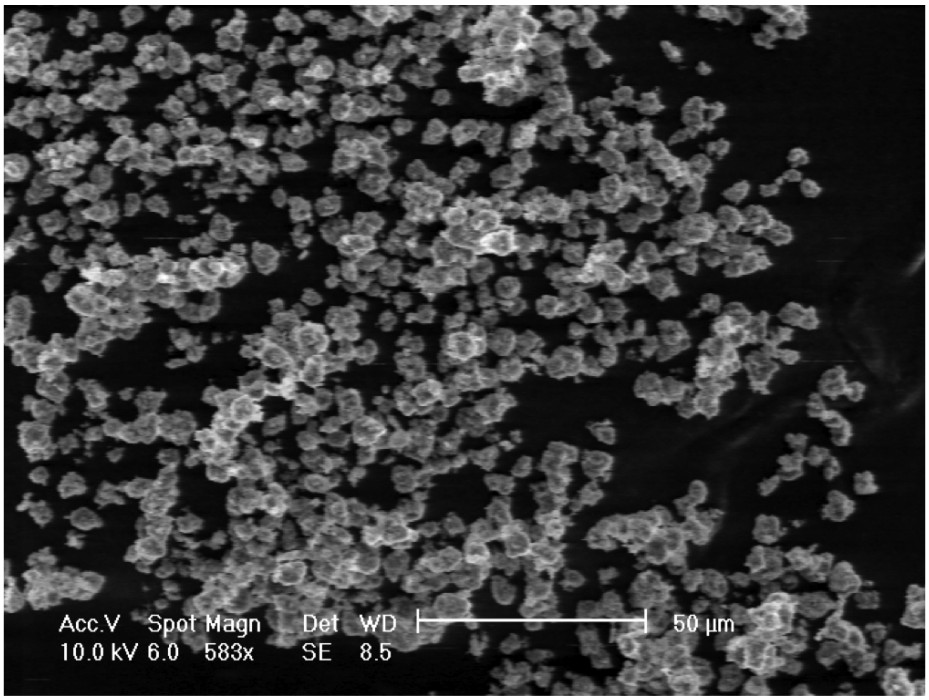

Figure 6.10: SEM image of fresh calcined HZSM-5, before reactions.

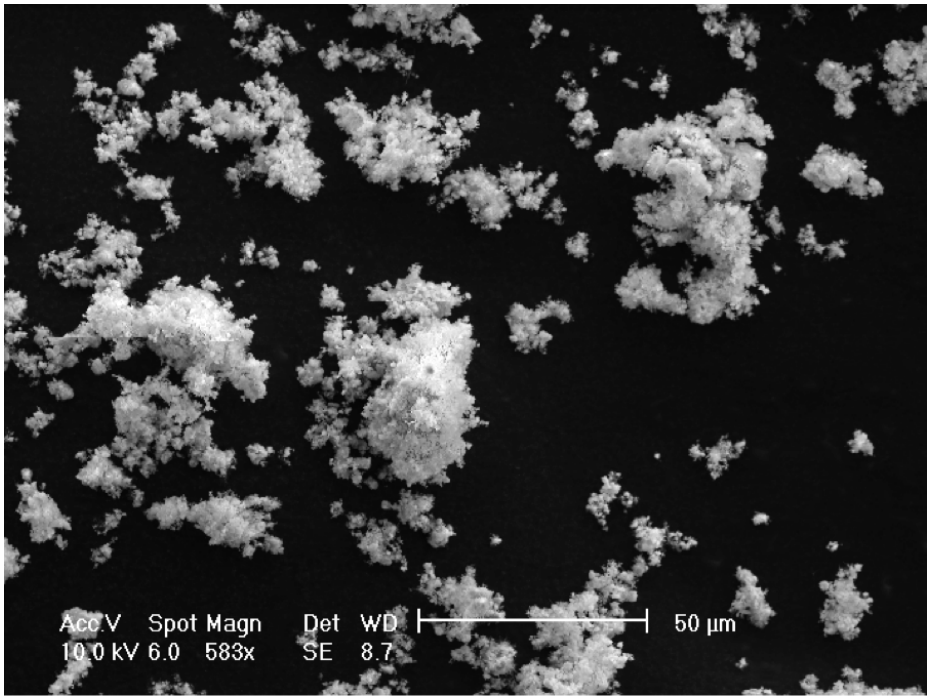

Figure 6.11: SEM image of HZSM-5 that has been used in reactions and without regeneration, reaction condition: 400℃, 180 minutes, water density of 0.1 g/mL, PA-to-catalyst ratio of 1.

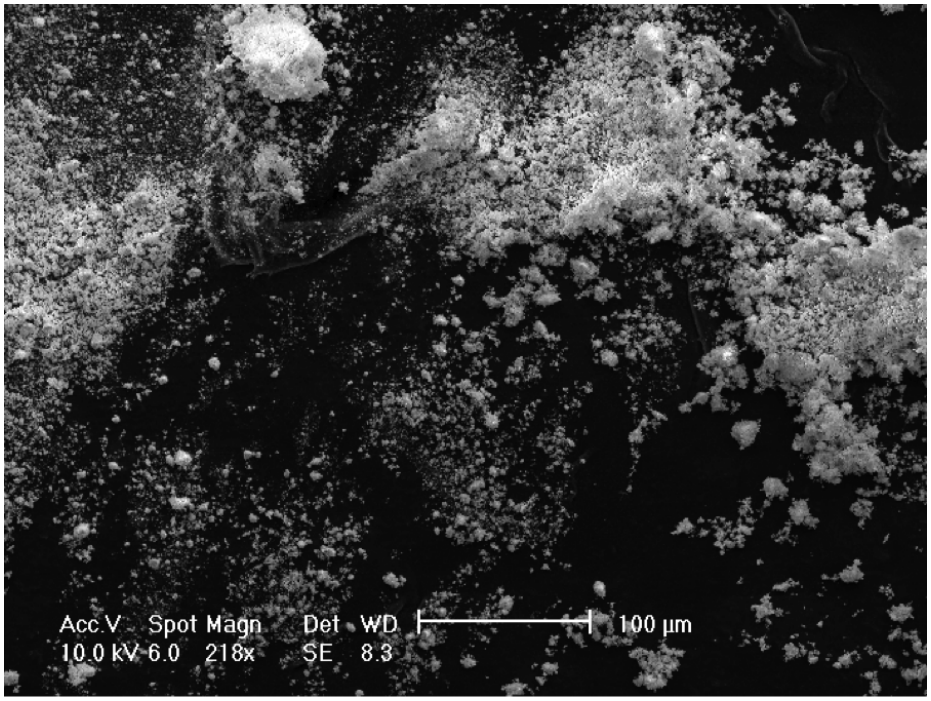

Figure 6.12: SEM image of HZSM-5 after one time usage and regeneration, reaction condition: 400℃, 180 minutes, water density of 0.1 g/mL, PA-to-catalyst ratio of 1.

used in hydrothermal reaction at 400 ℃ for 180 minutes, and HZSM-5 that has been used and regenerated once. The regeneration procedures were described in Chapter 3, section 3.1.2. The SEM images of these three types of catalyst samples appear as Figure 6.10, Figure 6.11, and Figure 6.12 respectively. More of the SEM images of catalyst samples at different magnifications were included in Appendix C.

The fresh catalyst sample has more uniform particle sizes. Close inspection shows that those particles are composed of smaller particles as well. The particle size (radius) of the catalyst can be estimated to be $3.57*10^{-4}$ cm from Figure 6.10 for the fresh sample.

For catalyst that experienced hydrothermal reaction, but was not regenerated, it seems that some catalyst particles combined and some also crumbled. The change in particle sizes suggested that the catalyst may lost some stability under the experimental conditions. There was a broad range of particle sizes for both used and used and regenerated sample. By comparing the SEM results of catalyst after reaction and catalyst after regeneration, it seems that the regeneration procedure did reduce the prevalence of larger particles.

6.4 Diffusion Limitation Calculation

In a heterogeneous reaction sequence, mass transfer of reactants first takes place from the bulk fluid to the external surface of the catalyst pellet. The reactants then diffuse from the external surface into and through the pores within the pellet. The reaction then takes place on the catalytic surface of the pores.[71]

The role of mass transfer may limit the overall reaction rate. Diffusion limitation includes both external and internal diffusion limitation. To minimize the external diffusion limitation, we used a wrist-action shaker during the reactions. The Weisz-Prater criterion was used to assess the significance of internal diffusion. The Weisz-Prater criterion uses measured values of the rate of reaction, $-r'_A$(obs), to determine

whether internal diffusion is limiting the reaction. The Weisz-Prater parameter (C_{wp}) is shown in equation 6.1.

$$C_{wp} = \eta * \phi^2 = \frac{-r'_{A,obs} * R^2 * \rho_c}{D_e * C_{AS}} \tag{6.1}$$

Where η is the effectiveness factor, ϕ is the Thiele modules, r'_A(obs) is the observed (actual) reaction rate, R is the radius of catalyst particle, ρ_c is the density of the solid catalyst, D_e is the effective diffusivity, and C_{AS} is the concentration of reactant at the catalyst surface.

All the terms in Equation 6.1 can be measured. Therefore, we can calculate C_{wp}. If C_{wp} <1, there are no internal diffusion limitations and consequently no concentration gradient exists within the pellet, and if C_{wp} >1, then internal diffusion limits the reaction severely. [71] We consider a reaction at 400 ℃, the highest temperature used in this study.

To calculate r'_A(obs), we took the ratio of the moles of converted reactant (palmitic acid) over the mass of catalyst (HZSM-5) in gram, and reaction time in seconds. The calculation is shown in equation (6.2):

$$\begin{aligned} -r'_{A,obs} &= \frac{0.97 * 0.15gPA \div 256g/mol}{0.15g \text{ catalyst} * 180 * 60sec} \\ &= 3.51 * 10^{-7} mol/g - s \end{aligned} \tag{6.2}$$

To calculate ρ_c, the density of the solid catalyst, we measured the weight and the volume of a fixed amount of the catalyst, and the following equation (6.3) presents the calculation:

$$\begin{aligned} \rho_c &= \frac{2.469g}{5mL} \\ &= 0.49g/mL \end{aligned} \tag{6.3}$$

R, the radius of catalyst particle, can be estimated from the SEM images of the fresh calcined HZSM-5 (e.g. Figure 6.10) to be 3.57*10^{-4} cm. Therefore R^2 can be calculated simply as in equation 6.4:

$$\begin{aligned} R^2 &= (3.57 * 10^{-4})^2 cm^2 \\ &= 1.27 * 10^{-7} cm^2 \end{aligned} \tag{6.4}$$

C_{AS}, the concentration of reactant at the catalyst surface, was calculated by taking the ratio of the moles of the reactant(PA) and the total volume of the reactor, which is 4 mL. Equation 6.5 shows the calculation for C_{AS}:

$$\begin{aligned} C_{AS} &= \frac{0.15gPA \div 256g/mol}{4mL \text{ reactor}} \\ &= 1.46 * 10^{-4} mol/mL \end{aligned} \tag{6.5}$$

Next, D_e, the effective diffusivity was estimated from the literature. Haag et al.[72] provided the effective diffusivity of 2,2-dimethylpentane in zeolite ZSM-5 as 3 * 10^{-8} cm^2/s.

Finally, since we have all the values we need for the Weisz-Prater criterion, we now calculate the C_{wp} by applying the values to equation 6.1, and the calculation is illustrated in the following:

$$
\begin{aligned}
C_{wp} &= \eta * \phi^2 \\
&= \frac{-r'_{A,obs} * R^2 * \rho_c}{D_e * C_{AS}} \\
&= \frac{3.51 * 10^{-7} \text{ mol/g-s} * 1.27 * 10^{-7} cm^2 * 0.49 \text{ g/mL}}{3 * 10^{-8} cm^2/s * 1.46 * 10^{-4} \text{ mol/mL}} \\
&= 4.99 * 10^{-3}
\end{aligned}
$$

Since the Weisz-Prater criterion (C_{wp}) is 4.99*10^{-3}, which is much less than 1, it is believed that there are no diffusion limitations in the reactions with fresh catalyst. (The SEM images used for measuring the range of particle sizes for regenerated catalyst samples can be found in Appendix B).

CHAPTER VII

Application on Triglyceride Feedstocks

From Chapter 4, we know that high yields of aromatics can be produced from fatty acids in water near the critical point using zeolite catalyst, and the major liquid-phase products were mixed xylenes and toluene. Chapter 5 on effect of reaction variables provided important insights of the process, for example, that more double bonds in the fatty acids led to lower yield of aromatics. To move the potential technology forward, one needs to confront it with real triglyceride feedstock. Therefore, we are motivated to apply this catalytic hydrothermal method to bio-based triglyceride feedstocks. Fatty acids are a major component of many types of plant oils, including algae and coconut, as well as animal fat. This chapter presents results of application of the best reaction conditions found from work with palmitic acid to various types of bio-based triglyceride feedstocks.

7.1 Results and Discussion

This section first reports results from control experiments that validate the methods used in the experiments and determine the extent of chemical transformation from thermal energy alone. Next, we discuss the yields with different types of feedstock by using the catalytic hydrothermal reaction that we had successfully used on fatty acids. The feedstocks we studied are crude algal oil, cold-pressed coconut oil,

peanut oil, and lard.

7.1.1 Control Experiments

The control experiments involved loading algal oil, coconut oil, peanut oil, or lard and water into reactors without any catalyst present. The reactions were conducted at the same reaction conditions (400℃, 200 bar, 180 minutes). All experiments have at least 3 replicates, and we report standard deviations as the experimental uncertainties in these cases.

The gas products for algal oil reactions are light gases, such as hydrogen, methane, carbon dioxide, ethylene, and ethane. The total gas product yield was 8.8 wt% with a standard deviation of 3.4 wt%. There were no significant liquid products detected for reactions with algal oil without catalyst.

For control experiments with coconut oil, the gas products were also light gases, including hydrogen, carbon monoxide, methane, carbon dioxide, ethylene, and ethane. It is similar to the gas products of algal oil but with additional carbon monoxide. The total gas product yield was 4.4 wt% with a standard deviation of 1.3 wt%. However, unlike algal oil, reaction with coconut oil without catalyst generated a total liquid product yield of 26 wt% with a standard deviation of 1.6 wt%. The liquid products were mainly 2-methyl-pentane, xylene, and 2-ethyl-toluene (none of which were originally in the feedstock).

For control experiments with peanut oil, the gas products were light gasses (hydrogen, carbon monoxide, methane, carbon dioxide, ethylene, and ethane) and propane. The total gas product yield was 3.4 wt% with standard deviation of 1.2 wt%. The liquid products with reactions of peanut oil were mainly 2-methyl-pentane, xylene, and 2-ethyl-toluene, which together gave a total liquid product yield of 8.5 wt% with standard deviation of 1.4 wt%.

Finally, we conducted control reactions of lard in water without catalyst, which

gave no significant liquid products that we were able to detect by GC-FID. The gas products included light gases and propane, which were the same types of gas products from control reactions with peanut oil. The total gas product yield for control reactions with lard was 5.4 wt% with a standard deviation of 1.7 wt%.

7.1.2 Algal Oil

The algae crude oil we extracted from Nanochloropsis microalgae hydrochar contains about 51% fatty acids, which are expressed as FAMEs (fatty acid methyl esters). The fatty acid profile for this algal oil is shown in Table 7.1. The fatty acids range from C14 to C22, and are both saturated and unsaturated. We use the omega notation system for fatty acids, where the first number is the total number of carbon atoms in the chain. The number following the colon is the number of double bonds in the chain, and the number following the n- is the location (carbon atom number) of the first double bond. [34] The algal oil production method was in Chapter 3 section 3.2.1.

Table 7.1: Fatty Acid Profile of Crude Algal Oil

FA Type	**wt% in total FAs**
C14:0	2.7%
C14:1n5	6.5%
C16:0	19.0%
C16:1n7	22.4%
C17:0	1.0%
C18:0	0.7%
C18:1n7	0.5%
C18:1n9	0.2%
C18:2n6	3.8%
C18:3n3	5.6%
C20:0	0.7%
C20:4n6	4.9%
C22:1n9	32.0%

The results from from the catalytic hydrothermal reactions of algal oil are summarized in Table 7.2 ("std" refers to "standard deviation"). Besides the major liquid

products listed in Table 7.2, which were the only significant peaks detected by GC-FID, the reactions also led to many products in yields too low to quantify reliably on an individual basis. Because the FID is a carbon counter, and also because the products are primarily hydrocarbons, we used the total peak area of all of the products appearing in the GC/FID chromatogram to estimate the total liquid product yield shown in Table 7.2. We also converted the yield per total mass of algal oil to the yield per total FAMEs by the factor of 51% (the total composition of all FAMEs in algal oil). As we can see from the table, the most abundant liquid products were 2-methyl-pentane, mixed xylenes, and toluene. The reactions also generated an appreciable amount of gas products, including hydrogen, carbon monoxide, carbon dioxide, and C1 to C5 hydrocarbons. Most of these can be used as fuel gases. The most abundant gas-phase products were ethylene and carbon dioxide (6 wt% per total algal oil or 12 wt% per total FAMEs) as shown in Figure 7.1.

Table 7.2: Product Yields (wt%) for Reactions of 150 mg Algal Oil with 150 mg HZSM-5 (silica/alumina ratio of 23), reaction condition: 400 ℃ 180 minutes, water density of 0.1 g/mL

	per total algal oil		per total FAMEs	
wt%	average	std	average	std
Pentane, 2-methyl-	3.56	0.66	6.98	1.29
2-methyl-hexane	0.42	0.29	0.83	0.57
2-pentanone	0.07	0.09	0.14	0.17
Heptane	0.06	0.07	0.12	0.13
Toluene	0.89	0.27	1.75	0.52
Mixed xylenes	2.02	0.49	3.97	0.95
Propyl-benzene	0.62	0.77	1.21	1.51
2-ethyl-toluene	0.21	0.07	0.42	0.14
Total major liquid products	11.79	1.19	23.12	2.33
Estimated total liquid products	18.52	2.47	36.31	4.84
Total gas products	27.49	5.39	53.90	10.57
Total yield	46.01	5.18	90.21	10.15

The total liquid-phase product yield from algal oil was lower than from pure fatty acid, such as palmitic acid. The total liquid product yield was 36 wt% per FAMEs with standard deviation of 4.8 wt% for reactions with algal oil, while the total liquid

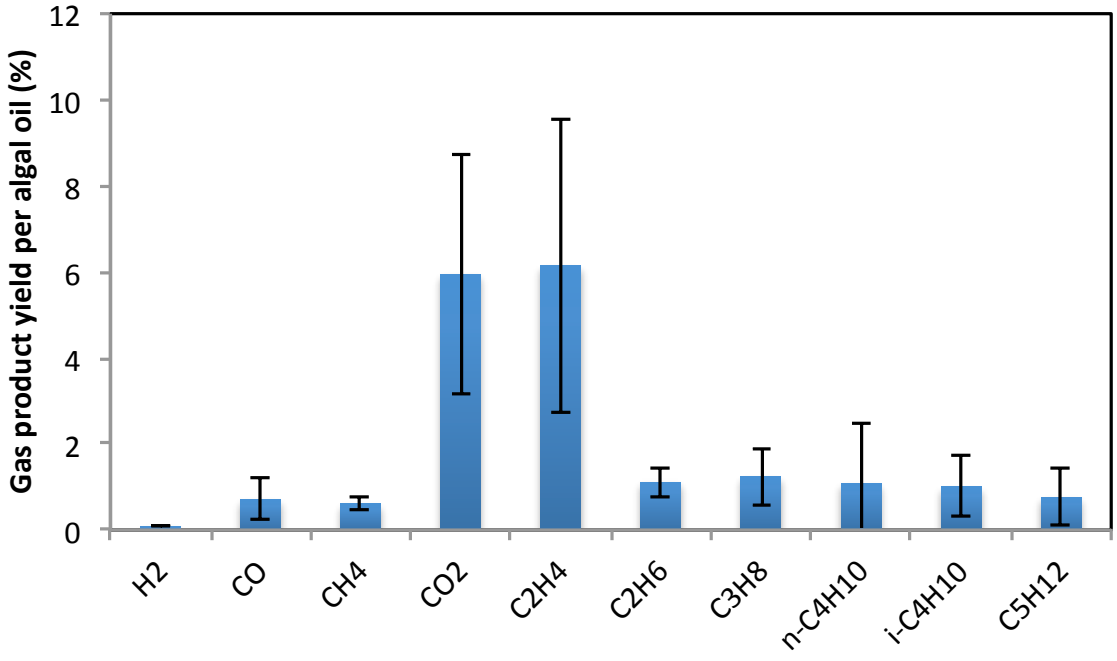

Figure 7.1: Gas product yields from catalytic hydrothermal reactions with 150 mg algal oil with 150 mg HZSM-5 (silica/alumina ratio of 23), at water density of 0.1 g/mL, 400℃, 180 minutes

product yield for reactions with palmitic acid was 86 wt% with standard deviation of 1 wt%.[73] However, the reactions with algal oil generated more gas-phase products (54 wt% with std of 11 wt%) than the reactions with palmitic acid (11 wt% with std of 3 wt%). We know that the algal oil has the highest gas-phase product yield (8.8 wt%) for non-catalyzed thermal cracking among all tested feedstocks and palmitic acid (4.0 wt% gas product yield). This means that algal oil is easier to be cracked into small gas phase molecules compared to fatty acid and the other feedstocks under thermal heating alone.

A possible explanation for a significantly higher gas-to-liquid product ratio is that the reaction condition at 400 ℃ is too severe for the algal oil cracking reaction, and some liquid products were cracked further into gases. To test this hypothesis, we carried out catalytic hydrothermal reactions of algal oil at a lower temperature (380 ℃) and at the same water density of 0.1 g/mL, this led to a reaction pressure of 184 bar. Therefore the reactions occurred in sub-critical pressure region. We kept all the other reaction conditions the same as for reactions at 400 ℃.

Table 7.3 shows the product yields of the algal oil reactions with zeolite HZSM-5 (silica/alumina ratio of 23) at 380 ℃. The total liquid product yield was 32 wt% per total FAMEs, which is lower than 36 wt% of the reactions at 400 ℃. The major liquid products were the same as the reactions at 400 ℃, which were 2-methyl-pentane, mixed xylenes, and toluene. The total gas product yield of reactions at 380 ℃ (27 wt%) was lower than the total gas product yield of reactions at 400 ℃ (54 wt%). Together, this contributed to a lower total yield for reactions at a lower temperature, indicating that hydrothermal reactions further occurred past 380 ℃. The most abundant gas product is carbon dioxide as shown in Figure 7.2. There was significantly less ethylene product for reactions at 380 ℃ compared to that at 400 ℃.

We also noticed that from 380 ℃ to 400 ℃, the total liquid product yield per FAMEs dropped 5 wt%, and the total gas product yield per FAMEs climbed 27 wt%,

though there is a large experimental uncertainty for the gas product yield at 400 ℃. The ratio of gas product yield to liquid product yield increased from 0.84 to 1.48 when the temperature increased from 380 ℃ to 400 ℃. This suggests that temperature has an effect on the product distribution between liquid and gas phases, and it is possible that liquid products were further cracked into gas products under the 400 ℃ catalytic hydrothermal condition.

Table 7.3: Product Yields (wt%) for Reactions of 150 mg Algal Oil with 150 mg HZSM-5 (silica/alumina ratio of 23), reaction condition: 380 ℃ 180 minutes, water with density of 0.1 g/mL

	per total algal oil		per total FAMEs	
wt%	average	std	average	std
Pentane, 2-methyl-	3.47	0.17	6.81	0.34
2-methyl-hexane	0.51	0.14	1.00	0.27
2-pentanone	0.23	0.01	0.45	0.03
Heptane	0.16	0.01	0.31	0.02
4-methyl-heptane	0.26	0.01	0.50	0.01
Toluene	1.29	0.10	2.53	0.20
Mixed Xylenes	2.91	0.35	5.71	0.69
Propyl-benzene	0.42	0.04	0.83	0.07
2-ethyl-toluene	0.21	0.01	0.41	0.02
Total major liquid products	9.46	0.71	18.54	1.39
Estimated total liquid products	16.13	2.01	31.63	3.94
Total gas products	13.63	1.01	26.72	1.99
Total yield	29.76	1.52	58.35	2.97

After applying the catalytic hydrothermal method to crude algal oil, we found there was a difference in product distribution between the crude algal oil, and pure palmitic acid. The reactions with crude algal oil gave a higher ratio of gas-to-liquid product yield and a higher alkane percentage in the total liquid product yield than those of palmitic acid. Also, the liquid product yields were lower with crude algal oil compared to the reactions with a pure fatty acid. As we have discussed earlier in the FAME analysis of algal oil, the total composition of fatty acids in the crude algal oil was only 51 wt%, which could be a reason for a lower yield. It is also possible the components in the crude algal oil interfered with the conversion of triglycerides. Therefore, we examined additional real, but better refined, renewable triglycerides

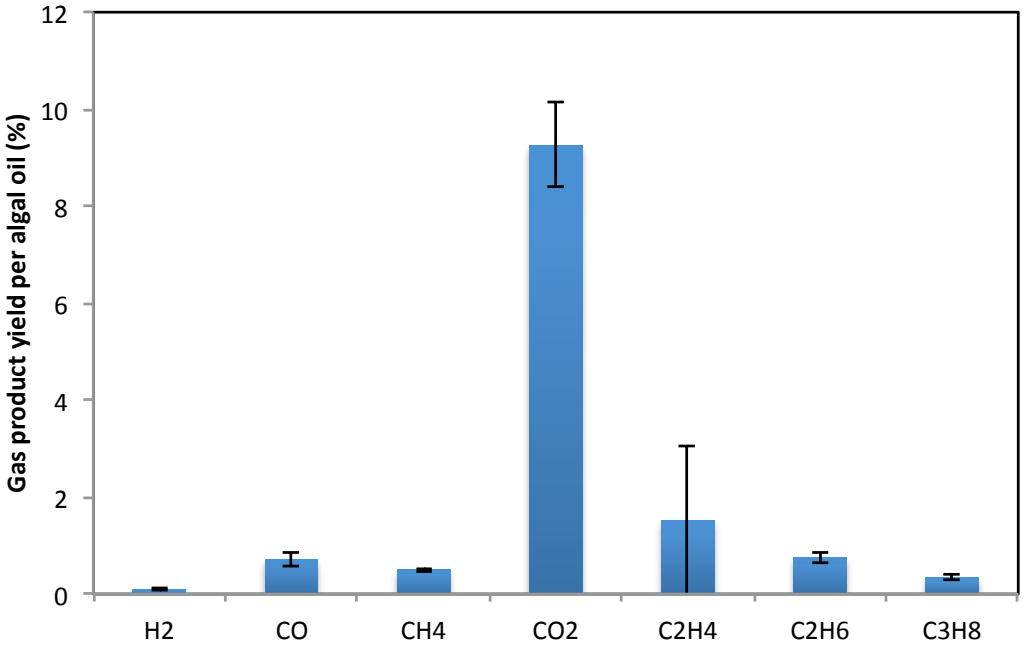

Figure 7.2: Gas product yields of catalytic hydrothermal reactions with 150 mg algal oil, 150 mg HZSM-5 (silica/alumina ratio of 23), at water density of 0.1 g/mL, 380℃, 180 minutes

feedstocks to test this zeolite catalytic hydrothermal cracking method.

7.1.3 Other Triglyceride Feedstocks

The use of vegetable oils as renewable fuel rather than petroleum has a long history. However, there are many disadvantages for using vegetable oils to produce diesel fuel, including high cost, competition with food, high viscosity, lower volatility, and the reactivity of unsaturated hydrocarbon chains of the product.[74] If the products from vegetable oil were at higher value than bio-fuel, the process would be more attractive. There are some studies of conversion of vegetable oil to chemicals using zeolite HZSM-5, but none were in water near its critical point.[75–78] Since we have successfully applied the catalytic hydrothermal process to pure fatty acids for production of industrial bulk chemicals, we would like to use the same process for vegetable oil, which normally contains a large percentage of fatty acids.

We chose coconut oil and peanut oil. Coconut oil is known for its high degree of saturation. The label of the coconut oil sample indicates a 87 wt% saturated fatty acids composition. earlier work showed that the more saturated the fatty acids were, the higher aromatic yield we would obtain.[73]. We also included animal fat, lard, as one of our feedstocks for testing this method. The cost of lard, for example, is about 60% lower than the cost of coconut oil.

Before we started the reaction experiments with different oils and fat, we carried out FAME analysis on these feedstock to understand the exact composition of fatty acids in them. Table 7.4, 7.5,and 7.6 show the fatty acid profile in coconut oil, peanut oil and lard respectively. Coconut oil contains a total fatty acids content of 84% with a standard deviation of 1.6%, peanut oil contains a total fatty acids content of 89% with a standard deviation of 1.3%, and lard contains a total fatty acids content of 88% with a standard deviation of 0.3%. We found that the most abundant fatty acid in coconut oil was C12:0 (50%), followed by C14:0 (19%). The saturated fatty

acids composition of total fatty acids was 91.2%. The most abundant fatty acid in peanut oil was C18:1n11 (58%), followed by C18:2n6 (24%). The saturated fatty acids composition of total fatty acids was only 19.4%. For lard, the most abundant fatty acid was C18:1n11 (36%), followed by C18:1n9 (16%). The saturated fatty acids composition of total fatty acids was 27.9%.

Table 7.4: Fatty Acid Profile of Coconut Oil

FA Type	**wt% in total FAs**
C8:0	8.0%
C10:0	6.3%
C12:0	49.6%
C14:0	18.9%
C16:0	8.3%
C18:1n9	2.9%
C18:1n11	5.1%
C18:2n6	0.8%

Table 7.5: Fatty Acid Profile of Peanut Oil

FA Type	**wt% in total FAs**
C16:0	9.4%
C18:1n9	2.6%
C18:1n11	57.8%
C18:2n6	23.9%
C20:0	0.3%
C20:1	1.2%
C20:2	1.7%
C22:1	3.1%

Table 7.7, 7.8, and 7.9 showed the product yields for reactions with coconut oil, peanut oil, and lard respectively. Mixed xylenes are the most abundant products in the liquid phase, with yields of 21 wt% for coconut oil, 34 wt% for peanut oil, and 33 wt% for lard. Toluene has the second highest liquid product yield, 7 wt% for coconut oil, 14 wt% for peanut oil, and 11 wt% for lard. Peanut oil and lard have the same types of major liquid products as listed in Table 7.8 and Table 7.9, while coconut oil generated very similar types of liquid products, except there was no 4-methyl-heptane detected. Summing the mass yields of the major aromatic hydrocarbons in Table 7.7,

Table 7.6: Fatty Acid Profile of Lard

FA Type	**wt% in total FAs**
C14:0	1.4%
C16:0	25.5%
C16:1	1.9%
C17:0	0.4%
C18:1n9	16.1%
C18:1n11	36.3%
C18:2n6	16.3%
C20:0	0.6%
C20:1	0.3%
C20:2	0.7%
C20:3n3	0.6%

7.8, and 7.9, shows that the major aromatics yield of coconut oil was 31 wt% with a standard deviation of 7 wt%, the major aromatics yield of peanut oil was 52 wt% with a standard deviation of 15 wt%, and the major aromatics yield of lard was 48 wt% with a standard deviation of 4 wt%. All these aromatic yields were based on the mass of oils/fat instead of mass of FAMEs. In the feedstock, this result shows that the most saturated fatty acid feedstock (coconut oil) gave the lowest major aromatic yield. This indicates that the real feedstock does not follow the trend with higher degree of saturation of the fatty acids, as observed in the pure fatty acid reactions. The reason for this difference is not clear at present. The complexity of the fatty acid profile in the feedstock may make it more difficult to observe the effect of degree of saturation since some other factors may affect the product yield as well, such as the alkyl chain length of fatty acids.

The total product yields of reactions with peanut oil and lard per FAMEs did exceed 100%. Probably because non-triglycerides components in the feedstocks can also form products.

By comparing Tables 7.2,7.3 (algal oil) and Tables 7.7,7.8,7.9 (vegetable oils and lard) for the product profiles of reactions with different feedstocks, it is interesting that unlike pure fatty acids or all the other types of triglyceride feedstocks, crude algal

oil gave a high percentage yields of alkanes, including the most abundant product, 2-methyl-pentane. The other feedstocks gave a high percentage yields of aromatics with the abundant product as mixed xylenes. Pie charts of the distribution of liquid products from these various types of renewable feedstocks are included in Appendix C.

Table 7.7: Product Yields (wt%) for Reactions of 150 mg coconut Oil with 150 mg HZSM-5 (silica/alumina ratio of 23), reaction condition: 400 ℃ 180 minutes, water with density of 0.1 g/mL

	per total coconut oil		per total FAMEs	
wt%	average	std	average	std
Pentane, 2-methyl-	3.86	0.06	4.59	0.07
2-methyl-hexane	1.35	0.73	1.61	0.87
2-pentanone	0.26	0.12	0.31	0.15
Heptane	0.23	0.07	0.28	0.09
Toluene	7.00	2.04	8.34	2.42
Mixed xylenes	21.41	4.64	25.49	5.52
Propyl-benzene	2.43	0.30	2.89	0.36
2-ethyl-toluene	0.47	0.16	0.56	0.20
1,2,4-trimethylbenzene	0.09	0.16	0.11	0.19
Total major liquid products	37.11	7.26	44.18	8.65
Estimated total liquid products	56.07	5.33	66.75	6.34
Total gas products	10.18	2.67	12.12	3.18
Total yield	66.25	5.46	78.87	6.51

While Tables 7.7, 7.8, and 7.9 listed the total gas product yields of the hydrothermal catalytic reactions of coconut oil, peanut oil, and lard with zeolite HZSM-5, Table 7.10 shows the profile of the gas phase products with the different feedstocks. Carbon dioxide was the most abundant gas product for coconut oil, followed by ethylene. Similarly, carbon dioxide was also the most abundant gas product for peanut oil, but followed by n-butane, while for lard, the major gas products were carbon dioxide, n-butane, and ethylene. Carbon dioxide could be generated through different pathways in the reactions, such as steam reforming reaction, water gas shift reaction, and decarboxylation. Ethylene is a common gas product from catalytic cracking reactions, for example cracking of ethane to ethylene and hydrogen. However, to confirm the actual pathways that led to those gas products, more studies would be required.

Table 7.8: Product Yields (wt%) for Reactions of 150 mg peanut Oil with 150 mg HZSM-5 (silica/alumina ratio of 23), reaction condition: 400 ℃ 180 minutes, water with density of 0.1 g/mL

	per total peanut oil		per total FAMEs	
wt%	average	std	average	std
Pentane, 2-methyl-	4.59	0.48	5.16	0.54
2-methyl-hexane	1.40	0.71	1.57	0.79
2-pentanone	0.77	0.54	0.86	0.60
Heptane	0.44	0.19	0.50	0.21
4-methyl-heptane	0.28	0.06	0.32	0.07
Toluene	14.01	6.88	15.74	7.73
Mixed xylenes	34.36	8.73	38.60	9.81
Propyl-benzene	3.55	1.17	3.99	1.32
2-ethyl-toluene	0.69	0.12	0.77	0.13
1,2,4-trimethylbenzene	0.25	0.26	0.29	0.29
Total major liquid products	60.34	16.43	67.79	18.46
Estimated total liquid products	88.33	11.66	99.25	13.11
Total gas products	12.23	3.95	13.74	4.43
Total yield	100.56	8.60	112.99	9.67

Table 7.9: Product Yields (wt%) for Reactions of 150 mg lard with 150 mg HZSM-5 (silica/alumina ratio of 23), reaction condition: 400 ℃ 180 minutes, water with density of 0.1 g/mL

	per total lard		per total FAMEs	
wt%	average	std	average	std
Pentane, 2-methyl-	3.55	0.39	4.04	0.44
2-methyl-hexane	2.01	0.40	2.29	0.46
2-pentanone	0.32	0.03	0.37	0.04
Heptane	0.27	0.04	0.31	0.05
4-methyl-heptane	0.22	0.01	0.25	0.01
Toluene	11.24	1.03	12.77	1.17
Mixed xylenes	32.69	2.64	37.14	3.00
Propyl-benzene	3.23	0.34	3.67	0.39
2-ethyl-toluene	0.66	0.04	0.75	0.04
1,2,4-trimethylbenzene	0.28	0.13	0.32	0.15
Total major liquid products	54.47	3.98	61.90	4.52
Estimated total liquid products	86.72	5.47	98.55	6.21
Total gas products	16.58	7.33	18.84	8.33
Total yield	103.30	3.36	117.39	3.82

Table 7.10: Gas Product Yields for Reactions of different feedstocks with 150 mg HZSM-5 (silica/alumina ratio of 23), reaction condition: 400 ℃ 180 minutes, water with density of 0.1 g/mL

wt%	coconut oil		peanut oil		lard	
	average	std	average	std	average	std
H2	0.11	0.02	0.08	0.03	0.07	0.01
CO	0.34	0.11	0.06	0.07	0.28	0.09
CH4	0.14	0.05	0.11	0.01	0.15	0.03
CO2	4.60	0.58	3.90	0.81	4.12	1.26
C2H4	2.12	0.37	1.01	0.98	3.33	2.66
C2H6	0.20	0.04	0.13	0.01	0.19	0.07
C3H8	0.67	1.16	2.11	0.53	2.55	1.67
n-C4H10	0.98	0.88	2.88	0.96	3.44	2.40
i-C4H10	0.68	0.62	1.05	0.33	1.38	0.91
C5H12	0.45	0.41	0.97	0.34	1.14	0.75

Figure 7.3 demonstrated the total major aromatic, total liquid, and total gas product yield for different types of feedstocks, including crude algal oil, coconut oil, peanut oil, lard and palmitic acid. Figure 7.4 indicates that peanut oil (88 wt%) and lard (87 wt%) gave the highest total liquid product yield, followed by coconut oil (56 wt%) and algal oil (19 wt%). Peanut oil and lard behaved as good as the pure palmitic acid for aromatics production under the same catalytic hydrothermal reaction condition, where the total liquid product yield with pure palmitic acid was 86 wt%. Therefore, we conclude that among the feedstocks we tested, lard is the most promising feedstock for aromatic chemical production because of the high yield and also because it costs less than peanut and coconut oil. We suspect that if the crude algal oil were purified to a much more refined oil like the peanut oil we used, it would lead to a much higher aromatic product yield.

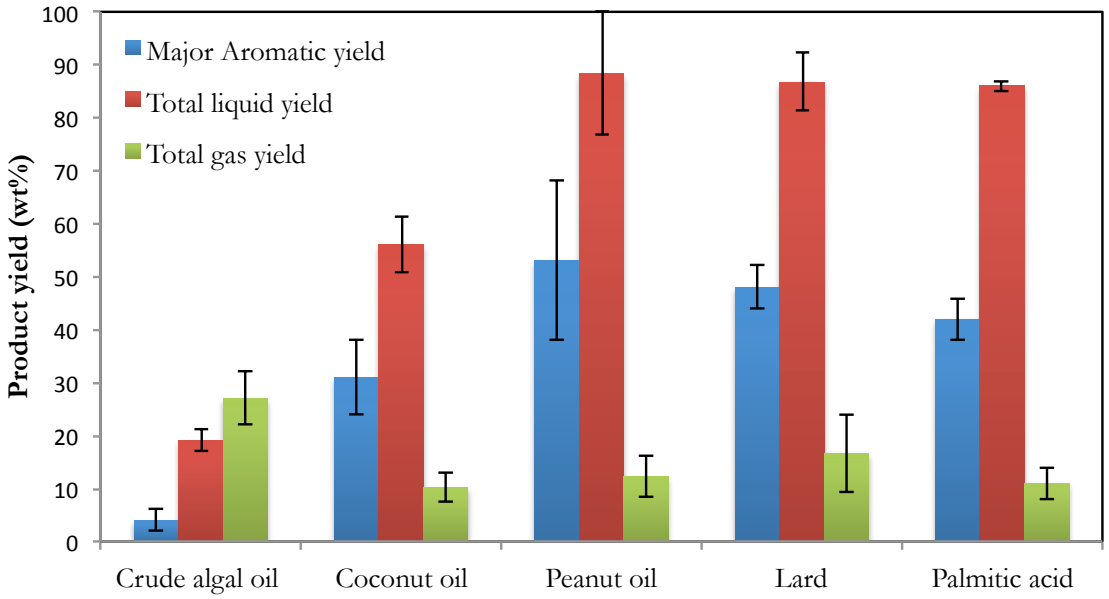

Figure 7.3: Total major aromatic, liquid, and gas product yield of different types of feedstocks, reaction condition: reactant-to-catalyst ratio of 1, silica/alumina ratio of 23, 400 ℃, 180 minutes, water density of 0.1 g/mL

7.2 Summary of Method Application on Triglycerides Feedstocks

This work is the first that applied catalytic hydrothermal reaction method with zeolite to triglyceride feedstocks for hydrocarbon chemical production (e.g.aromatics). The results presented herein demonstrate a total product yield of 46 wt% from reactions of algal oil under catalytic hydrothermal method. More specifically, for reactions with algal oil, water, and zeolite HZSM-5 (silica/alumina ratio of 23), at 400℃, the total yield was 90 wt% per FAMEs in algal oil. This includes 36 wt% of liquid products and 54 wt% of gas products. The major liquid products were 2-methyl-pentane, mixed xylenes, and toluene, and the most abundant gas product was carbon dioxide.

At a lower temperature, 380℃, the total yield was 45 wt% per FAMEs in algal oil, which includes 19 wt% of liquid products and 27 wt% of gas products. Again, 2-methyl-pentane, mixed xylenes, and toluene were the most abundant liquid products

in this case. The temperature has an effect on the total yield as well as the liquid-to-gas product ratio.

Besides algal oil, this work also broadens to other common renewable feedstocks, such as coconut oil, peanut oil, and lard. We have successfully applied this catalytic hydrothermal method on these various types of feedstock, and have achieved considerable yields of aromatics. FAME analysis has been done on those samples to get the fatty acid profiles. Coconut oil has the most saturated fatty acids, followed by lard then peanut oil. This suggested that the real feedstock does not follow the trend we observed from pure fatty acids: the higher product yields with higher degree of saturation of the fatty acids.

More work on upgrading the crude algal oil would be a great direction for improving the product yield of reactions with algal oil. Study of different reaction factors on the reactions with the real feedstocks could be another future work to pursue in order to find potential tools for tuning the product distribution as desired.

CHAPTER VIII

Conclusions and Future Work

This thesis concludes by identifying the key findings from the work, and the significance of those findings, while also providing some suggestions for future work on the foundations laid herein.

The key findings of this work may be concluded as follows:

(1) Aromatics can be produced via zeolite-catalyzed hydrothermal reactions of palmitic acid. At 400 ℃, and 180 minutes, the major aromatic products include toluene, 1,4-dimethyl-benzene (p-xylene), 1-ethyl-2-methyl-benzene, and 1,2,4-trimethyl-benzene. The other xylene isomers and propylbenzene are also present. The major alkanes include 2-methyl-pentane, 2-methyl-hexane, heptane, and 4-methyl-heptane. Among the gas phase products, there were C1 to C5 alkanes, CO, CO_2, and H_2. There were more liquid products than gas products at our tested reaction conditions, and among different liquid products, mixed xylenes (p,m,o-xylene) took up 50 wt% of the total of all identified and quantified liquid products.

(2) The palmitic acid conversion at 400 ℃ was consistent with first-order kinetics. The activation energy for PA disappearance was determined to be 31 +/- 1 kJ/mol, and the Arrhenius pre-exponential factor was $5.6 * 10^{-2} \pm 2.2 * 10^{-3} s^{-1}$ or $1.5 * 10^{-3} \pm 5.9 * 10^{-5} L * gcat^{-1} s^{-1}$. Some possible reaction pathways were deduced from the product analysis, such as catalytic cracking, decarboxylation, decarbonylation, and

transalkylation between toluene, 1,2,4-trimethyl-benzene, and p,m,o-xylene. This finding provides a foundation for completing the reaction pathways and kinetics in the future.

(3) Among all the water densities we have examined, a water density of 0.1 g/mL provided the highest yields of xylenes and toluene, and the highest yield of total liquid products. The yields of the various products responded differently to the presence of water and to its density. The yield of acetic acid, for example, increased nearly 50-fold as the water density increased from zero to 0.15 g/mL. Other products showing consistently increasing yields with increasing water density (though less dramatic than acetic acid) include 2-methyl-pentane, butanal, 2-methyl hexane, 2-ethyl toluene, and pentane. In contrast to the behavior of the products just listed, the yields of other products either consistently decrease with increasing water density or exhibit a maximum yield at some intermediate density. Toluene, trimethyl-benzene, 2-pentanone, CO, methane, ethane, and propane are examples of the former, and heptane, 4-methyl-heptane, xylenes, propyl benzene, butanes, and CO_2 are examples of the latter. The water density could be a potential tool for improving the desired product yield based on the different responses that products have to the variation of water density.

(4) Zeolite ZSM-5 is active in water near its critical point. Among the catalysts we have studied, zeolite ZSM-5 is the most promising catalyst for hydrothermal reaction with fatty acids for aromatic hydrocarbon production. The reaction results showed that under reaction condition of 400℃, 180 mins, reactant-to-catalyst ratio of 1, and water density of 0.15 g/mL, ZSM-5 gave the highest conversion of 95 ± 4%. The conversion with zeolite Y was about 50%, and zeolite beta gave the lowest PA conversion (30%). Zeolites beta and Y gave 2-methyl-pentane as the most abundant liquid product, while ZSM-5 gave toluene and xylenes as the major products.

(5) The reaction that forms single-ring aromatics is first-order in catalyst, which

means operating at even lower palmitic acid-to-ZSM-5 ratios should offer even higher yields of aromatics. The PA conversions and the total product yields both decreased as the reactant-to-catalyst ratio increased, as expected. Though one prefers a high reactant-to-catalyst ratio, the highest total product yield (76 wt%) and the highest PA conversion (95%) were achieved at the lowest reactant-to-catalyst ratio (1) examined.

(6) The yields of the aromatic products decreased as the degree of unsaturation of fatty acids increased. The ratio of the total liquid product yield to the total gas product yield decreased with increasing unsaturation. This shift in the product distribution with the extent of unsaturation shows that changing the number of double bonds in the fatty acids can be a potential tool for controlling the product distribution for catalytic hydrothermal reactions with fatty acids.

(7) The silica/alumina ratio of the zeolite catalyst can be used for tuning the product distribution. Among zeolites with different silica/alumina ratios (23, 30, 50, and 80), ZSM-5 with silica/alumina = 23 gave the highest total product yield of 97 ± 2 wt% and the highest conversion of 98 ± 1%. As the silica/alumina ratio increased, the yields of the major products, toluene and xylenes, decreased. In addition, silica/alumina ratio has influence on the distribution between liquid and gaseous products. ZSM-5 with a silica/alumina ratio of 23 gave the largest difference between the liquid and gas yields, with the liquid products dominating.

(8) Zeolite ZSM-5 can be regenerated and reused in this hydrothermal process. Even though the molar yields of the major products (toluene and xylenes) decreased slightly with each reuse and regeneration of the catalyst, appreciable yields of these desirable aromatic products were still obtained. The total product yield decreased from 76 ± 13 wt% with the fresh catalyst to 53 ± 1.9 wt% upon its second use. This irreversible deactivation in the first reaction regeneration cycle is typical of HZSM-5 zeolites, and one reason is the loss of a certain fraction of the Bronsted strong acid sites in hot compressed water, which are required for the cracking reactions.

The total product yields were about the same for the second and third uses of the catalyst, which suggests that this hydrothermal reaction regeneration process might be effective for hydrothermal conversion of fatty acids to hydrocarbons with value as fuels or chemicals.

X-ray Powder Diffraction (XRD), Brunauer-Emmett-Teller (BET), and Scanning Electron Microscope (SEM) techniques were applied on the zeolite catalyst used in the reactions for assessing the catalyst characterization. XRD results verified that the HZSM-5 retained its major structural elements during the reaction, while BET results suggested the use and regeneration of the catalysts decreased both the surface area and the pore volume, but not the average pore diameter, which implies that a modest reduction in activity with regeneration and reuse noted previously could be due to loss of surface area and pore volume. SEM results indicated that the fresh sample has more uniform particle sizes, and some particles combined and some crumbled after hydrothermal reactions. The regeneration procedure reduced the prevalence of larger particles.

The study in catalyst reuse is important for applying the process in industry, and this finding showed the potential to use this proposed process in real world.

(9) This zeolite catalytic hydrothermal cracking method can be applied to other bio-based triglyceride feedstocks (crude algal oil, coconut oil, peanut oil, or lard).

The product yield from reactions with crude algal oil was lower than that from pure fatty acids. When applying the catalytic hydrothermal method to crude algal oil at 400 ℃, the total liquid-phase product yield was lower than when applied to pure fatty acid, such as palmitic acid. The total liquid product yield was 36 wt% per FAMEs with standard deviation of 4.5 wt% for reactions with algal oil, while the total liquid product yield for reactions with palmitic acid was 86 wt% with a standard deviation of 1 wt%. However, the reactions with algal oil generated more gas-phase products (47 wt% with std of 15 wt%) than the reactions with palmitic acid (11 wt%

with std of 3 wt%).

Mixed xylenes were the most abundant products in the liquid phase with yields of 21 wt% for coconut oil, 34 wt% for peanut oil, and 33 wt% for lard. Toluene has the second highest liquid product yield, 7 wt% for coconut oil, 14 wt% for peanut oil, and 11 wt% for lard. The major aromatics yield of coconut oil, peanut oil, and lard was 31 $\pm$ 7 wt%, 52 $\pm$ 15 wt%, and 48 $\pm$ 4 wt% respectively. (All these aromatic yields were based on per oils/fat instead of per FAMEs) These results showed that the catalytic hydrothermal method with those renewable feekstocks is facilitated to produce considerable yields of aromatic hydrocarbons and are very close to the yields from reactions with pure fatty acids.

The suggestions for future work can be summarized as follows:

(1) Further study of the reaction pathways and kinetics would be one direction for future work. It could provide a clearer picture of how each aromatic hydrocarbon was generated, and therefore provide potential information on product selectivity. Analyze products from reactions at different times in a continuous flow reactor would be a good way to identify the primary products and the secondary products.

(2) Apply other types of solvent instead of acetone to collect products from reactions for potential improvement of mass balance.

(3) We only carried out three cycles of experiments due to time constraints, but one can further study the product yield and catalyst behavior in the long run, such as in ten cycles in batch reactors or carry it in a flow reactor, which would be helpful for understanding the hydrothermal stability of the catalyst.

(4) Experiments of algal oil with zeolite ZSM-5 without water would be an interesting approach to try, since crude algal oil doesn't behave well in hydrothermal condition.

(5) Refine the crude algal oil to have a higher concentration of fatty acid content and less of other inorganic minerals. This would be helpful for improving the desired

product yields from algal oil.

(6) Carry out economic analysis of this process to provide information for potential application in industry.

(7) Access the environmental impact of the process to compare with the conventional chemical production process from fossil fuel. An Life Cycle Analysis (LCA) study would be helpful to understand the potential sustainability benefits and risks of the renewable feedstocks. GHG emissions and energy consumption are possible emphasis for minimizing environmental impacts by using renewable feedstocks.

Overall, this research provided several unique and interesting findings, which have direct applications in high-value chemical production using the catalytic hydrothermal process. We believe that the results presented herein serve as a foundation that can be built upon by some of the further studies that we mentioned above, to attain better understanding of this process and to push forward the real implementation of this "green" methodology in the real-world chemical industry.

APPENDICES

APPENDIX A

Experimental procedures of making amorphous silica-alumina catalyst

Amorphous silica-alumina was introduced as an unstructured catalyst in order to compare with the activity of HZSM-5 in hydrothermal environment. The amorphous silica-alumina catalyst was prepared by the following steps. First, 16 g of tetraethyl orthosilicate (TEOS) was hydrolyzed with 10 g of 0.2 M aqueous hydrochloric acid at room temperature for 45 minutes, which formed solution A. Once the initially two phase system in solution A became monophasic, solution B, which contained 0.523 g of aluminum isopropoxide in 7 g of isopropyl alcohol, was added to solution A, and the mixture was stirred for 10 minutes to complete the hydrolysis of the Si and Al alkoxides. Drop-wise addition of ammonia hydroxide was used to bring the mixture to the gel point. The co-gel obtained was left for aging at room temperature overnight without stirring, followed by vacuum filtering and a wash with DI water. It was ready to use after drying at 110 ℃ overnight and crushed into powder. The last step was to activate the catalyst by calcination at 550 ℃ for 14 hours.

APPENDIX B

SEM images of catalyst HZSM-5

Figure B.1 to B.6 are SEM images of fresh calcined HZSM-5 at different magnification or angles. The figures were arranged in the order of a decreasing magnification, and the magnification ranged from 2333 times to 593 times.

Figure B.7 to B.12 are SEM images of HZSM-5 that have been used once for reaction and not get regenerated, at different magnification or angles. The figures were arranged in the order of a decreasing magnification, and the magnification ranged from 4667 times to 146 times.

Figure B.13 to B.17 are SEM images of the HZSM-5 that has been used and regenerated once, at different magnification or angles. The figures were arranged in the order of a decreasing magnification, and the magnification ranged from 3492 times to 55 times.

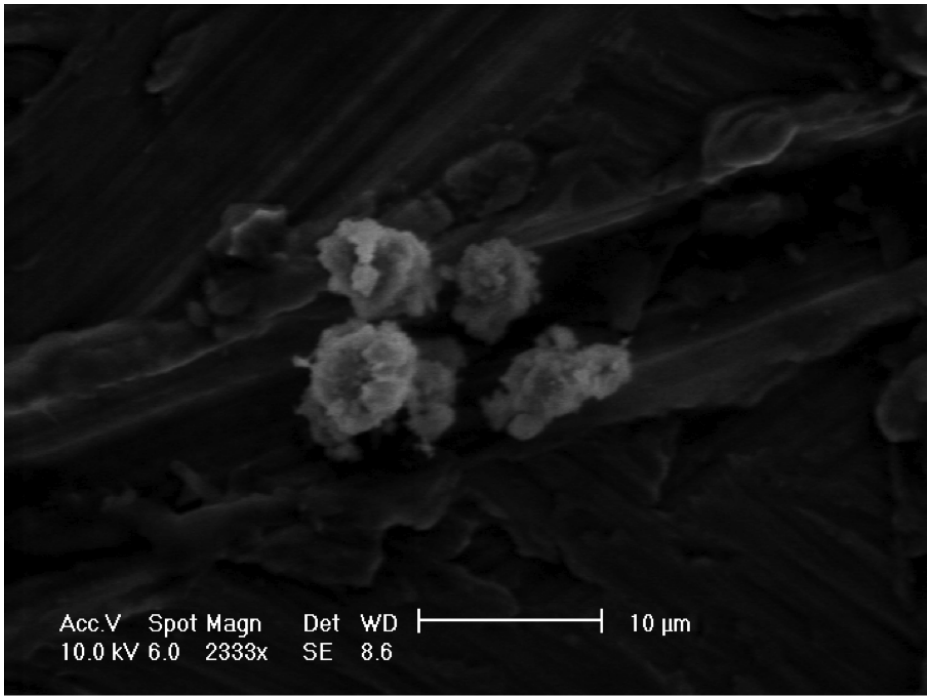

Figure B.1: SEM image of fresh calcined HZSM-5, before reactions.

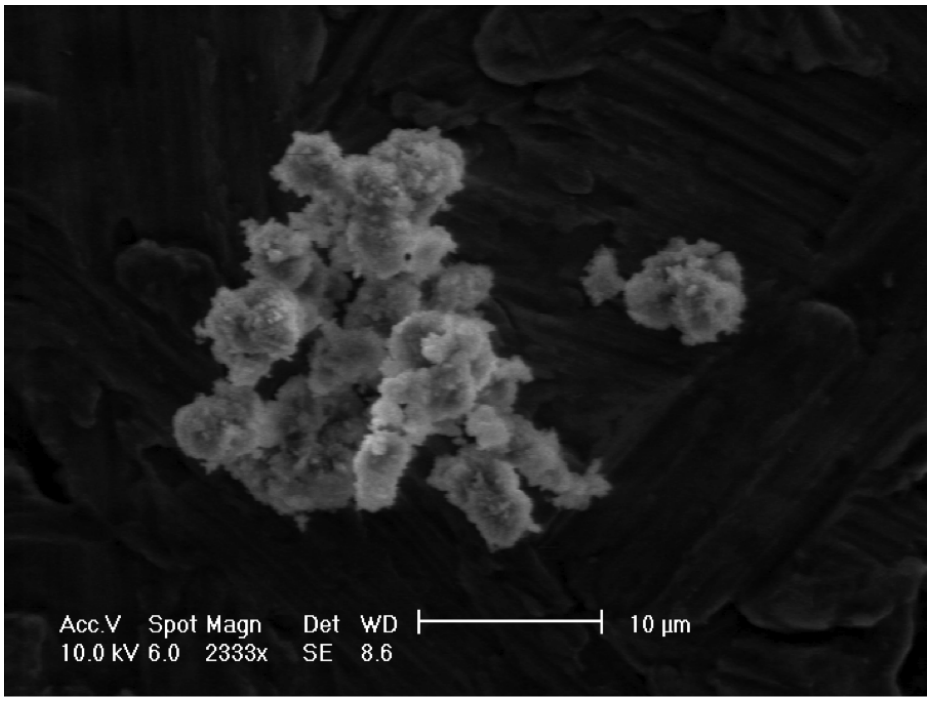

Figure B.2: SEM image of fresh calcined HZSM-5, before reactions.

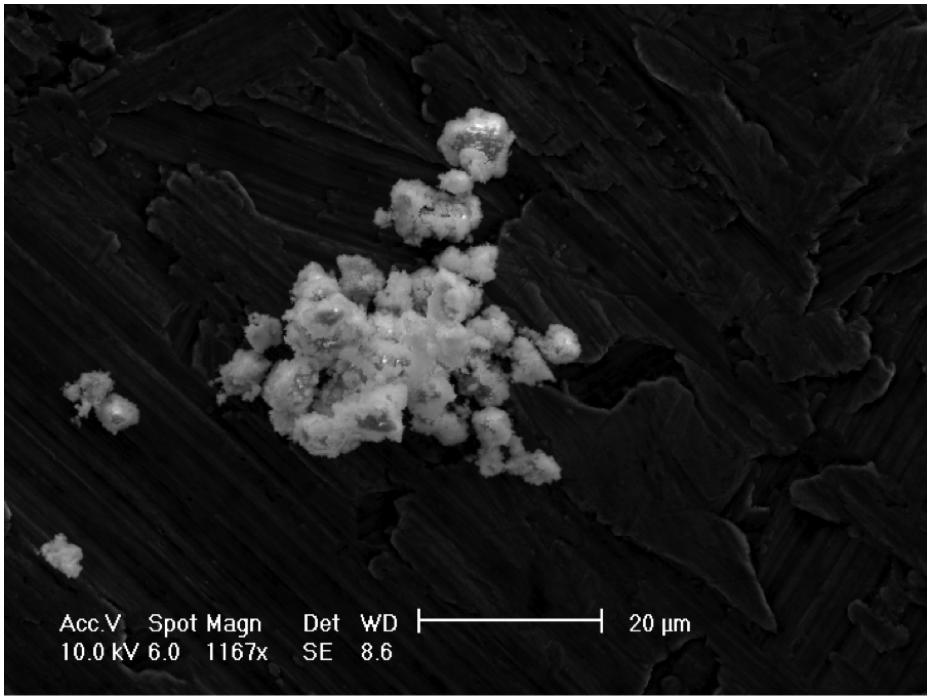

Figure B.3: SEM image of fresh calcined HZSM-5, before reactions.

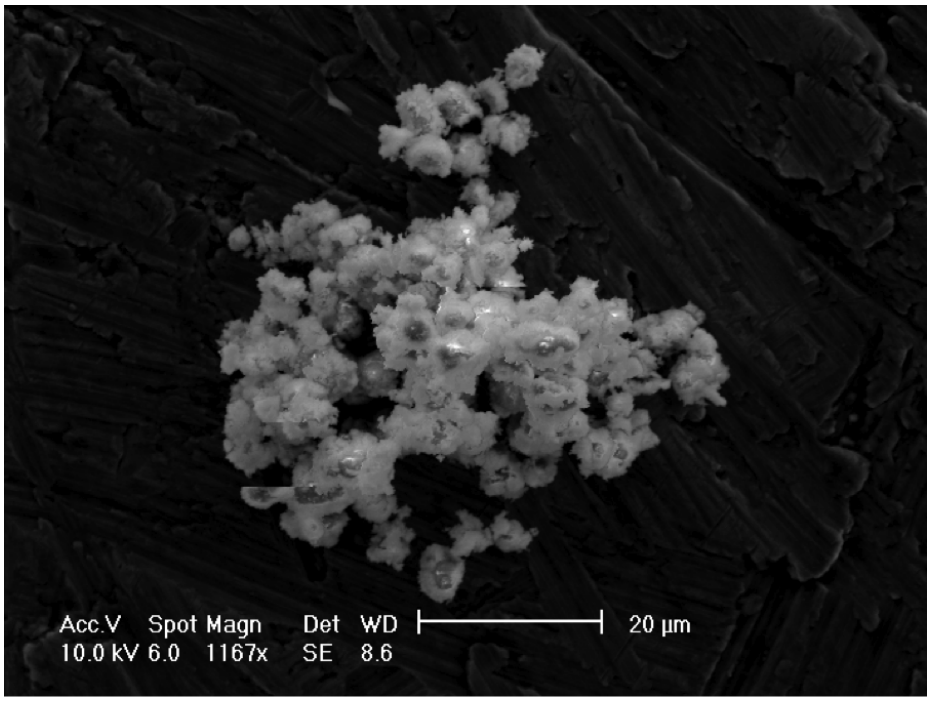

Figure B.4: SEM image of fresh calcined HZSM-5, before reactions.

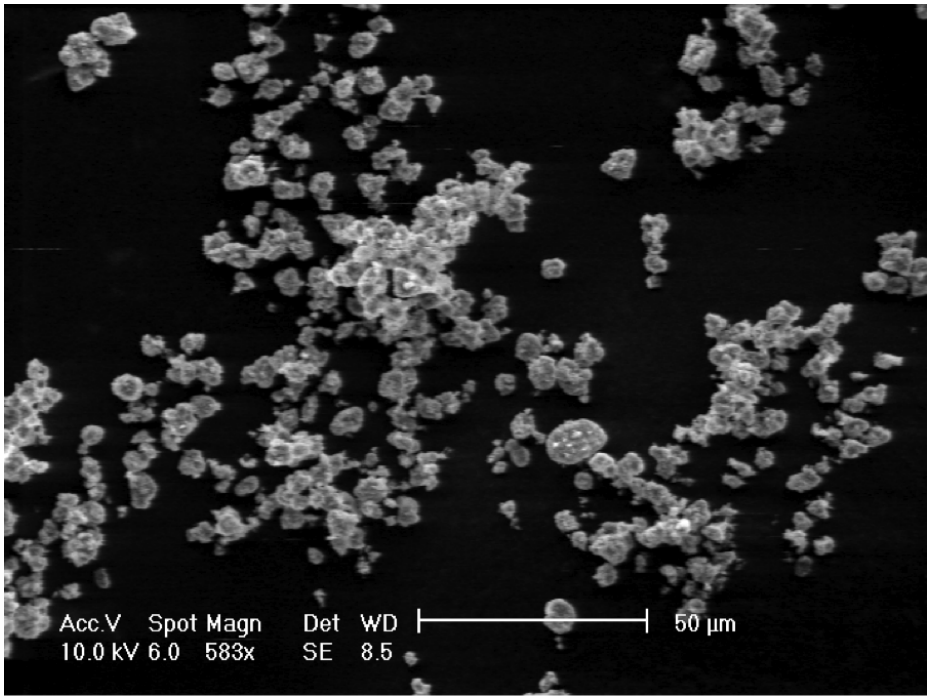

Figure B.5: SEM image of fresh calcined HZSM-5, before reactions.

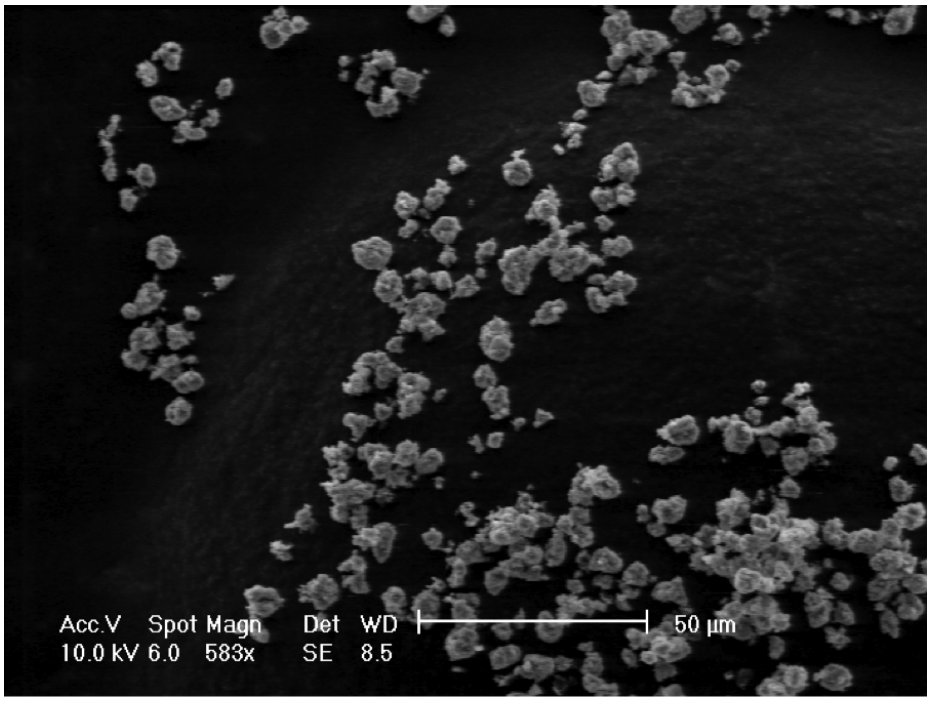

Figure B.6: SEM image of fresh calcined HZSM-5, before reactions.

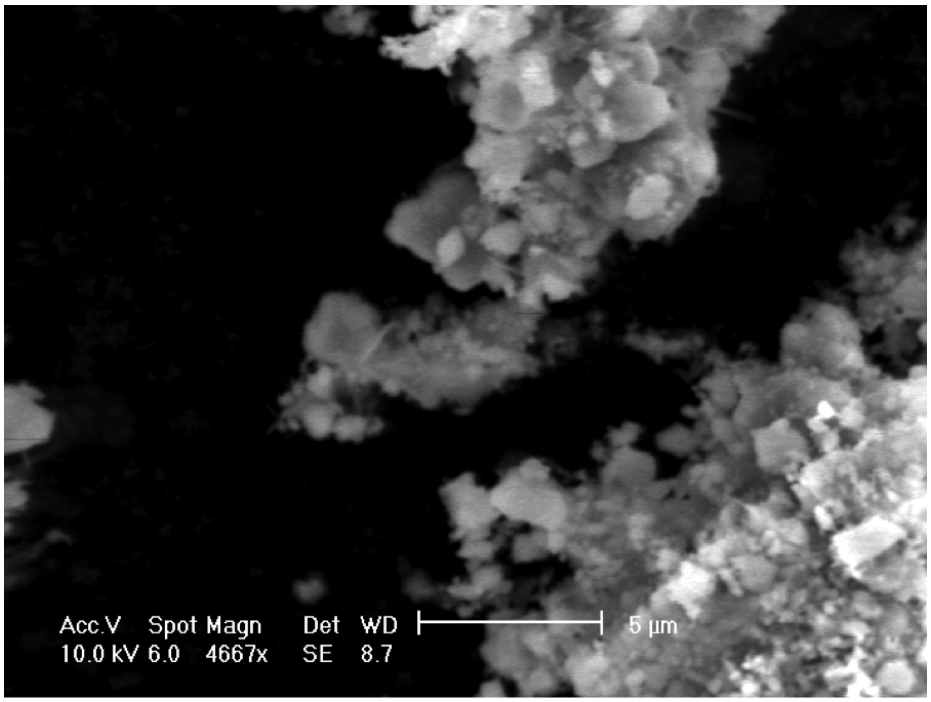

Figure B.7: SEM image of HZSM-5 that has been used in reactions and without regeneration, reaction condition: 400℃, 180 minutes.

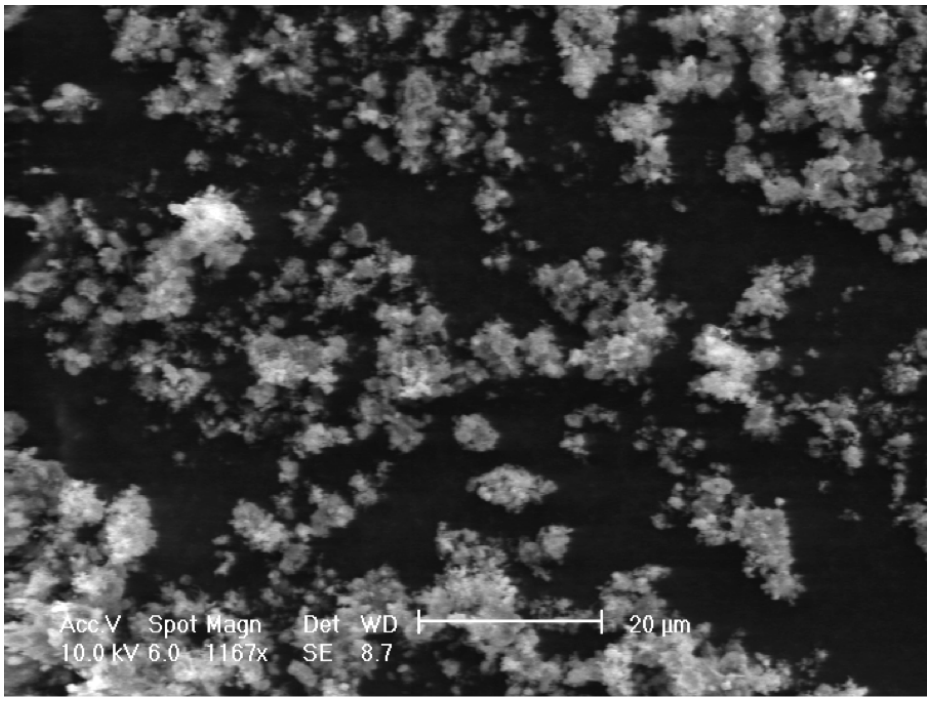

Figure B.8: SEM image of HZSM-5 that has been used in reactions and without regeneration, reaction condition: 400℃, 180 minutes.

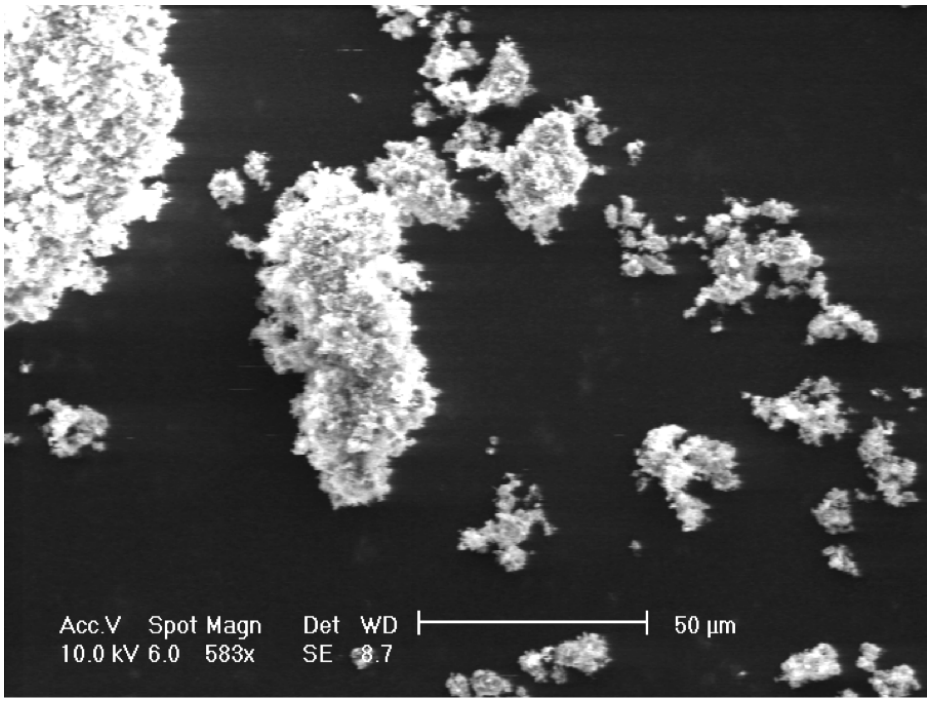

Figure B.9: SEM image of HZSM-5 that has been used in reactions and without regeneration, reaction condition: 400℃, 180 minutes.

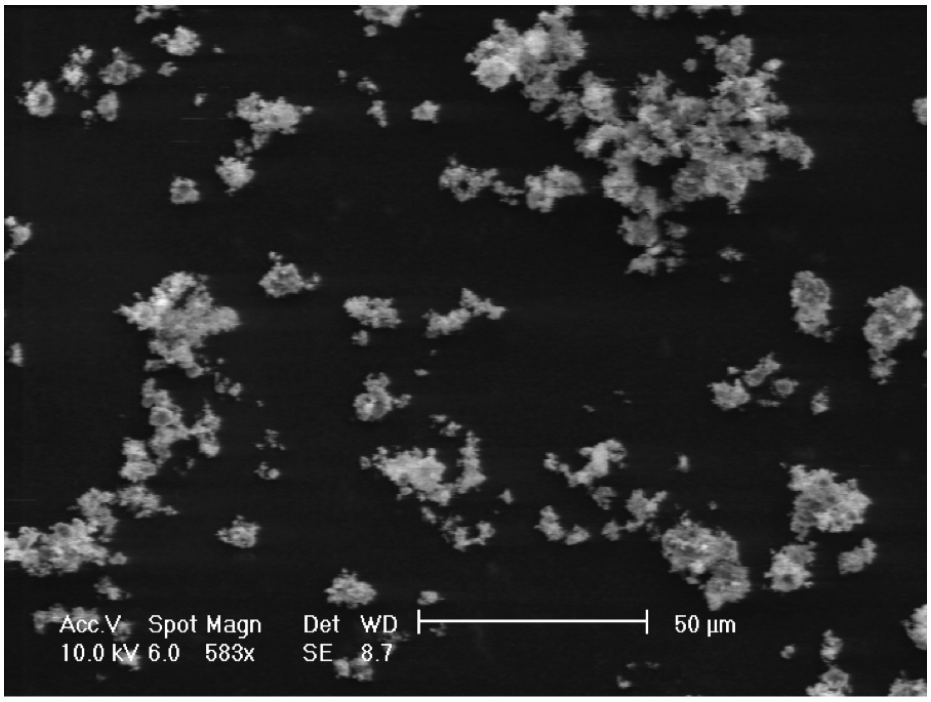

Figure B.10: SEM image of HZSM-5 that has been used in reactions and without regeneration, reaction condition: 400℃, 180 minutes.

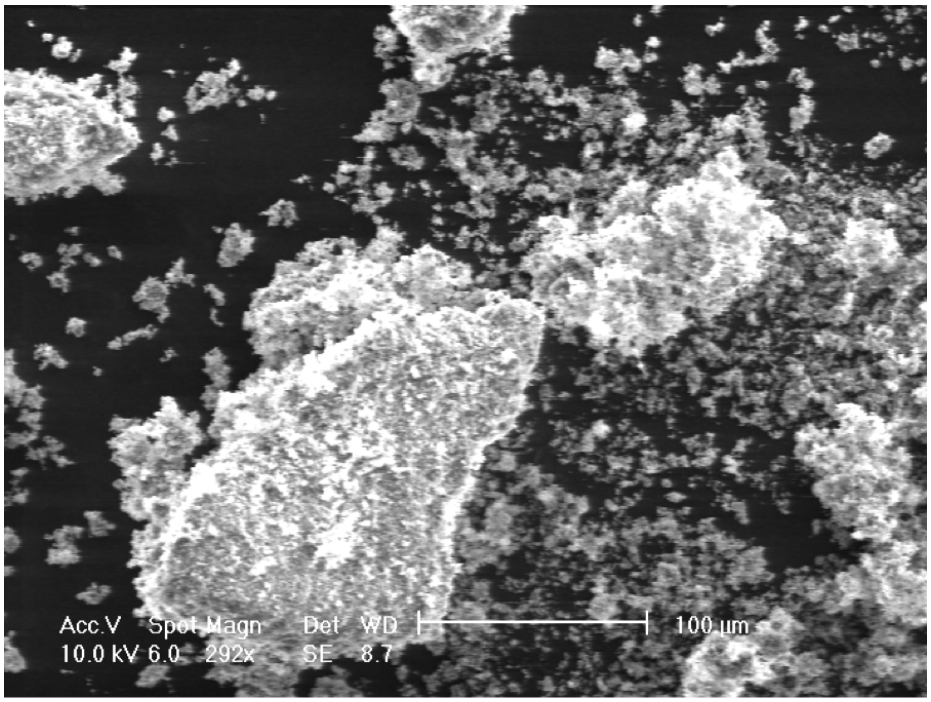

Figure B.11: SEM image of HZSM-5 that has been used in reactions and without regeneration, reaction condition: 400℃, 180 minutes.

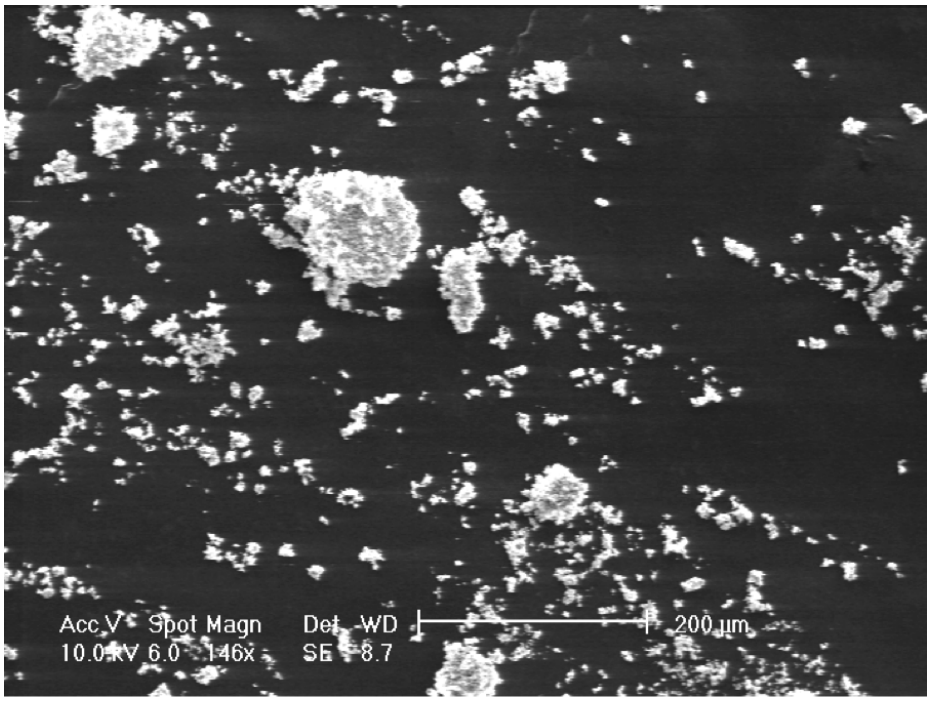

Figure B.12: SEM image of HZSM-5 that has been used in reactions and without regeneration, reaction condition: 400℃, 180 minutes.

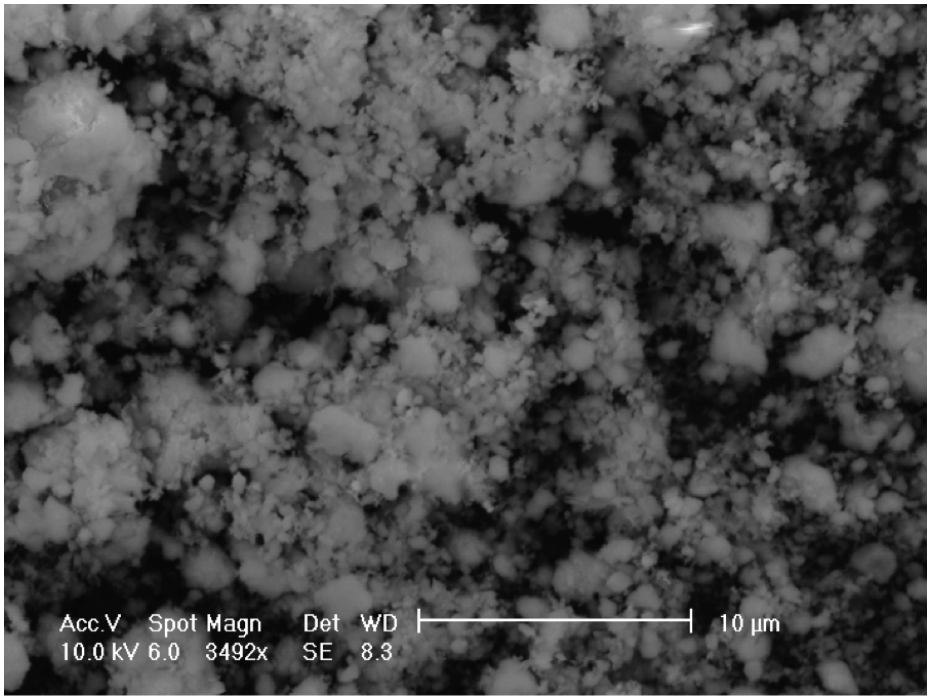

Figure B.13: SEM image of HZSM-5 after one time usage and regeneration.

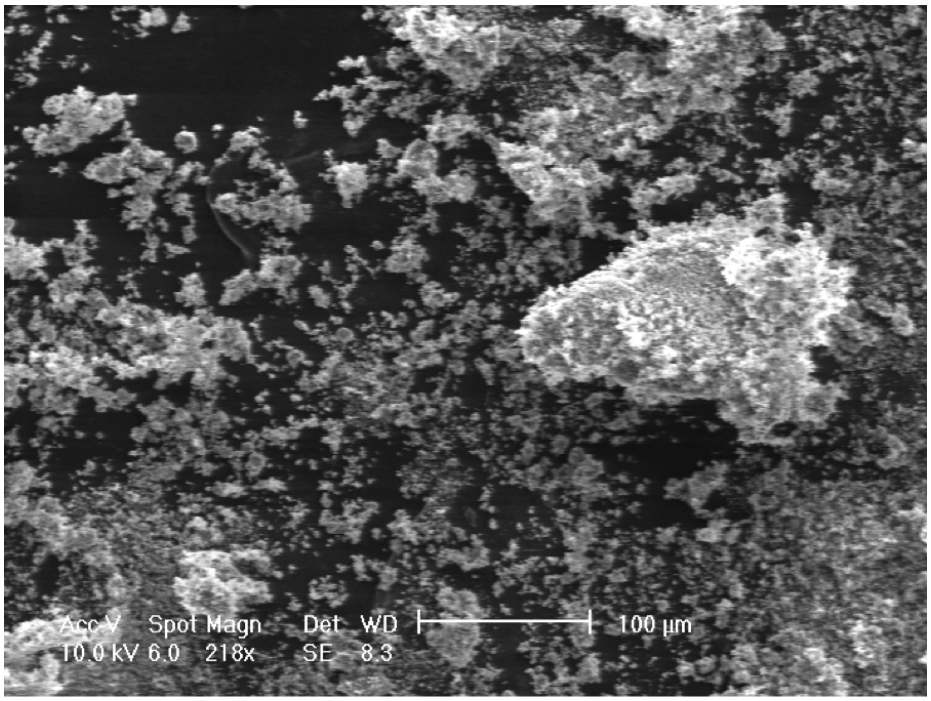

Figure B.14: SEM image of HZSM-5 after one time usage and regeneration.

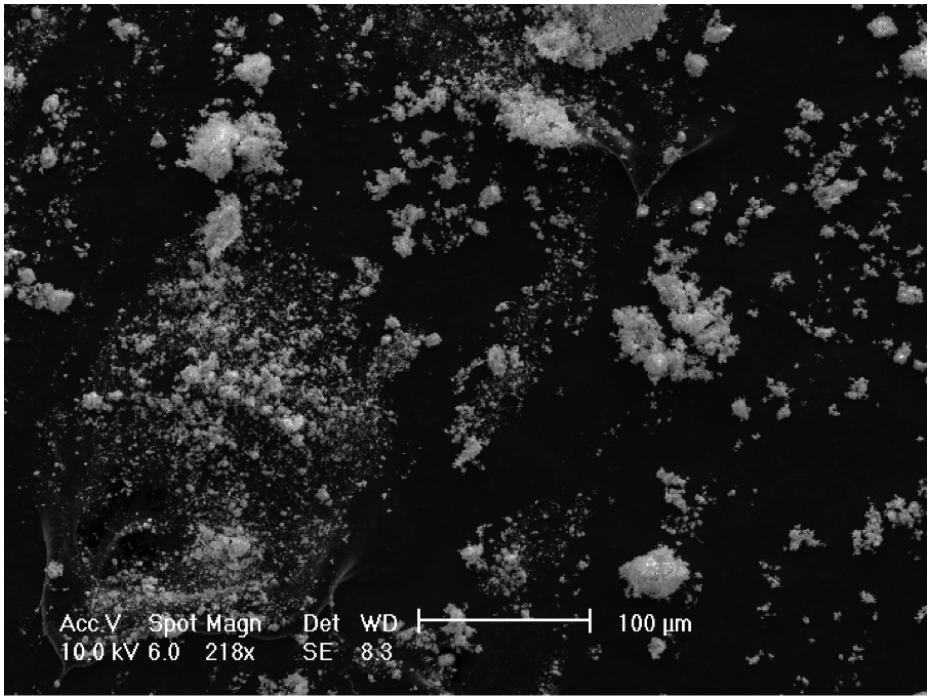

Figure B.15: SEM image of HZSM-5 after one time usage and regeneration.

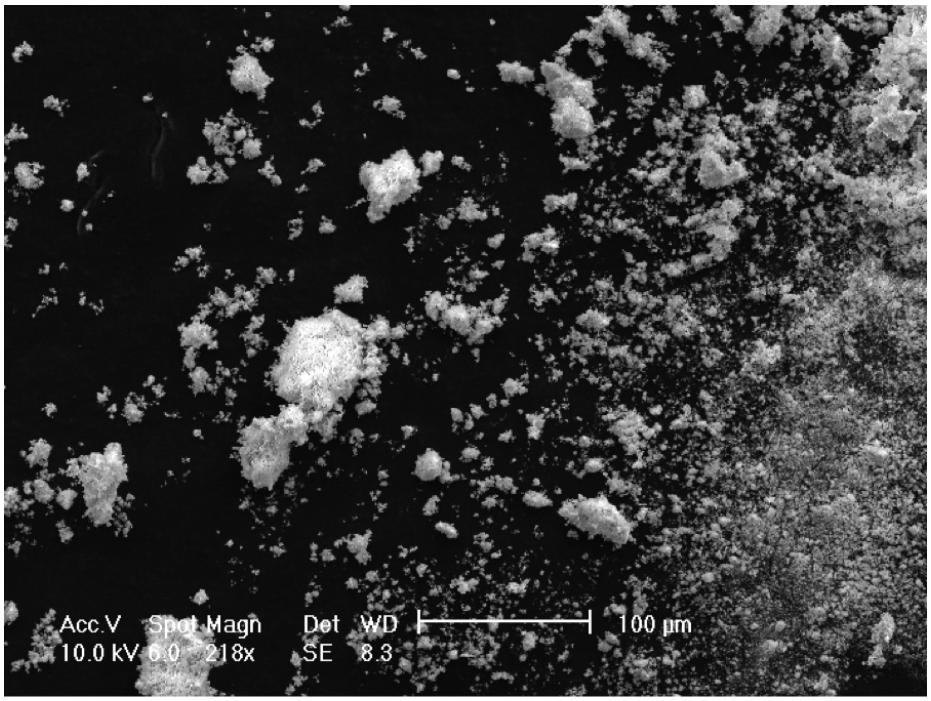

Figure B.16: SEM image of HZSM-5 after one time usage and regeneration.

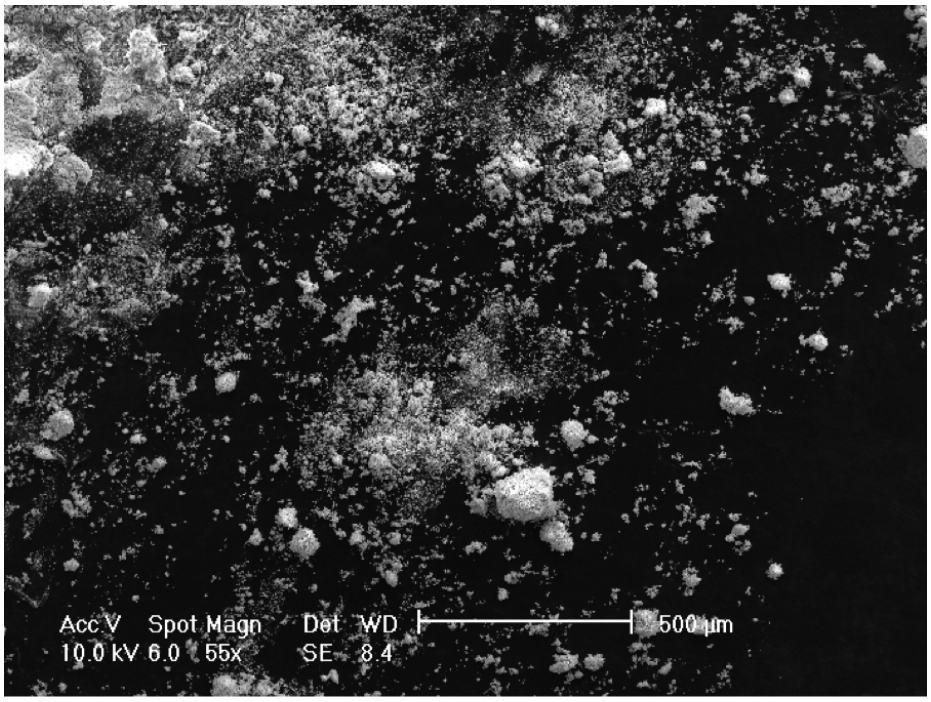

Figure B.17: SEM image of HZSM-5 after one time usage and regeneration.

APPENDIX C

Distribution of liquid products from reactions of different feedstocks

Figure C1 to Figure C4 are pie-charts of distribution of liquid products from catalytic hydrothermal cracking reactions of different real feedstocks with zeolite HZSM-5. Those pie-charts gave very direct visual comparison of different product profiles among various types of renewable feedstocks, including crude algal oil, cold pressed coconut oil, refined peanut oil, and lard (solid animal fat).

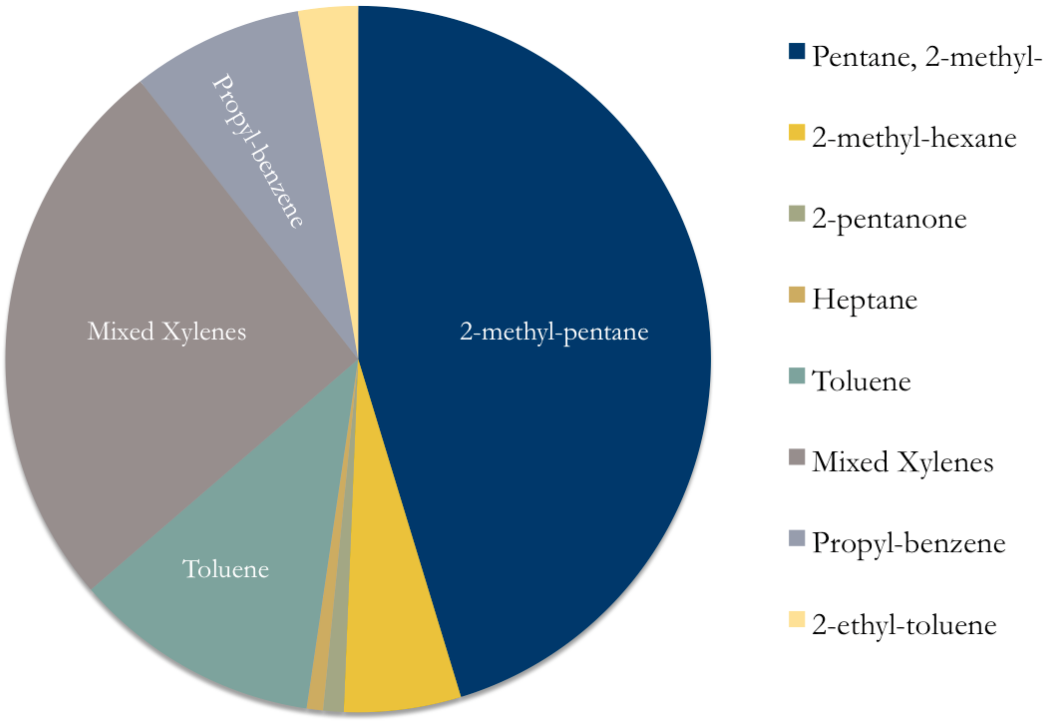

Figure C.1: Distribution of liquid products of crude algal oil, reaction condition: 150 mg algal oil with 150 mg HZSM-5 (silica/alumina ratio of 23), 400°C, 180 minutes, water density of 0.1 g/mL

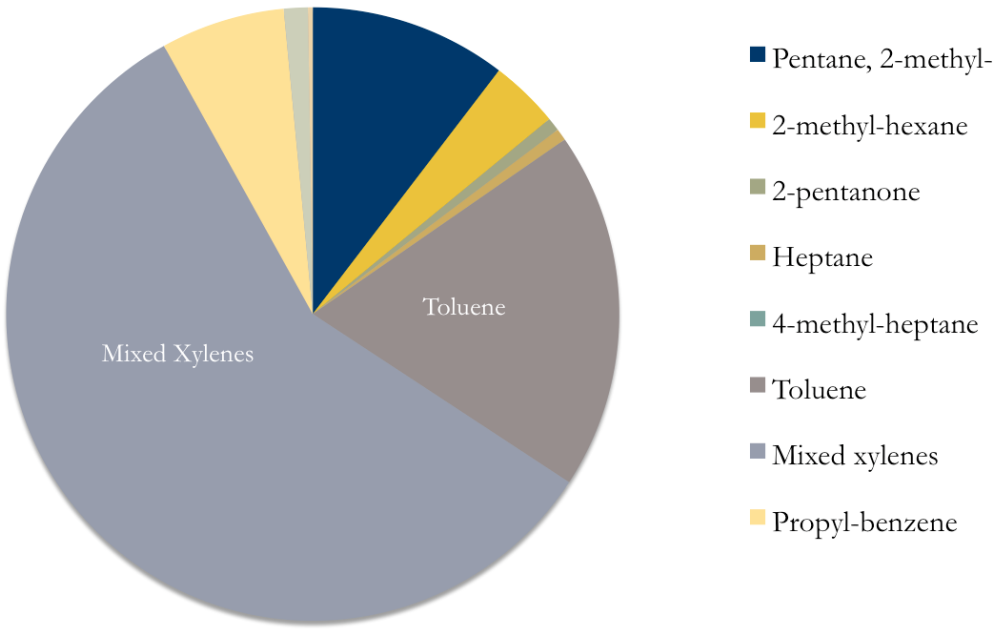

Figure C.2: Distribution of liquid products of coconut oil, reaction condition: 150 mg algal oil with 150 mg HZSM-5 (silica/alumina ratio of 23), 400℃, 180 minutes, water density of 0.1 g/mL

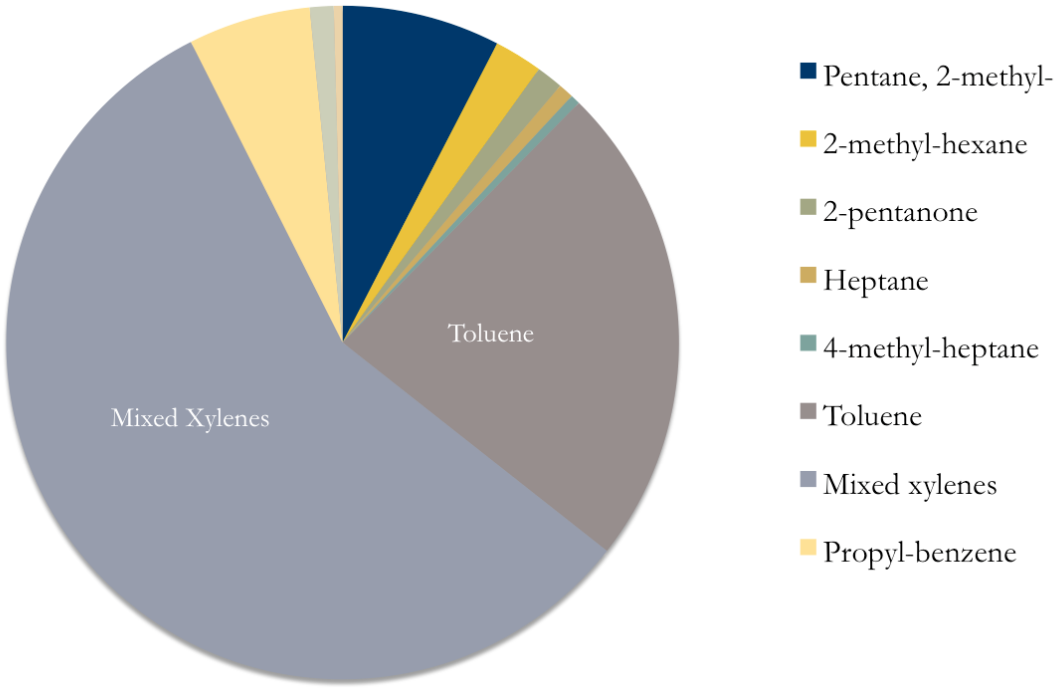

Figure C.3: Distribution of liquid products of peanut oil, reaction condition: 150 mg algal oil with 150 mg HZSM-5 (silica/alumina ratio of 23), 400℃, 180 minutes, water density of 0.1 g/mL

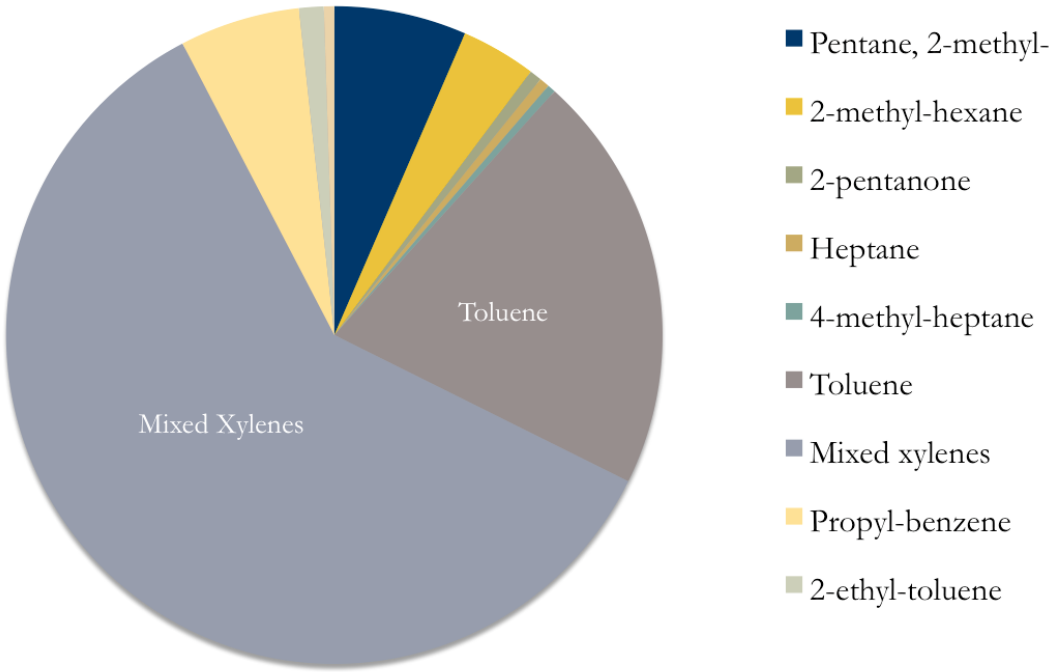

Figure C.4: Distribution of liquid products of lard, reaction condition: 150 mg algal oil with 150 mg HZSM-5 (silica/alumina ratio of 23), 400℃, 180 minutes, water density of 0.1 g/mL

BIBLIOGRAPHY

BIBLIOGRAPHY

[1] Tylisha M. Brown, Peigao Duan, and Phillip E. Savage. Hydrothermal liquefaction and gasification of Nannochloropsis sp. *Energy and Fuels*, 24(6):3639–3646, June 2010.

[2] Dadan Kusdiana and Shiro Saka. Effects of water on biodiesel fuel production by supercritical methanol treatment. *Bioresource Technology*, 91(3):289–295, February 2004.

[3] Russell L. Holliday, Jerry W. King, and Gary R. List. Hydrolysis of Vegetable Oils in Sub- and Supercritical Water. (Edko 76):932–935, 1997.

[4] R. Alenezi, G. A. Leeke, R. C. D. Santos, and A. R. Khan. Hydrolysis kinetics of sunflower oil under subcritical water conditions. *Chemical Engineering Research and Design*, 87(6):867–873, 2009.

[5] Pierre Gallezot. Conversion of biomass to selected chemical products. *Chemical Society reviews*, 41(4):1538–58, February 2012.

[6] Jesse B. Thompson et al. Shale Revolution Feeds Petrochemical Profits as Production Adapts. *Southwest Economy*, (Q4):16–19, 2013.

[7] C. DooHoo. The effect of shale gas revolution on oil industry. *The Institute of Energy Economics Japan (IEEJ)*, 2035(January):1–10, 2013.

[8] Pieter C. A. Bruijnincx and Bert M. Weckhuysen. Shale Gas Revolution: An Opportunity for the Production of Biobased Chemicals? *Angewandte Chemie International Edition*, 52(46):11980–11987, November 2013.

[9] T.F. Slaper and T.J. Hall. The triple bottom line: what is it and how does it work? *Indiana Business Review*, 86(1):4–8, 2011.

[10] Evangelos C. Petrou and Costas P. Pappis. Biofuels : A Survey on Pros and Cons Biofuels : A Survey on Pros and Cons. (1):1055–1066, 2009.

[11] Anoop Singh and Stig Irving Olsen. A critical review of biochemical conversion, sustainability and life cycle assessment of algal biofuels. *Applied Energy*, 88(10): 3548–3555, 2011.

[12] Laurent Lardon, Arnaud Helias, Bruno Sialve, Jean-Philippe Steyer, and Olivier Bernard. Life-Cycle Assessment of Biodiesel Production from Microalgae. *Environmental Science & Technology*, 43:6475–6481, 2009.

[13] P. Kritzer and E. Dinjus. An assessment of supercritical water oxidation (SCWO): Existing problems, possible solutions and new reactor concepts. *Chemical Engineering Journal*, 83(3):207–214, 2001.

[14] Phillip E. Savage. A perspective on catalysis in sub- and supercritical water. *The Journal of Supercritical Fluids*, 47(3):407–414, 2009.

[15] Phillip E Savage, Sudhama Gopalan, Thamid I Mizan, Christopher J Martino, and Eric E Brock. Reactions at supercritical conditions: Applications and fundamentals. *AIChE Journal*, 41(7):1723–1778, 1995.

[16] Jeremy G. Immer, M. Jason Kelly, and H. Henry Lamb. Catalytic reaction pathways in liquid-phase deoxygenation of C18 free fatty acids. *Applied Catalysis A: General*, 375(1):134–139, February 2010.

[17] Wei-Cheng Wang, Nirajan Thapaliya, Andrew Campos, Larry F. Stikeleather, and William L. Roberts. Hydrocarbon fuels from vegetable oils via hydrolysis and thermo-catalytic decarboxylation. *Fuel*, 95:622–629, May 2012.

[18] International Energy Agency. *2012 Annual Report*. IEA, March 2013.

[19] K. A. O. Santos, A. A. Dantas Neto, M. C. P. A. Moura, and T. N. Castro Dantas. Separation of Xylene Isomers Through Adsorption on Microporous Materials: a Review. *Brazilian Journal of Petroleum and Gas*, 5(4):255–268, December 2011. ISSN 19820593.

[20] Peigao Duan and Phillip E. Savage. Hydrothermal liquefaction of a microalga with heterogeneous catalysts. *Industrial and Engineering Chemistry Research*, 50(1):52–61, 2011.

[21] Saruul Idesh, Shinji Kudo, Koyo Norinaga, and Jun-ichiro Hayashi. Catalytic Hydrothermal Reforming of Jatropha Oil in Subcritical Water for the Production of Green Fuels: Characteristics of Reactions over Pt and Ni Catalysts. *Energy & Fuels*, 27(8):4796–4803, August 2013. ISSN 0887-0624.

[22] Lixiong Li, Edward Coppola, Jeffrey Rine, Jonathan L. Miller, and Devin Walker. Catalytic Hydrothermal Conversion of Triglycerides to Non-ester Biofuels. *Energy & Fuels*, 24(2):1305–1315, February 2010.

[23] Siswati Lestari, Päivi Mäki-Arvela, Jorge Beltramini, G. Q. Max Lu, and Dmitry Yu Murzin. Transforming triglycerides and fatty acids into biofuels. *ChemSusChem*, 2(12):1109–19, January 2009.

[24] Tracy J. Benson, Rafael Hernandez, Mark G. White, W. Todd French, Earl E. Alley, William E. Holmes, and Bethany Thompson. Heterogeneous Cracking of an Unsaturated Fatty Acid and Reaction Intermediates on H^+ZSM-5 Catalyst. *CLEAN - Soil, Air, Water*, 36(8):652–656, August 2008.

[25] Peter Bielansky, Alexander Weinert, Christoph Schönberger, and Alexander Reichhold. Gasoline and gaseous hydrocarbons from fatty acids via catalytic cracking. *Biomass Conversion and Biorefinery*, 2(1):53–61, November 2011.

[26] Yean-Sang Ooi, Ridzuan Zakaria, Abdul Rahman Mohamed, and Subhash Bhatia. Catalytic Conversion of Fatty Acids Mixture to Liquid Fuel and Chemicals over Composite Microporous/Mesoporous Catalysts. *Energy & Fuels*, 19(3):736–743, May 2005.

[27] Yu-Ting Cheng, Jungho Jae, Jian Shi, Wei Fan, and George W. Huber. Production of Renewable Aromatic Compounds by Catalytic Fast Pyrolysis of Lignocellulosic Biomass with Bifunctional Ga/ZSM-5 Catalysts. *Angewandte Chemie*, 124(6):1416–1419, February 2012. ISSN 00448249.

[28] Zheng Li and Phillip E. Savage. Feedstocks for fuels and chemicals from algae: Treatment of crude bio-oil over HZSM-5. *Algal Research*, 2(2):154–163, March 2013.

[29] Thomas A. Milne, Robert J. Evans, and Nicholas Nagle. Catalytic conversion of microalgae and vegetable oils to premium gasoline, with shape-selective zeolites. *Biomass*, 21(3):219–232, January 1990. ISSN 01444565.

[30] R. A. Beyerlein, C. Choi-feng, J. B. Hall, B. J. Huggins, and G. J. Ray. Effect of steaming on the defect structure and acid catalysis of protonated zeolites. *Topics in Catalysis*, 4:27–42, 1997. ISSN 1022-5528.

[31] Costas S. Triantafillidis, Athanasios G. Vlessidis, Lori Nalbandian, and Nicholaos P. Evmiridis. Effect of the degree and type of the dealumination method on the structural, compositional and acidic characteristics of H-ZSM-5 zeolites. *Microporous and Mesoporous Materials*, 47(2-3):369–388, 2001.

[32] Costas S. Triantafillidis, Athanasios G. Vlessidis, and Nicholaos P. Evmiridis. Dealuminated HY Zeolites: Influence of the Degree and the Type of Dealumination Method on the Structural and Acidic Characteristics of HY Zeolites. *Industrial & Engineering Chemistry Research*, 39(2):307–319, 2000.

[33] Shujauddin M. Changi, Julia L. Faeth, Na Mo, and Phillip E. Savage. Hydrothermal Reactions of Biomolecules Relevant for Microalgae Liquefaction. *Industrial and Engineering Chemistry Research*, 54(47):11733–11758, 2015.

[34] Yingda Lu, Robert B. Levine, and Phillip E. Savage. Fatty Acids for Nutraceuticals and Biofuels from Hydrothermal Carbonization of Microalgae. *Industrial & Engineering Chemistry Research*, 54(16):4066–4071, April 2015.

[35] J. K. Satyarthi, D. Srinivas, and P. Ratnasamy. Hydrolysis of vegetable oils and fats to fatty acids over solid acid catalysts. *Applied Catalysis A: General*, 391 (1-2):427–435, 2011.

[36] Peigao Duan and Phillip E Savage. Upgrading of crude algal bio-oil in supercritical water. *Bioresource technology*, 102(2):1899–906, January 2011.

[37] Tomoyuki Fujii, Pramote Khuwijitjaru, Yukitaka Kimura, and Shuji Adachi. Decomposition kinetics of monoacyl glycerol and fatty acid in subcritical water under temperature-programmed heating conditions. *Food Chemistry*, 94(3):341–347, 2006.

[38] Masaru Watanabe, Toru Iida, and Hiroshi Inomata. Decomposition of a long chain saturated fatty acid with some additives in hot compressed water. *Energy Conversion and Management*, 47(18-19):3344–3350, November 2006.

[39] Jie Fu. Fuels of the future. *Energy & Environmental Science*, 3(3):253, 2010.

[40] Jie Fu, Xiuyang Lu, and Phillip E. Savage. Hydrothermal decarboxylation and hydrogenation of fatty acids over Pt/C. *ChemSusChem*, 4(4):481–486, April 2011.

[41] Jie Fu, Fan Shi, L. T. Thompson, Xiuyang Lu, and Phillip E. Savage. Activated Carbons for Hydrothermal Decarboxylation of Fatty Acids. *ACS Catalysis*, 1(3): 227–231, March 2011.

[42] Jing Yang and Huai Sun. A theoretical study of hydrothermal stability of P-modified ZSM-5 zeolites. *Science in China, Series B: Chemistry*, 52(3):282–287, 2009.

[43] Tushar P Vispute, Huiyan Zhang, Aimaro Sanna, Rui Xiao, and George W Huber. Renewable chemical commodity feedstocks from integrated catalytic processing of pyrolysis oils. *Science (New York, N.Y.)*, 330(6008):1222–7, November 2010.

[44] Kaige Wang and Robert C. Brown. Catalytic pyrolysis of microalgae for production of aromatics and ammonia. *Green Chem*, 15(3):675–681, 2013.

[45] Yu-Ting Cheng, Zhuopeng Wang, Christopher J Gilbert, Wei Fan, and George W Huber. Production of p-xylene from biomass by catalytic fast pyrolysis using ZSM-5 catalysts with reduced pore openings. *Angewandte Chemie (International ed. in English)*, 51(44):11097–100, October 2012.

[46] Ryan M. Ravenelle, Florian Schü, Andrew DAmico, Nadiya Danilina, Jeroen A. van Bokhoven, Johannes A. Lercher, Christopher W. Jones, and Carsten Sievers. Stability of Zeolites in Hot Liquid Water. *The Journal of Physical Chemistry C*, 114(46):19582–19595, 2010.

[47] Pan Pan, Changwei Hu, Wenyan Yang, Yuesong Li, Linlin Dong, Liangfang Zhu, Dongmei Tong, Renwei Qing, and Yong Fan. The direct pyrolysis and catalytic pyrolysis of Nannochloropsis sp. residue for renewable bio-oils. *Bioresource technology*, 101(12):4593–9, June 2010.

[48] Chen Zhao and Johannes A. Lercher. Upgrading pyrolysis oil over Ni/HZSM-5 by cascade reactions. *Angewandte Chemie - International Edition*, 51(24): 5935–5940, 2012.

[49] C. W. Hoerr and H. J. Harwood. The Solubilities of Oleic and Linoeic Acids in Common Organic Solvents. *The Journal of Physical Chemistry*, 56(9):1068–1073, 1952.

[50] Rudi Heryanto, Masitah Hasan, Ezzat Chan Abdullah, and Andri Cahyo Kumoro. Solubility of Stearic Acid in Various Organic Solvents and Its Prediction using Non-ideal Solution Models. *ScienceAsia*, 33:469–472, 2007.

[51] Hee-Yong Shin, Jae-Hun Ryu, Sang-Yeob Park, and Seong-Youl Bae. Thermal stability of fatty acids in subcritical water. *Journal of Analytical and Applied Pyrolysis*, 98:250–253, November 2012.

[52] J. H. Gary, G. E. Handwerk, and M. J. Kaiser. Petroleum Refining: Technology and Economics, Fourth Edition, 2001. URL `http://www.dekker.com`.

[53] Robert A. Meyers. *Handbook of Petroleum Refining Processes*. McGraw-Hill Professional, Third Edition, 2004.

[54] T. Tsai. Disproportionation and transalkylation of alkylbenzenes over zeolite catalysts. *Applied Catalysis A: General*, 181(2):355–398, 1999.

[55] Jiri Cejka, Herman van Bekkum, A. Corma, and F. Schueth. *Introduction to Zeolite Molecular Sieves*, volume 168. Elsevier, 2007.

[56] Peigao Duan and Phillip E. Savage. Catalytic hydrothermal hydrodenitrogenation of pyridine. *Applied Catalysis B: Environmental*, 108-109:54–60, October 2011.

[57] Jacob G. Dickinson, Jack T. Poberezny, and Phillip E. Savage. Deoxygenation of benzofuran in supercritical water over a platinum catalyst. *Applied Catalysis B: Environmental*, 123-124:357–366, 2012.

[58] Steven F. Rice, Richard R. Steeper, and Jason D. Aiken. Water Density Effects on Homogeneous Water-Gas Shift Reaction Kinetics. *The Journal of Physical Chemistry A*, 102(16):2673–2678, 1998.

[59] Xiwen Zhang, Qun Guo, Bo Qin, Zhizhi Zhang, Fengxiang Ling, Wanfu Sun, and Ruifeng Li. Structural features of binary microporous zeolite composite Y-Beta and its hydrocracking performance. *Catalysis Today*, 149(1-2):212–217, January 2010.

[60] J Meusinger. Activation of Hydrogen on Zeolites: Kinetics and Mechanism of n-Heptane Cracking on H-ZSM-5 Zeolites Under High Hydrogen Pressure. *Journal of Catalysis*, 152(1):189–197, 1995.

[61] Panagiotis G. Smirniotis and Eli Ruckenstein. Comparison of the Performance of ZSM-5, beta Zeolite, Y, USY, and their Composites in the Catalytic Cracking of n-Octane, 2, 2, 4-Trimethylpentane, and 1-Octene. *Industrial & Engineering Chemistry Research*, 33(4):800–813, 1994.

[62] Joeri F. Denayer, Wim Souverijns, Pierre A. Jacobs, Johan A. Martens, and Gino V. Baron. High-Temperature Low-Pressure Adsorption of Branched C 5 C 8 Alkanes on Zeolite Beta, ZSM-5, ZSM-22, Zeolite Y, and Mordenite. *The Journal of Physical Chemistry B*, 102(23):4588–4597, 1998.

[63] Ch. Baerlocher and L. B. McCusker. Database of Zeolite Structures, 2014. URL `http://www.iza-structure.org/databases/`. Accessed March 2016.

[64] Dimitris K. Liguras and David T. Allen. Structural models for catalytic cracking. 1. Model compound reactions. *Industrial & Engineering Chemistry Research*, 28 (6):665–673, June 1989.

[65] Beatriz Valle, Ana G. Gayubo, Ainhoa Alonso, Andrés T. Aguayo, and Javier Bilbao. Hydrothermally stable HZSM-5 zeolite catalysts for the transformation of crude bio-oil into hydrocarbons. *Applied Catalysis B: Environmental*, 100(1-2): 318–327, October 2010.

[66] Paula A. Zapata, Jimmy Faria, M. Pilar Ruiz, Rolf E. Jentoft, and Daniel E. Resasco. Hydrophobic zeolites for biofuel upgrading reactions at the liquid-liquid interface in water/oil emulsions. *Journal of the American Chemical Society*, 134 (20):8570–8, May 2012.

[67] Sharelle M. Campbell, David M. Bibby, Jan M. Coddington, Russell F. Howe, and Richard H. Meinhold. Dealumination of HZSM-5 zeolites. *Journal of Catalysis*, 161(1):338–349, 1996.

[68] Kendall T. Thomson. Reactivity in Zeolite Systems. URL `https://engineering.purdue.edu/~thomsonk/projects.html`. Accessed March 2016.

[69] Rajamani Gounder. Hydrophobic microporous and mesoporous oxides as Bronsted and Lewis acid catalysts for biomass conversion in liquid water. *Catal. Sci. Technol.*, 4(9):2877–2886, 2014.

[70] D.P. Serrano, R. A. García, M. Linares, and B. Gil. Influence of the calcination treatment on the catalytic properties of hierarchical ZSM-5. *Catalysis Today*, 179(1):91–101, January 2012.

[71] H. Scott Fogler. *Elements of Chemical Reaction Engineering*. Pearson Education, Inc., Fourth Edition, 2006. ISBN 0-13-047394-4.

[72] Werner O. Haag, Rudolph M. Lago, and Paul B. Weisz. Transport and reactivity of hydrocarbon molecules in a shape-selective zeolite. *Faraday Discussions of the Chemical Society*, 72:317, 1981.

[73] Na Mo, Wincent Tandar, and Phillip E. Savage. Aromatics from saturated and unsaturated fatty acids via zeolite catalysis in supercritical water. *The Journal of Supercritical Fluids*, 102:73–79, July 2015.

[74] Ayhan Demirbas. Biodiesel production from vegetable oils via catalytic and non-catalytic supercritical methanol transesterification methods. *Progress in Energy and Combustion Science*, 31(5-6):466–487, January 2005.

[75] Witchakorn Charusiri, Withaya Yongchareon, and Tharapong Vitidsant. Conversion of used vegetable oils to liquid fuels and chemicals over HZSM-5, sulfated zirconia and hybrid catalysts. *Korean Journal of Chemical Engineering*, 23(3): 349–355, 2006.

[76] Yean-Sang Ooi, Ridzuan Zakaria, Abdul Rahman Mohamed, and Subhash Bhatia. Catalytic Conversion of Fatty Acids Mixture to Liquid Fuel and Chemicals over Composite Microporous/Mesoporous Catalysts. *Energy & Fuels*, 19(3):736–743, May 2005.

[77] A. Bayat and S. M. Sadrameli. Conversion of canola oil and canola oil methyl ester (CME) to green aromatics over a HZSM-5 catalyst: a comparative study. *RSC Adv.*, 5(36):28360–28368, 2015.

[78] Y. S. Prasad, N. N. Bakhshi, J. F. Mathews, and R. L. Eager. Catalytic conversion of canola oil to fuels and chemical feedstocks: Part II Effect of co-feeding steam on the performance of HZSM-5 catalyst. *The Canadian Journal of Chemical Engineering*, 64(2):285–292, 1986.